Year : 2024

Developmental transcriptomics of sexual dimorphism and sexual conflict

Djordjevic Jelisaveta

Djordjevic Jelisaveta, 2024, Developmental transcriptomics of sexual dimorphism and sexual conflict

Originally published at : Thesis, University of Lausanne

Posted at the University of Lausanne Open Archive http://serval.unil.ch
Document URN : urn:nbn:ch:serval-BIB_709899674DF68

UNIL | Université de Lausanne
Faculté de biologie et de médecine

Département d'Ecologie et Evolution

Developmental transcriptomics of sexual dimorphism and sexual conflict

Thèse de doctorat ès sciences de la vie (PhD)

présentée à la

Faculté de biologie et de médecine
de l'Université de Lausanne

Jelisaveta Djordjevic

Master of science in Behaviour, Evolution and Conservation de l'Université de Lausanne

Jury

Prof. Jan Roelof van der Meer, Président
Prof. Tanja Schwander, Directrice de thèse
Prof. Jennifer Perry, Experte
Prof. Abderrahman Khila, Expert

Lausanne, 2024

UNIL | Université de Lausanne
Faculté de biologie et de médecine

Ecole Doctorale
Doctorat ès sciences de la vie

Imprimatur

Vu le rapport présenté par le jury d'examen, composé de

Président·e	Monsieur	Prof.	Jan Roelof	**van der Meer**
Directeur·trice de thèse	Madame	Prof.	Tanja	**Schwander**
Expert·e·s	Madame	Prof.	Jennifer	**Perry**
	Monsieur	Prof.	Abderrahman	**Khila**

le Conseil de Faculté autorise l'impression de la thèse de

Jelisaveta Djordjevic

Master - Maîtrise universitaire ès Sciences en comportement, évolution et conservation, Université de Lausanne

intitulée

Developmental transcriptomics of sexual dimorphism and sexual conflict

Lausanne, le 23 février 2024

pour le Doyen
de la Faculté de biologie et de médecine

Prof. Jan Roelof van der Meer

Table of Contents

Acknowledgments

I would like to express my gratitude to Tanja Schwander for mentoring me over the past seven years during my master's and PhD journey. I am proud to have had the chance to work with a scientist like her. Not only do I admire her knowledge, but I also appreciate her integrity concerning research quality and its accessibility.

I extend my thanks to Jan Roelof van der Meer, Abderrahman Khila, and Jennifer Perry for being part of my jury and for providing valuable feedback.

I am deeply grateful to Darren Parker, who introduced me to bioinformatics. He was an amazing supervisor during my master's, and I am still learning from him. His encouragement and support throughout these years have meant a great deal to me.

A sincere thank you to Marjorie Labédan and Zoé Dumas for your valuable help in the lab, your advice, and support. I also appreciate the contributions of Emelyne Gaudichau, William Toubiana, Alexander Brandt, Luca Soldini, Iulia Darolti, Kristine Jecha, Morgane Massy, Guillaume Lavanchy, Vincent Merel, and all current and past “Schwanderinos”.

I want to express my appreciation for all laughs, and joy, coffee breaks and talks, in the DEE with Jelena Bujan, Olivia Bates, Tomas Kay, Gyda Fenn-Moltu, Charles Mullon, Miya Pan, Céline Stoffel, Julie Guenat, Tanuj Kafle, Hanna Nomoto and Camille-Sophie Cozzarolo.

Finally, thanks to my husband, Amaury Avril for his enormous support, for helping me when I was stuck with R, for reading my thesis, and for listening to all my ideas about projects. I bet he now knows so much about sexual conflict that he could write a small review on it ☺.

Abstract

Sexes have distinct evolutionary interests, leading to the selection of different phenotypes in males and females. Sexual conflict, arises when a favored trait benefits one sex but harms the other, however a shared genome constrains each sex from achieving its optima. Sex-specific gene expression regulation can alleviate the conflict. Hence, sex-biased genes (genes with different levels of expression in males and females), likely reflect resolved conflicts over expression levels. Sex-bias typically increases during development, aligning with sexual differentiation. Yet, the ontogeny of sex-biased gene expression contributing to sexual dimorphism and its connection to sexual conflict remains poorly understood. In this thesis I analyzed the dynamics of sex-biased gene expression across development in different tissues in *Timema* stick insects. In chapter 1, I investigated the sex-biased gene expression in males and females at three developmental stages of *T. californicum* and *Drosophila melanogaster*. *Timema* show a gradual increase in sex-biased gene expression during development, while *D. melanogaster* has an abrupt increase in sex-biased gene expression in the adult stage, aligning with sexual differentiation patterns in two developmental types. In chapter 2, I examined sex-biased gene expression in various tissues across development of the closely related sister pair *T. poppense* and *T. douglasi*. Sexual differentiation at the tissue level is not gradual. The reproductive tract has extensive differences already in the first instar, while somatic tissue shows minimal sex-bias throughout development. In parthenogenetic species, selection acts on females only, consequently, their gene expression levels are expected to align with female optima. I assessed whether there is ongoing sexual conflict in sexual species, by comparing the expression levels of sex-biased genes between sexual and parthenogenetic females. I found signal of sexual conflict in the first nymphal stage of reproductive tissue. In the third chapter I examined the mechanism of dosage compensation in *T. poppense* (XX:X0). Males double the expression of X- linked genes, across somatic tissues. In reproductive tract dosage compensation is present in first instar, but later in development appears to be absent. This absence is the result of X chromosome inactivation during meiosis. Overall, these findings improve our understanding on sexual differentiation and sexual conflict during development.

Résumé

Les individus de sexe différents ont des intérêts évolutifs distincts, conduisant à la sélection de phénotypes différents chez les mâles et les femelles. Un génome partagé contraint chaque sexe dans l'atteinte de ses optima respectifs. La régulation de l'expression génique spécifique à chaque sexe peut atténuer ce conflit entre sexes. Généralement, les gènes biaisés sexuellement (gènes avec des niveaux d'expression différents chez les mâles et les femelles) augmentent pendant le développement, s'alignant avec la différenciation sexuelle. Cependant, l'ontogenèse de l'expression génique biaisée sexuellement contribuant au dimorphisme sexuel et sa connexion au conflit sexuel restent mal comprises. Dans cette thèse, j'ai analysé la dynamique de l'expression génique biaisée sexuellement tout au long du développement dans différents tissus chez les phasmes du genre *Timema*. Dans le chapitre 1, j'ai étudié l'expression génique biaisé sexuellement chez les mâles et les femelles à trois stades de développement chez *T. californicum* et *Drosophila melanogaster*. *Timema* montre une augmentation progressive de l'expression génique biaisée sexuellement pendant le développement, tandis que *D. melanogaster* connaît une augmentation brutale à l'âge adulte, s'alignant sur les schémas de différenciation sexuelle des deux types de développement. Dans le chapitre 2, j'ai examiné l'expression génique biaisée sexuellement dans différents tissus tout au long du développement dans deux espèces étroitement apparentées *T. poppense* et *T. douglasi*. La différenciation sexuelle au niveau tissulaire n'est pas progressive. Le tractus reproducteur présente d'importantes différences dès le premier stade, tandis que le tissu somatique montre un biais sexuel minimal tout au long du développement. Dans les espèces parthénogénétiques, la sélection n'agit que sur les femelles, par conséquent, on s'attend à ce que leurs niveaux d'expression génique s'alignent sur les optimaux féminins. J'ai évalué la présence d'un conflit sexuel en comparant les niveaux d'expression des gènes biaisés sexuellement entre les femelles sexuelles et parthénogénétiques. J'ai trouvé un signal de conflit sexuel au premier stade nymphe dans le tissu reproducteur. Dans le troisième chapitre, j'ai examiné le mécanisme de compensation de dosage chez *T. poppense* (XX:X0). Les mâles doublent l'expression des gènes liés au X dans les tissus somatiques. Dans le tractus reproducteur, la compensation de dosage est présente au premier stade, mais semble être absente plus tard dans le développement en raison de l'inactivation du chromosome X pendant la méiose. Dans l'ensemble, ces résultats améliorent notre compréhension de la différenciation sexuelle et du conflit sexuel pendant le développement.

General introduction

Reproduction is a fundamental biological process that in most multicellular organisms involves two sexes. Ancestrally, sexual reproduction (the exchange of genetic material) occurred via isogametes—i.e. gametes that are identical (Parker, et al. 1972; Kodric-Brown and Brown 1987). Sexual dimorphism, while not necessary for sexual reproduction, emerged early in evolution in the form of anisogamy, where male gametes are small and mobile while female gametes are large and nutritive. Anisogamy in turn led to the development of gonochorism, which distinguishes males from females. Sexual dimorphism goes beyond primary sexually differentiated traits, such as gonads, and encompasses all divergent morphological, physiological, and behavioral traits that differ between males and females of the same species (Darwin 1871; Williams and Carroll 2009). Sexually dimorphic traits result from natural and/or sexual selection favoring traits that increase the reproductive success, survival, or mating of one, but not the other, sex (Lande 1980). Some traits confer an advantage to males in male-male competition, such as horns in stag beetles, deers' antlers, or body size, and are favored by intrasexual selection (Rico-Guevara and Hurme 2019). Other traits increase mating success via female choice (intersexual selection), such as male traits that signal health, like feather pigmentation, or vocalization (Loyau, et al. 2005).

When a trait increases the fitness of one sex but decreases the fitness of the other sex, it is subject to sexually antagonistic selection, or sexual conflict (Bateman 1948; Trivers 1972; Parker 1979). Sexual conflict can occur at both the level of a single locus (intralocus sexual conflict) and between different genes or genomic regions (interlocus sexual conflict). Intralocus sexual conflict arises because the two sexes share the same genome but have different fitness optima. For example, experimental work in *Drosophila* (Drosophilidae: Diptera) has shown that certain haplotypes that increase male fitness lower fitness in females (Chippindale, et al. 2001). Interlocus sexual conflict occurs when the two sexes have a different optimal fitness outcome for a given interaction. Mating frequency is one example. In *Drosophila melanogaster*, males can increase their reproductive success through mating multiply, while multiple mating reduces longevity and reproductive success for females (Wigby and Chapman 2005).

These effects are attributed to male seminal proteins, which are transferred during mating and enhance sperm success while diminishing female receptivity (Wigby and Chapman 2005). Nevertheless, the conventional notion that the *Drosophila* seminal protein 'sex peptide' harms females for male advantage is now being questioned, as empirical research outcomes are mixed, and show potential benefits of seminal proteins to females (Hopkins and Perry 2022). Interlocus conflict can result in the coevolution of, for example, male traits for grasping females, and female traits that resist male grasping, resulting in exaggerated sexual armaments (Arnqvist and Rowe 2002; Perry and Rowe 2015).

Investigating how a single genome produces sexual dimorphism has become a key focus in evolutionary biology. Initially, it was assumed that sex chromosomes play a fundamental role in generating phenotypic sex differences, which seemed reasonable given their exclusive association with one sex in many cases and their involvement in sex determination. In mammals (XX:XY system), the Y chromosome carries the primary sex-determining gene (SRY) and is exclusively found in males (Goodfellow and Lovell-Badge 1993; Waters, et al. 2007). This gene triggers a series of gene expression changes that regulate testes development, and the subsequent development of all male phenotypes. However, sex-limited chromosomes driving differences between sexes is surprisingly rare. For example, in *Drosophila*, sex is determined by the dose of X chromosomes relative to autosomes (genomic regions shared between the sexes), despite males having a male-limited Y chromosome (Cline 1993). However, when sex chromosomes are present, they do contribute to sex differences to some extent (Dean and Mank 2014). For instance, in humans, beyond sex determination, genes on the Y chromosome play a crucial role in male fertility, and in *Drosophila*, X0 males are sterile (Kiefer 1966; Foresta, et al. 2000; Colaco and Modi 2018). In certain fish species, genes on the Y chromosome determine male-specific coloration (Kottler and Schartl 2018). Contrastingly, sex chromosomes are not essential for sex determination, and are absent in many species (Janzen and Paukstis 1991). Instead, the primary triggers of sex determination can be environmental factors, like temperature, that activate autosomal genes. In haplodiploid systems, such as Hymenoptera, sex is determined by allele combinations on autosomes (Evans, et al. 2004).

In species with differentiated sex chromosomes, males and females differ in their numbers of sex chromosome copies. In X0 and XY systems, for instance, males have a single copy of each gene on

the X chromosome, while females have two copies. The expected expression levels of X-linked genes in males are half that of autosomal genes and half that of the same X-linked genes in females. However, selection may act on sex-specific expression regulation, restoring balanced expression between the sexes, a process known as dosage compensation (Ohno 1967; Straub and Becker 2007; Mank 2013). Under complete dosage compensation, males express their single X chromosome to a level equivalent to that of the two X chromosomes in females. Hence, in cases where males are X0 and lack a sex-limited region like the Y chromosome, the differences between the sexes introduced by the varying number of chromosomes should be minimal.

Sex chromosomes have limited influence on sexual dimorphism, while autosomes play a significant role through sex-specific regulation of gene expression. Various mechanism can contribute to this: epigenetics, cis-trans regulation of gene expression, alternative splicing, post-transcriptional regulation, as well as regulation at the translational and post-translational levels (Chen and Rajewsky 2007; Signor and Nuzhdin 2018). The majority of research into sexual conflict and sexual dimorphism has focused on analyzing differences in gene expression between the sexes. Such genes with different expression levels between sexes are known as sex-biased genes (Ellegren and Parsch 2007; Grath and Parsch 2016). Sex-biased genes have been studied extensively, and the amount of sex-bias varies considerably between tissues and developmental stages (Ingleby, et al. 2015; Mank 2017). Studies using reproductive tissue often discover many sex-biased genes. In *Gallus gallus*, the number of sex-biased genes increases throughout development from around 10% to 50% (Mank, et al. 2010). In pre-gonad tissue in two pre-adult stages in *Drosophila melanogaster* over 50% of the transcriptome was sex-biased (Perry, et al. 2014). Consistently, in 5th instar *Bombyx mori* (Bombycidae: Lepidoptera) larvae there was little sex-biased gene expression in somatic tissues (ranging from 0.2% to 4.6%), while in gonads 29% of genes were sex-biased (Xia, et al. 2007). However, it is difficult to relate patterns of sex-biased gene expression in sexually differentiated tissues to total sexual dimorphism, because dimorphism also includes secondary sexual traits.

Nevertheless, levels of sex-biased gene expression correlate with the extent of sexual dimorphism (Mank 2017). For example, in wild turkeys (Phasianidae: Galliformes) with two male

morphs (dominant and subordinate), dominant males exhibit more prominent 'male' traits such as vivid coloration and subordinate males display a feminized gene expression compared to their dominant counterparts. This aligns with the observed phenotypic dimorphism (Pointer, et al. 2013). However, directly linking sex-biased genes to a phenotypic trait is a challenging process that requires a functional genetic approach. In water striders, *Microvelia longipes* (Veliidae: Hemiptera), males have exaggerated long legs used in male-male competition (Toubiana, Armisén, Dechaud, et al. 2021). Knocking down a male-biased gene (a growth factor) revealed its crucial regulatory role in male leg size (Toubiana, Armisén, Viala, et al. 2021).

Sex-biased genes are expected to reflect resolved or partially resolved cases of intralocus sexual conflict over optimal expression levels. Manipulating mating systems, for example through eliminating sexual selection, leads to changes in gene expression levels (Abbott, et al. 2023). But predicting the dynamics and directions of shifts in sex-biased gene expression is challenging and often tissue-specific (Veltsos, et al. 2017; Abbott, et al. 2023). For example, in *D. melanogaster*, enforced monogamy resulted in a feminized male transcriptome, while in *D. pseudoobscura*, it became masculinized (Hollis, et al. 2014; Veltsos, et al. 2017). In *Timema* stick insects (Timematidae: Phasmatodea), where sexual selection is naturally absent in parthenogenetic species, parthenogenetic females exhibited masculinized gene expression across multiple species, rather than the expected feminized expression (Parker, et al. 2019). However, it is not excluded that conflict occurs earlier in their development, and that different trajectories of sex-biased genes expression would be observed in pre-adult stages in parthenogenetic females.

Indeed, sex-biased gene expression is dynamic during development, suggesting that sex-specific selection may act at specific developmental stages. For instance, some sexual traits begin developing before the adult stage, marking a critical point when selection is likely to act. Examining sex-bias at multiple developmental stages is therefore necessary to understand the developmental aspects of sexual dimorphism.

Timema stick insects as a model system

Timema is a genus of hemimetabolous stick insects within which there have been multiple independent transitions to parthenogenetic reproduction. *Timema* eggs hatch in early winter, and the insects molt several times before reaching maturity in late spring. They have a relatively slow life cycle, and the exact number of molts has not previously been examined. The most critical period for survival in the laboratory is between the hatching stage and the second nymphal stage, which covers about two months. It takes about a month for *Timema* to develop from the second to the third nymphal stage. It then takes approximately two weeks each to develop from the third instar to the fourth, fourth to fifth, fifth to sixth, and from the sixth instar to the adult stage. The sixth nymphal stage is specific to females – i.e. males have one less nymphal stage (chapter 1). *Timema* are sexually dimorphic (Vickery and Sandoval 2001). Males are smaller than females, they have different coloration on the body and legs, and they have conspicuous cerci for holding on to the female during copulation. Sex is genetically determined: females have two X chromosomes while males have only one (XX:XO sex determination system) (Schwander and Crespi 2009). There are no sex-limited regions of the genome. Hence, differences between males and females stem from differences in gene expression, or post transcriptional changes.

Parthenogenetic species do not have males in their populations, and eggs are produced through automictic parthenogenesis (Larose, et al. 2023). Parthenogenetic females are characterized by decayed sexual traits, including reduced pheromone production and spermatheca size, and are less attractive to males than sexual females. Otherwise they morphologically resemble closely related, sexually reproducing females (Schwander, et al. 2013).

The transition to parthenogenetic reproduction eliminated sexually antagonistic selection, because selection acts only on one sex, namely the females. This makes *Timema* an excellent system to study the evolutionary consequences of sexual selection and sexual conflict. Importantly, differences between sexual and parthenogenetic females can result from both the release from sexual conflict, and from adaptions to parthenogenetic reproduction itself.

Aims of the thesis

The aim of this thesis is to gain a deeper understanding of how the two sexes develop from the same genetic foundations. My research delves into sex-biased gene expression at various developmental stages, examining both whole bodies and specific tissues. We additionally analyze gene expression in a pair of sister species, one parthenogenetic and one sexually reproducing, to evaluate ongoing sexual conflict. The primary focus is on incorporating a developmental perspective when studying sex-biased gene expression, sexual dimorphism, and sexual conflict.

In the first chapter, we investigated the dynamics of gene expression in males and females at three developmental stages in *T. californicum* (sexually reproducing and hemimetabolous). The aim was to test whether the extent of sex-biased gene expression was related to the extent of sexual dimorphism. We compared the first nymphal stage, where there is little to no sexual dimorphism, the 3rd nymphal stage, where there are some sexually dimorphic traits, and adults, which have fully developed sexual dimorphism. We further assessed sex-biased gene expression across three developmental stages in a holometabolous insect, *Drosophila melanogaster*. We then contrasted patterns of sex-biased gene expression between the two developmental strategies above.

In the second chapter of this thesis, we analyzed sex-biased gene expression in two *Timema* species; the sexually reproducing *T. poppense* and its parthenogenetic sister species *T. douglasi*. The first aim of this project is a follow up on the first chapter, where we analyzed whole body samples. Here we analyzed separately contribution of reproductive tissues and different somatic tissues to sex-biased gene expression across postembryonic development. The second aim is to assess whether there is ongoing sexual conflict in *T. poppense*. This was done by identifying sex-biased genes in the sexual species, and then testing whether parthenogenetic females (which do not experience sexual conflict) shift their expression levels at those genes.

The last chapter of my thesis is focused on dosage compensation in *T. poppense*. In this species, females have two X chromosomes, while males have a single X chromosome (XX: X0 system). We

tested whether gene expression is balanced between the sexes despite the imbalance in X chromosome copy number. We further examined the levels of gene expression of X-linked and autosomal genes in both males and females. We also analyzed expression levels in multiple somatic tissues, as well as in the reproductive tract. Finally, we studied dosage compensation across development to see whether it is ubiquitously present across development and tissues.

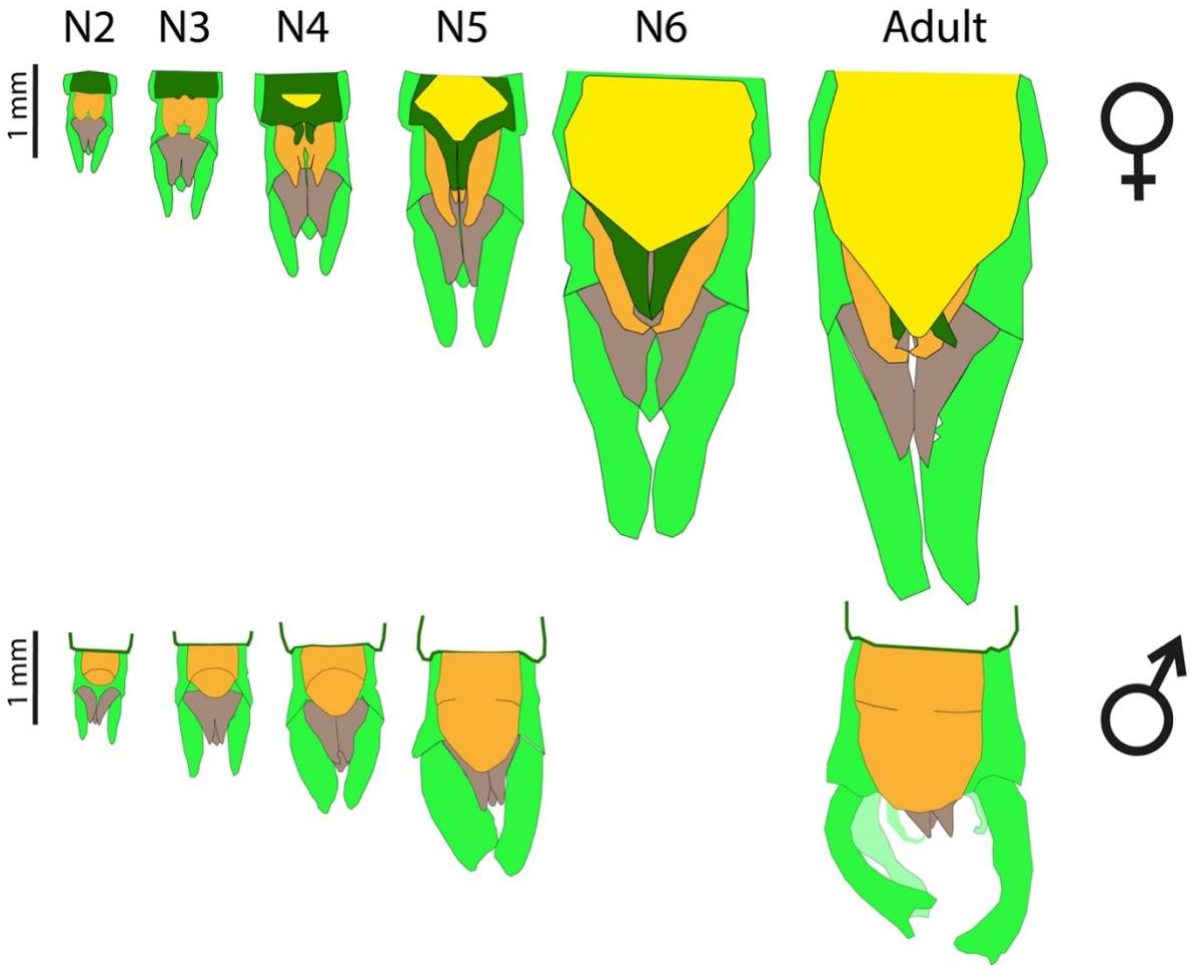

Figure 1. Schematic image depicting development of male and female subgenital parts from the second nymphal (N2) stage to adult.

Chapter 1

Dynamics of sex-biased gene expression during development in the stick insect *Timema californicum*

Jelisaveta Djordjevic, Zoé Dumas, Marc Robinson-Rechavi, Tanja Schwander and Darren J Parker

In this chapter, we explored the dynamics of sex-biased gene expression in the hemimetabolous species *Timema californicum*, examining three developmental stages: hatchlings, juveniles, and adults. The proportion of sex-biased genes gradually increased during development, paralleling the increase in phenotypic sexual dimorphism. We then contrasted the dynamics of sex-biased gene expression during development in *T. californicum* with those in the holometabolous fly *Drosophila melanogaster*. Our findings support the prediction that the dynamics of sex-biased gene expression during development differs extensively between holometabolous and hemimetabolous insect species.

This chapter was published in Heredity in 2022.

Author contributions:

JD, DJP, TS, and MRR designed the study. JD conducted the analyses, with input from DJP, TS and MRR. JD curated the data. ZD conducted the lab work with assistance of JD. JD wrote the manuscript with DJP and TS, with input from all authors

the geneticssociety

www.nature.com/hdy

ARTICLE OPEN

Check for updates

Dynamics of sex-biased gene expression during development in the stick insect *Timema californicum*

Jelisaveta Djordjevic[1]✉, Zoé Dumas[1], Marc Robinson-Rechavi[1,2], Tanja Schwander[1,4] and Darren James Parker[1,2,3,4]✉

Sexually dimorphic phenotypes are thought to arise primarily from sex-biased gene expression during development. Major changes in developmental strategies, such as the shift from hemimetabolous to holometabolous development, are therefore expected to have profound consequences for the dynamics of sex-biased gene expression. However, no studies have previously examined sex-biased gene expression during development in hemimetabolous insects, precluding comparisons between developmental strategies. Here we characterized sex-biased gene expression at three developmental stages in a hemimetabolous stick insect (*Timema californicum*): hatchlings, juveniles, and adults. As expected, the proportion of sex-biased genes gradually increased during development, mirroring the gradual increase of phenotypic sexual dimorphism. Sex-biased genes identified at early developmental stages were generally consistently male- or female-biased at later stages, suggesting their importance in sexual differentiation. Additionally, we compared the dynamics of sex-biased gene expression during development in *T. californicum* to those of the holometabolous fly *Drosophila melanogaster* by reanalyzing publicly available RNA-seq data from third instar larval, pupal and adult stages. In *D. melanogaster*, 84% of genes were sex-biased at the adult stage (compared to only 20% in *T. californicum*), and sex-biased gene expression increased abruptly at the adult stage when morphological sexual dimorphism is manifested. Our findings are consistent with the prediction that the dynamics of sex-biased gene expression during development differ extensively between holometabolous and hemimetabolous insect species.

Heredity (2022) 129:113–122; https://doi.org/10.1038/s41437-022-00536-y

INTRODUCTION

Males and females often have divergent evolutionary interests, resulting in sex-specific selection pressures and ultimately the evolution of sexually dimorphic phenotypes (Khila et al. 2012; Lande 1980). Studies investigating how sexually dimorphic phenotypes are generated have shown the importance of differential gene expression between the sexes, suggesting that sex-specific selection is the major driving force behind the evolution of sex-biased gene expression (Mank 2017). The relationship between sexual dimorphism and sex-biased gene expression has been largely studied at the adult stage when sexual dimorphism is completely manifested and reproductive interests between males and females are most different (Mank 2017). However, sex-biased gene expression has also been found at early developmental stages of many species, well before any phenotypic sexual dimorphism becomes apparent (Lowe et al. 2015; Paris et al. 2015). This suggests that expression patterns in early developmental stages are also under sex-specific selection pressures (Hale et al. 2011; Ingleby et al. 2015; Mank et al. 2010; Perry et al. 2014; Zhao et al. 2011).

Because we lack detailed studies of sex-biased gene expression during development, we do not know how consistent or dynamic the expression of the sex-biased genes is, nor how these dynamics relate to changes in phenotypic sexual dimorphism. For example, although we expect to see an overall increase in sex-biased gene expression during development (Ingleby et al. 2015; Mank 2017), it is not clear whether this results from the gradual increase of sex-bias of a set of genes or if sex-biased genes at early stages are largely different to those at later stages (Mank 2017). Furthermore, sex-biased gene expression can be considered to reflect a broad measure of sexual dimorphism, including physiological and behavioral traits, and may therefore be more representative than dimorphism quantified using external morphology. However, whether the extent of sexual dimorphism and of sex-biased gene expression are generally correlated remains poorly known.

In insects there are two major developmental strategies, and developmental patterns of sex-biased gene expression could differ between them. Holometabolous insects have morphologically and ecologically distinct larval, pupal, and adult stages, and phenotypic sexual dimorphism is commonly prominent only at the adult stage. Contrastingly, hemimetabolous insects go through gradual morphological changes and sexual differentiation, and the nymphal stages morphologically resemble adults (Chen et al. 2010). These distinct dynamics for sexual morphological differentiation are expected to be mirrored by sex-biased gene expression, with abrupt versus gradual increases in the proportion of sex-biased genes during development. However, studies of sex-biased gene expression during development have

[1]Department of Ecology and Evolution, University of Lausanne, Lausanne, Switzerland. [2]Swiss Institute of Bioinformatics, Lausanne, Switzerland. [3]School of Natural Sciences, Bangor University, Bangor, Gwynedd, United Kingdom. [4]These authors contributed equally: Tanja Schwander, Darren James Parker. Associate editor: Louise Johnson.
✉email: jelisaveta.djordjevic@unil.ch; d.parker@bangor.ac.uk

Received: 4 February 2022 Revised: 4 April 2022 Accepted: 6 April 2022
Published online: 17 May 2022

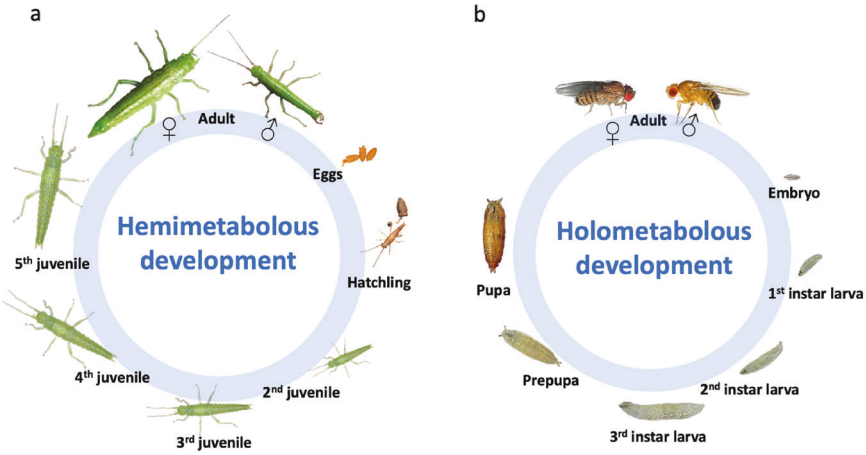

Fig. 1 Life cycles of the stick insect *T. californicum* and the fly *D. melanogaster*. **a** Life cycle of *T. californicum* showing the stages present in females. *Timema* males have one moult fewer than females. **b** Life cycle of *D. melanogaster*. Hatchling and egg photographs of *Timema were* kindly provided by Bart Zijlstra (http://www.bartzijlstra.com), juvenile and adult stages by Jelisaveta Djordjevic. Life cycle of *D.melanogaster* modified from Weigmann et al. (2003).

thus far only been conducted in holometabolous insects (Magnusson et al. 2011; Rago et al. 2020), with the main focus on *Drosophila* (Ingleby et al. 2015; Perry et al. 2014), precluding comparisons between species with different developmental strategies. For example, more than 50% of the transcriptome is sex-biased in pre-gonad tissue in juvenile stages of *Drosophila melanogaster* (Perry et al. 2014) but similar data are not available for hemimetabolous species. Furthermore, sex-biased genes in reproductive tissues provide only partial insight into total sexual dimorphism, since it excludes differences beyond sexual organs, such as secondary sexual traits.

Here, we studied the dynamics of sex-biased gene expression across development in a hemimetabolous insect, *Timema californicum*. *Timema* are sexually dimorphic walking-stick insects, found in California (Vickery and Sandoval 2001). Males are smaller than females, with different coloration, and have conspicuous cerci used for holding on to the female during copulation. We selected three developmental stages (Fig. 1a): the hatchling stage where sexes are phenotypically identical, the third juvenile stage with minor phenotypic differences, and the adult stage, with pronounced sexual dimorphism. We investigated whether sex-biased genes are recruited in a stage-specific manner, and if the magnitude of sex-bias increases with development. We further explored sequence evolution rates of sex-biased genes in pre-adult stages, to determine if they show elevated rates as commonly observed for sex-biased genes at adult stages in many species (Ellegren and Parsch 2007; Grath and Parsch 2012; Perry et al. 2014).

We then compared the dynamics of sex-biased gene expression during development in the hemimetabolous stick insect to those of the holometabolous fly *Drosophila melanogaster* by reanalyzing publicly available RNA-seq data from 3rd. instar larvae, pupal and adult stages, using the same pipeline as for *T. californicum*. In *D. melanogaster*, both larval and pupal stages have little morphological sexual dimorphism, while the adult stage has extensive dimorphism (Fig. 1b). We hypothesized that sex biased gene expression follows the establishment of morphological sexual dimorphism, with a gradual increase in sex-biased gene expression during development in *T. californicum*, and an abrupt increase at the adult stage in *D. melanogaster*.

We showed that the proportion of sex-biased genes gradually increases during development in *T. californicum*, mirroring the gradual differentiation of phenotypic sexual dimorphism in hemimetabolous insects. We also showed that sex-biased genes from early developmental stages largely remained sex-biased at later stages. Finally, our findings are also consistent with the prediction that the dynamics of sex-biased gene expression during development differ greatly between holometabolous and hemimetabolous insect species. As this is the first study to examine sex-biased gene expression during development in a hemimetabolous insect it is unclear if the differences we describe will apply generally, however, we hope that our study will stimulate similar studies across a broad range of insect species.

METHODS

Sample collection and preservation

T. californicum eggs hatch in early winter. Upon hatching, insects moult several times before reaching maturity in late spring (Sandoval 1993). Developmental stages (especially adults and hatchlings) do not co-occur temporally, hence samples from different stages cannot be collected simultaneously. Adults (4 males, 4 females) and juveniles (4 males, 3 females) were collected in California (Saratoga County) in 2015 and 2016, respectively. They were fed with artificial medium for two days to prevent contamination with plant cells from the gut, and subsequently frozen at −80 °C. Hatchlings were obtained from the eggs laid by field-collected adults in 2015. Hatchlings were flash frozen and stored at −80 °C. Sexes cannot be distinguished morphologically at the hatchling stage, thus single individuals were extracted to allow for later identification of sex via genotyping (see below) and 5 male and 4 female hatchlings were used.

RNA extraction and sequencing

Individuals (whole-bodies) from all developmental stages were mechanically homogenized with beads (Sigmund Linder) in liquid nitrogen. We then added 900 ul Trizol (Life Technologies), followed by 180 ul chloroform and 350 ul ethanol. The aqueous layer was then transferred to RNeasy MinElute Columns (Qiagen). Upon RNA extraction, samples were treated with DNase Turbo Kit (Life Tech) following the manufacturer's protocol. Total RNA from the hatchlings was extracted with MagMaxTM Express Robot (AB Applied Biosystems) using a MagMAXTM-96 Total RNA Isolation Kit from Ambion (Life Technologies) following the manufacturer's protocol, but without DNAse at this step to preserve DNA for the sex determination of hatchlings via genotyping (see below). Following RNA extraction, hatchling samples were treated with DNase Turbo Kit (Life Tech) following the manufacturer's protocol. The quality and quantity of the extracted RNA was then measured using a NanoDrop and Bioanalyzer. Library preparations (one for each individual) were done using the Illumina TruSeq Stranded Total RNA kit, upon which samples were sequenced together in six lanes. Paired-end sequencing with a read length of 100 bp was done on a HiSeq2000 platform at the GTF (Genomic Technologies Facility, Centre of Integrative Genomics, Lausanne, Switzerland).

Hatchling sex identification

To identify the sex of *T. californicum* hatchlings, we developed microsatellite markers on the *T. californicum* X chromosome scaffolds reported by Parker et al. (2022). *Timema* have an XX/X0 sex determination system (Schwander and Crespi 2009) meaning X-linked regions will be present in two copies in females and one copy in males. Consequently, females can feature heterozygous genotypes for polymorphic X-linked markers, while males are invariably hemizygous. Candidate microsatellite markers were designed with msatcommander (v. 1.08, default options) (Faircloth 2008). A selection of four candidate markers were tested for polymorphism and sex-linkage using 15 adult males and 15 adult females in two Multiplex PCR Kit reactions (Qiagen; see Supplementary Table 1 for primer sequences and Supplementary Table 2 for PCR conditions). Microsatellite alleles were then determined with an ABI3100 machine (Applied Biosystem) and Genemapper v.4.1 (Currie-Fraser et al. 2010). Across microsatellite markers, all 15 tested females were heterozygous at minimum two markers, whereas males were invariably hemizygous at all markers, confirming the predictions for *Timema* X-linked markers (Supplementary Table 2). We thus genotyped the nine hatchlings at the four microsatellite markers to identify their sex, and were able to identify four females and five males that were used for the transcriptome study (Supplementary Table 2).

Raw data quality control, mapping and read counting

The quality of the reads was checked using FastQC v.0.11.2 (Andrews 2010). We used Cutadapt v. 2.3 with Python v. 3.5.2 (Martin 2011) to remove adapter sequences. Low quality bases at both ends of the reads were trimmed when below a Phred score of 10. Bases with an average Phred score below 20 in a 4 bp sliding window were trimmed. Finally, reads with a length below 80 bp were removed with Trimmomatic v. 0.36 (Bolger et al. 2014). Trimmed reads were then mapped to the reference *T. californicum* genome from (Jaron et al. 2022) using STAR v. 2.6.0c (Dobin et al. 2013). HTSeq v.0.9.1 (Anders et al. 2014) was used to count the number of reads uniquely mapped to each gene, with the following options (htseq-count -f bam -r name -s reverse -t gene -i ID -m union –nonunique none).

Drosophila melanogaster data

D. melanogaster RNA-seq whole body data from Ingleby et al. (2016) was downloaded from SRA (accession number SRP068235). To mirror the data available for *Timema* and to facilitate comparisons, four replicates per sex and three developmental stages from different hemiclonal lines were used. A complete list of samples is provided in the supplementary materials (Supplementary Table 3). Although reads were deposited as paired-end, we found that most of them were unpaired, thus we used only the forward reads for analysis. Reads were trimmed, mapped to the reference genome (FlyBase, r6.23) (Gramates et al. 2017) and counted using the methods described above.

Differential gene expression analysis

Differential expression between the sexes was performed using edgeR v.3.16.5 (McCarthy et al. 2012; Robinson et al. 2009) in RStudio v.1.2.501 (Team 2019). This analysis fits a generalized linear model following a negative binomial distribution to the expression data and calculates a *p* value associated with the hypothesis that gene counts are similar between experimental groups. EdgeR implements a normalization method (trimmed mean of M values, TMM) to account for composition bias. We analyzed data separately for each developmental stage. We filtered out genes with low counts; we required a gene to be expressed in a majority of male or female libraries dependent on the number of replicates per sex (i.e., a minimum three libraries when replicate number is ≥4, two libraries when replicate number is =3), with expression level >0.5 CPM (counts per million). To test for differential gene expression between the sexes, we used a generalized linear model with a quasi-likelihood F- test, with contrasts for each stage between females and males (Chen et al. 2016). To correct for multiple testing, we applied the Benjamini–Hochberg method (Benjamini and Hochberg 1995) with an alpha of 5%. Genes with significantly higher expression in males were considered as male-biased, genes with significantly higher expression in females as female-biased, and the genes without significant differential expression between sexes as unbiased. To identify genes showing a significant sex by developmental stage interaction we used a similar GLM modeling approach but with all stages included. We used SuperExactTest v.0.99.4 (Wang et al. 2015) to test if the overlap of sex-biased genes between the three developmental stages was greater than what is expected by chance. To visualize the overlap of sex-biased genes between developmental stages we used VennDiagram v.1.6.20 (Chen and Boutros 2011). We visualized the $\log_2$FC sex-biased gene expression across developmental stages, using pheatmap v.1.0.12 (Kolde 2018). We tested the Spearman's correlation of sex-bias ($\log_2$FC) between the developmental stages, using cor.test from the R package stats v 4.1.1. To describe the increases in the number of sex-biased genes during development, we calculated the effect sizes for each of the two proportions of neighboring developmental stages, using the pwr v. 1.3-0 (Cohen 1988).

Stage specific gene expression

Median gene expression (CPM) values were calculated for each developmental stage and sex. These values were used to calculate Tau, an index of gene expression specificity during development (Liu and Robinson-Rechavi 2018; Yanai et al. 2004). Values of Tau range from zero (broadly expressed during development) to one (gene expressed in only one stage). Tau is generally used to quantify the tissue-specificity of gene expression (Yanai et al. 2004). Here we applied the same principle and formula to calculate stage specificity. To visualize the results, we made boxplots using ggplot2 v. 3.3.2 (Wickham 2016).

Divergence rates

We calculated values of sequence divergence rates (dN/dS) along the branch leading to *T. californicum* after the split with *T. poppensis* as described in (Jaron et al. 2022). Briefly, branch-site models with rate variation at the DNA level (Davydov et al. 2019) were run using the Godon software (https://bitbucket.org/Davydov/godon/, version 2020-02-17, option BSG –ncat 4) for each gene with an ortholog found in at least 6 species of *Timema* (including *T. poppensis*). Godon estimates the proportion of sites evolving under purifying selection (p0), neutrality (p1), and positive selection. We used only sites evolving under purifying selection or neutrality to calculate dN/dS. To test for differences in sequence divergence rates (dN/dS) between different gene categories (female-biased, male-biased and un-biased), we used Wilcoxon tests (ggpubr v.0.2.5, in R) with *p* values adjusted for multiple comparisons using the Benjamini–Hochberg method (Haynes 2013). Note that some of the *T. californicum* sex-biased genes had no identified ortholog in other *Timema* species, thus we do not have sequence evolution rates for all sex-biased genes.

Furthermore, we used a partial correlation between the strength of the sex bias ($\log_2$FC) and the sequence divergence rate (dN/dS) on sex-biased genes only, while controlling for the average expression level (CPM) of the gene, and GC- content (ppcor v.01 (Kim 2015), in R) in order to determine if genes with higher $\log_2$FC values have faster sequence divergence rates. Per gene GC content was calculated for the coding sequences from the *T. californicum* genome.

Functional analysis of sex-biased genes

We performed Gene Ontology (GO) enrichment analysis using TopGO v.2.26.0 (Alexa and Rahnenfuhrer 2010) on sex-biased genes obtained with EdgeR (see above) at each developmental stage. We used a functional annotation derived from blasting sequences to *Drosophila melanogaster* database. Only GO terms with minimum ten annotated genes were used. Enrichment of terms was determined using a weighted Kolmogorov–Smirnov-like statistical test, equivalent to the gene set enrichment analysis (GSEA method). We applied the "elim" algorithm, which considers the Gene Ontology hierarchy, i.e., it first assesses the most specific GO terms, and then more general ones (Alexa et al. 2006). Our analysis focused on gene sets in the Biological Processes (BP) GO category. We considered terms as significant when $p < 0.05$. Enriched GO terms were then semantically clustered using ReviGO (Supek et al. 2011) to aid interpretation.

RESULTS

Sex-biased gene expression increases during development in *T. californicum*

Sex-biased gene expression gradually increased during the three developmental stages, with 0.2% (26) of the expressed genes sex-biased at the hatchling stage, 4.7% (568) at the juvenile, and 20.3% (2485) at the adult stage (Fig. 2). There are significantly

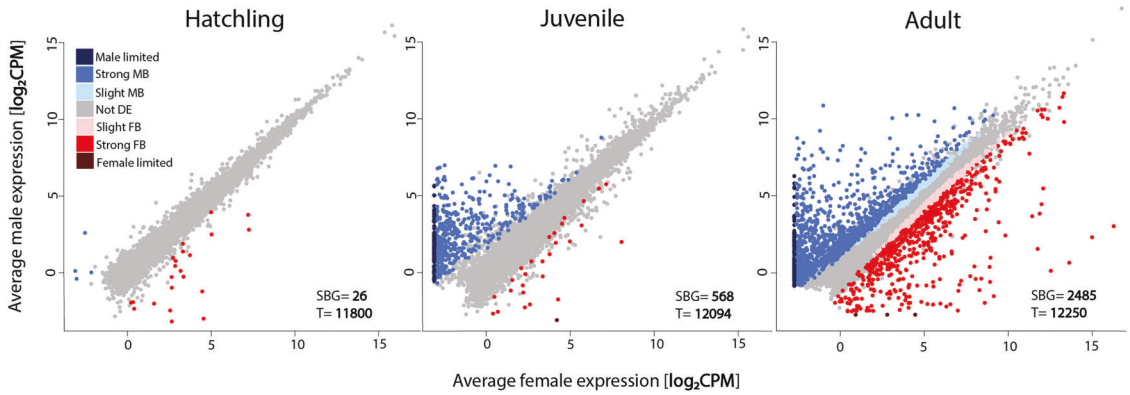

Fig. 2 Gene expression (log_2CPM) in *T. californicum* males and females at the hatchling (left), juvenile (middle) and adult stage (right). The number of differentially expressed genes (SBG) is shown at the bottom right corner of each plot, as well as the total number of expressed genes at each stage (T). Genes are classified based on their sex-bias into seven categories: "slight FB"- female bias (<2 FC), "strong FB"- female bias (>2 FC), "female limited"- with no expression in males, "slight MB"- male bias (<2 FC), "strong MB"- male bias (>2 FC), "male limited"- no expression in females, "Not DE"- not differentially expressed genes.

fewer sex-biased genes both at the hatchling stage compared to the juvenile stage ($x^2_{(1)} = 498.11$, $p_{adj.} = 2.2 \times 10^{-16}$) and at the juvenile compared to the adult stage ($x^2_{(1)} = 1347$, $p_{adj.} = 2.2 \times 10^{-16}$). In addition, the two effect sizes are similar; $h_{(hatchling\text{-}juvenile)} = 0.34$, $h_{(juvenile\text{-}adult)} = 0.49$ (Cohen 1988), supporting a gradual rather than abrupt increase. The hatchling stage had more female than male biased genes ($x^2_{(1)} = 11.13$, $p = 0.0004$), while the juvenile and adult stages had more male biased genes ($x^2_{juvenile\ (1)} = 467.1$, $x^2_{adult\ (1)} = 85.915$, $p < 2.2 \times 10^{-16}$) (Supplementary Table 4). All except one of the sex-biased genes at the two preadult stages had strong sex-bias (>2 FC), while at the adult stage 77% had strong sex-bias (>2 FC) (Fig. 2, see also Supplementary Table 4 and Fig. 8). The intensity of sex-bias varied greatly during development, with 1137 genes showing a significant sex by development interaction.

To characterize the dynamics of sex-biased expression during development, we then classified the 2671 genes which are sex-biased at one or more developmental stages into 13 categories, dependent on their expression patterns during development (Supplementary Fig. 1). This classification showed that sex-biased genes are added gradually during development, with genes sex-biased at earlier stages generally remaining sex-biased in the same direction at later stages (Supplementary Figs. 1 and 2). Only a single gene shifted from male-biased to female-biased expression (Supplementary Fig. 1). Out of 26 sex-biased genes at the hatchling stage, 18 (69%) were also significantly sex-biased in at least one of the later stages, with 9 (35%) remaining sex-biased throughout development (Fig. 3), while out of 568 sex-biased genes at the juvenile stage, 390 (69%) stayed sex-biased at the adult stage (Fig. 3). This classification is conservative, as it depends on the sex-biased gene expression detection threshold, meaning sex-biased gene expression may be missed in some stages, inflating the number of differences we see. This is supported by the fact that only around 65% of genes that are sex-biased in two stages show a significant sex by development stage interaction (Supplementary Table 8, also see Supplementary Fig. 1). Furthermore, the fold changes of sex-biased genes were strongly correlated between all developmental stages ($\rho = 0.75$–0.9 Supplementary Fig. 3).

Sex-biased genes at the hatchling stage are particularly interesting because they reveal sexual differentiation prior to visible morphological differences. We therefore looked for functional annotations of the 26 genes sex-biased at the hatchling stage in the *T. californicum* reference genome (Jaron et al. 2022). However, only 16 out of the 26 sex-biased genes had functional annotations and only one (vitellogenin receptor) had a clear link to sexual differentiation (Fig. 3b). While key genes known to play a role in insect sex-determination and differentiation pathways (*doublesex*, *transformer-2* and *sex-lethal*) were expressed at the hatchling stage, *doublesex* had very low expression, preventing analysis of sex-bias, and *transformer-2* and *sex-lethal* did not feature sex-biased expression.

Sex-biased genes are enriched for development-related processes

Genes sex-biased at the hatchling stage were enriched for GO-terms related to developmental processes (e.g., "regulation of cell development", "regulation of cell proliferation", "cuticle development"), and GO-terms related to female specific functions such as oogenesis ("oocyte construction", "oocyte development") (Supplementary Fig. 5a and Supplementary Table 10). At the juvenile stage, sex-biased genes were enriched for GO-terms related to metabolic processes, in particular to catabolism (e.g., "lipid catabolic processes", "cellular catabolic processes", "regulation of catabolic processes") (Supplementary Fig. 5b and Supplementary Table 11). At the adult stage, sex-biased genes were enriched for GO-terms related to diverse metabolic and physiological processes with no clear association to sexual differentiation (Supplementary Fig. 5c and Supplementary Table 12); however, several terms were related to chemosensory and olfactory behavior, which may play a role in mate detection. Furthermore, sex-biased genes at the adult stage were enriched for pigmentation (e.g., "developmental pigmentation", "eye pigmentation"), which is a sexually dimorphic trait in *T. californicum* (Sandoval 2008).

Sex-biased genes have more stage-specific expression

Expression levels of sex-biased genes tend to be specific to only one developmental stage while unbiased genes have a more constant expression level across development (Fig. 4, Supplementary Fig. 4). Male-biased genes have the most stage specific expression in both males and females. Female-biased genes are only slightly more stage specific than un-biased genes, but the trend is consistent and the difference is significant notably in both male and female adults.

Sex-biased genes have faster sequence evolution rates

Male-biased genes have faster rates of sequence evolution (dN/dS) compared to both un-biased and female-biased genes, at juvenile and adult stages (Fig. 5). Female-biased genes do not evolve significantly faster than un-biased genes, at any of the three developmental stages.

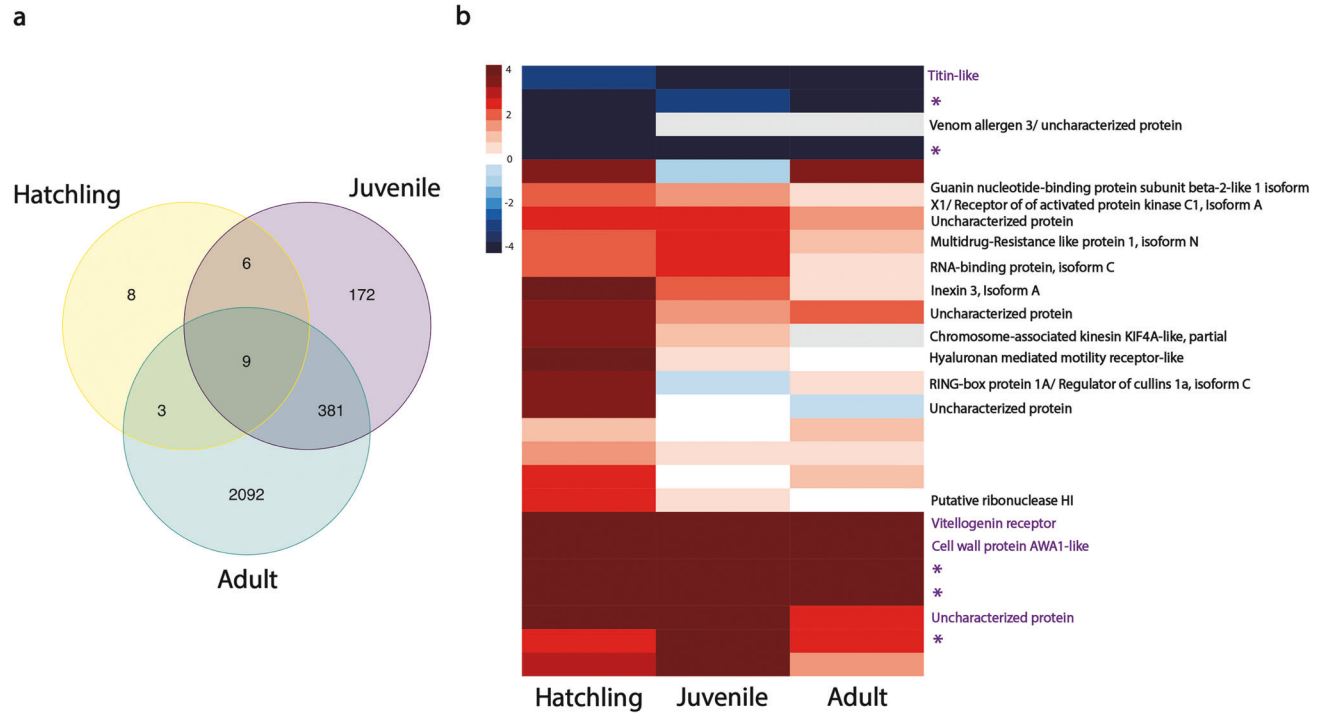

Fig. 3 Sex-biased genes shared across development. a Venn-diagram of sex-biased genes in three developmental stages: hatchling (yellow), juvenile (purple), and adult (green). The number of genes shared between all three stages was greater than expected by chance (observed overlap = 9, expected overlap = 0.21, Exact test of multi set interactions: $P_{adj.} = 5 \times 10^{-13}$). Note that all pairwise overlaps also contained more genes than expected by chance (detailed results in Supplementary Table 7). **b** A heatmap showing the 26 sex-biased genes at the hatchling stage with their annotations and their expression in three developmental stages. Genes in red are female-biased, blue are male-biased. Saturation of the colors increases with the $\log_2$FC. Genes without a label have no annotation, annotation in purple is for genes that were sex-biased in all three stages.

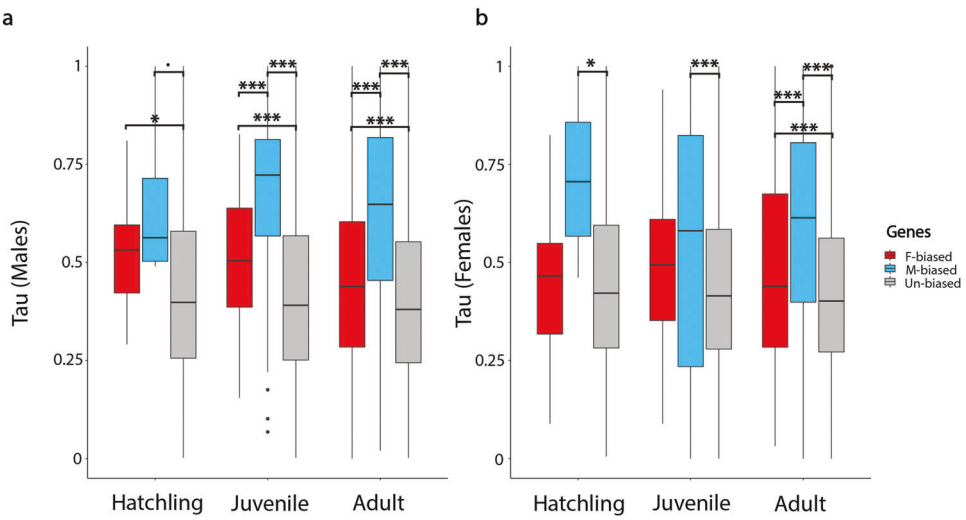

Fig. 4 Developmental gene expression specificity in *T. californicum*. Tau index of gene expression at three developmental stages in males (**a**) and females (**b**). Tau ranges from zero (similarly expressed during development) to one (gene expressed in only one stage). Three gene categories are depicted with different colors; female-biased in red, male-biased in blue, and un-biased in gray. Boxplots represent the median, lower and upper quartiles, and whiskers the minimum and maximum values (in the limit of 1.5× interquartile range). Adjusted p values of Wilcoxon rank sum tests are summarized above the box plots (***$p < 0.001$, *$p < 0.05$, $p = 0.06$).

We performed partial correlation analyses to test the effect of sex bias strength on sequence evolutionary rate, controlling for the average expression level of the gene, and GC-content (Supplementary Table 6). For both male-biased and female-biased genes, stronger sex-bias is associated with faster sequence evolution at the adult stage (Fig. 6). Partial correlations are not significant at juvenile or hatchling stages.

Sex-biased gene expression increases abruptly in adult *D. melanogaster*

In order to compare the dynamics of sex-biased gene expression during development between hemimetabolous and holometabolous insects, we reanalyzed publicly available data from *D. melanogaster* (Ingleby et al. 2016), using the same pipeline as for *T. californicum*. This experiment was chosen for comparison as it has a similar design,

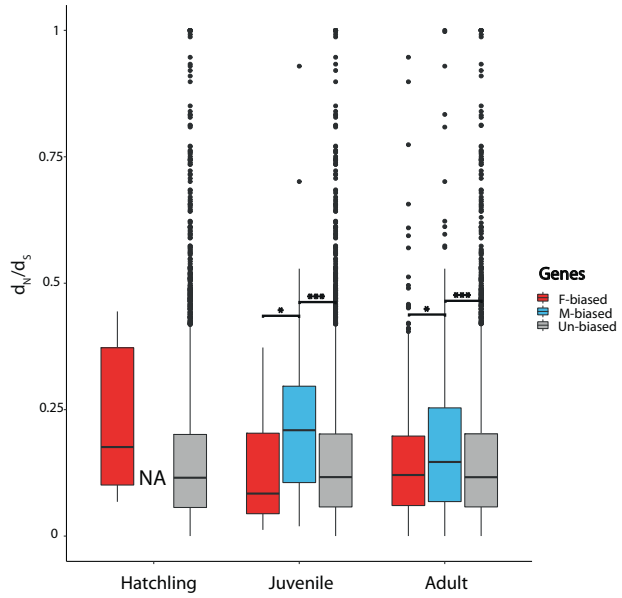

Fig. 5 Divergence rates (the ratio of nonsynonymous to synonymous substitutions, dN/dS), at three developmental stages; hatchling, juvenile and adult stage. Boxplots represent the median, lower and upper quartiles, and whiskers the minimum and maximum values (in the limit of 1.5× interquartile range). Adjusted *p* values of Wilcoxon rank sum tests are summarized above the box plots (***$p < 0.001$, *$p < 0.05$). Note that the four male-biased genes at the hatchling stage had no identified ortholog in other *Timema* species and therefore no associated dN/dS value.

i.e., whole-body RNA-seq data from several developmental stages. In addition, although *D. melanogaster* from this experiment were lab-reared, they had a similar between sample variance as *T. californicum* (biological coefficient of variation at the adult stage: *D. melanogaster* = 0.274, *T. californicum* = 0.348).

In contrast to the gradual increase in the amount of sex-biased expression during development observed in *T. californicum*, sex-biased gene expression increased abruptly at the adult stage in *D. melanogaster* (Figs. 7 and 8), from 22 to 84% of sex-biased genes (20 to 69% restricting to >2 FC) (Fig. 8). There were significantly fewer sex-biased genes both at the larval compared to the pupal stage ($\chi^2_{(1)} = 19.445$, $p_{adj.} = 5.18 \times 10^{-6}$) and at the pupal compared to the adult stage ($x^2_{(1)} = 9607.2$, $p_{adj.} = 4.40 \times 10^{-16}$). The two effect sizes were very different, with a more extensive shift from pupa to adult ($h_{larva\text{-}pupa} = 0.06$, $h_{pupa\text{-}adult} = 1.35$) supporting the abrupt increase. Moreover, adult *D. melanogaster* had a significantly larger proportion of sex-biased genes than *T. californicum* ($x^2_{(1)} = 10061$, $p < 2.2 \times 10^{-16}$). Overall, at each developmental stage, there were more male than female-biased genes (Supplementary Table 5). The majority of sex-biased genes had a strong sex bias at every developmental stage (>2 FC: 83, 94 and 82%, in larval, pupal, and adult stage, respectively) (Supplementary Table 5). Out of 2113 sex-biased genes at the larval stage, 1262 (60%) were significantly sex-biased in at least one of the later stages, with 1226 (58%) remaining sex-biased throughout development (Fig. 7b), while out of 2643 sex-biased genes at the pupal stage, 2423 (92%) stayed sex-biased at the adult stage (Fig. 7b). The fold changes of sex-biased genes were also low to moderately correlated between larvae and pupae or adults (ρ = 0.30 and 0.69; Supplementary Fig. 3) but strongly correlated between pupae and adults (ρ = 0.85; Supplementary Fig. 3).

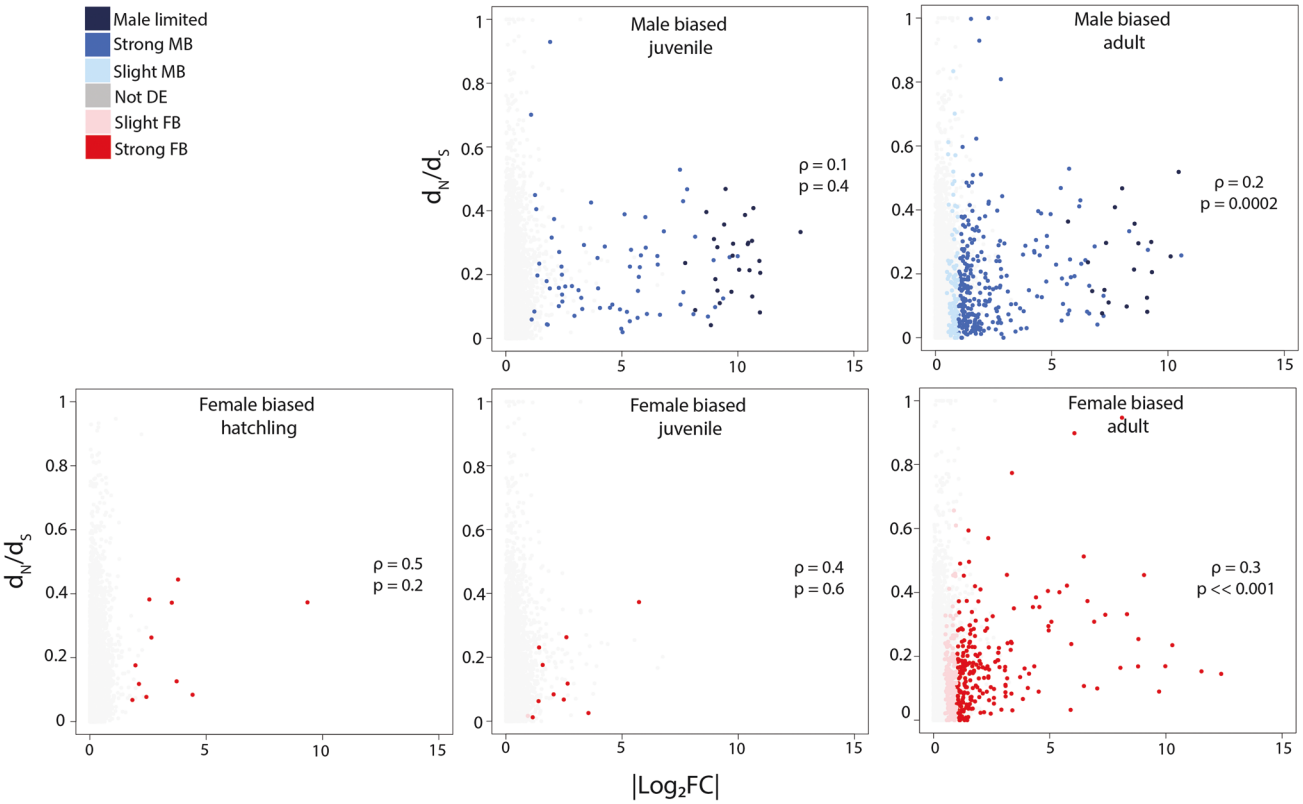

Fig. 6 Partial Spearman's rank correlations between the divergence rate of genes, dN/dS, and their strength of the sex bias $|\log_2 FC|$ at three developmental stages. Note that all genes are displayed on each plot but only male- respectively female-biased ones are used for correlation tests. Adjusted *p* values and partial correlation coefficients are shown in each plot.

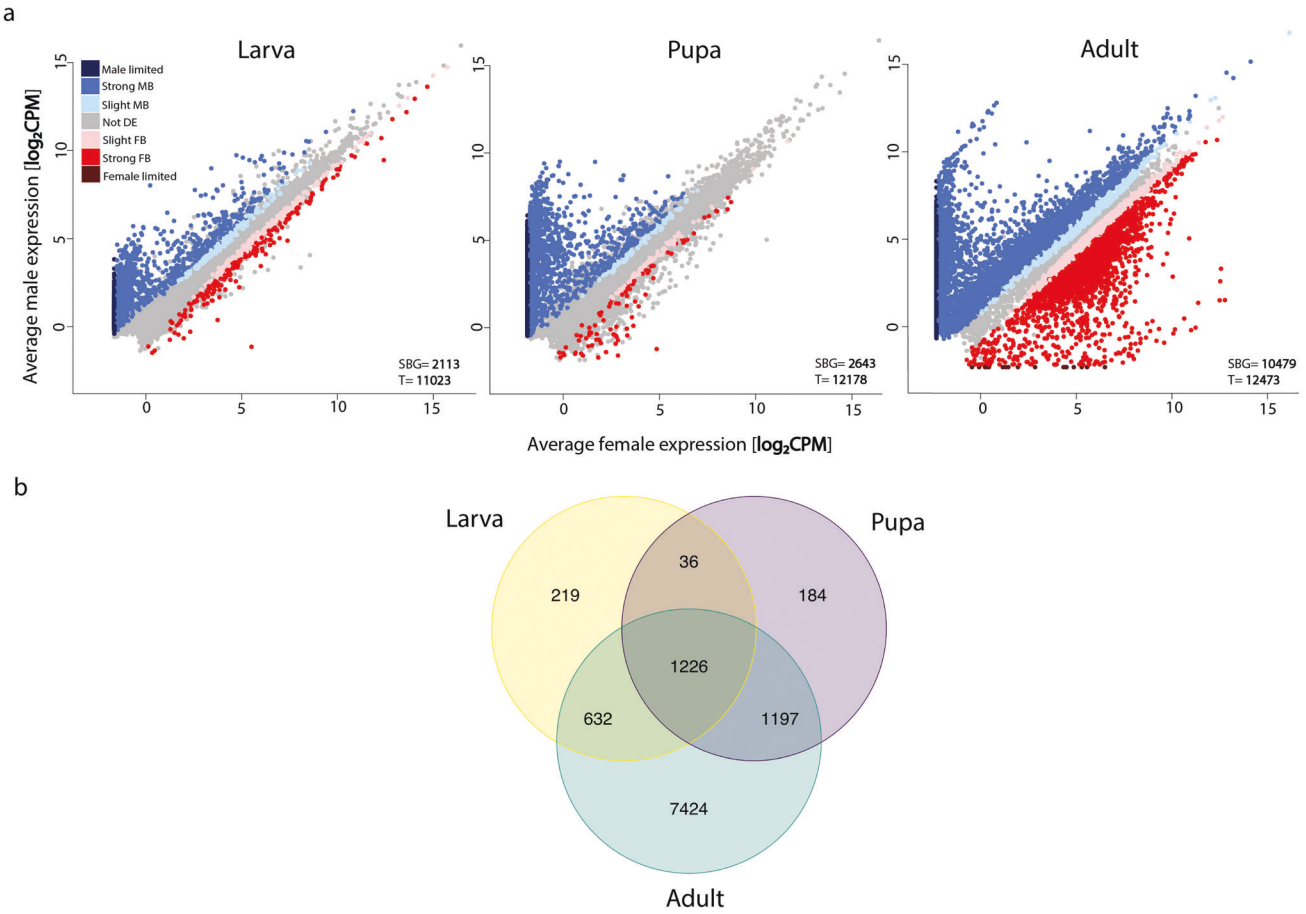

Fig. 7 Comparison of male and female gene expression in D. melanogaster. a Gene expression(log_2 CPM) in males and females at the larval (left), pupal (middle) and adult stage (right). The number of differentially expressed genes (SBG) is shown at bottom right corner of each plot, as well as the total number of expressed genes at each stage (T). Genes are classified based on their sex-bias into seven categories: "slight FB"- female bias (<2 FC), "strong FB"- female bias (>2 FC), "female limited"- with no expression in males, "slight MB"- male bias (<2 FC), "strong MB"- male bias (>2 FC), "male limited"- no expression in females, "Not DE"- not differentially expressed genes. **b** Venn-diagram of sex-biased genes in three developmental stages: larval (yellow), pupal (purple), and adult (green). The number of genes shared between all three stages was greater than expected by chance (observed overlap = 1226, expected overlap = 334.7), Exact test of multi set intersections: p value ≈ 0).

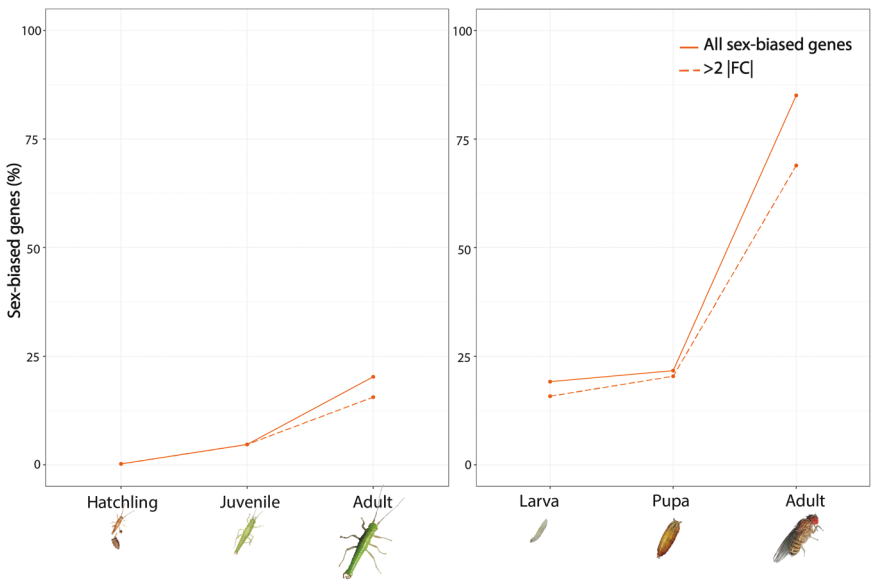

Fig. 8 Percentage of sex-biased genes (SBG) in *T. californicum* (left panel) and *D. melanogaster* (right panel) at three developmental stages. Note that the immature developmental stages in the two species are not homologous but serve to illustrate the gradual versus abrupt increase in sex-biased gene expression in adults.

DISCUSSION

In the stick insect *T. californicum*, gene expression differs between males and females before morphological sexual dimorphism. During development, most of the sex-biased genes are added gradually and cumulatively, meaning that once a gene gains sex-biased expression in *T. californicum*, it generally remains sex-biased at later developmental stages. In addition, genes were consistent in their sex-bias direction; only a single gene shifted from male- to female-biased expression. Surprisingly, such a gradual and consistent addition of sex-bias does not appear to be a general pattern over animal development. For example, in humans and mosquitos, some stages have bursts of sex-biased gene expression, suggesting that specific developmental stages contribute discretely to sexual differentiation, and that sexual phenotypes are not gradually established (Magnusson et al. 2011; Shi et al. 2016).

Although only 26 genes were sex-biased in *T. californicum* at the hatchling stage, they all had a strong sex-bias and nine of them stayed significantly sex-biased at both the juvenile and adult stages. As such these 26 genes likely represent key genes involved in the sexual differentiation of *Timema*. Most of the sex-biased genes at the hatchling stage were female-biased. This might suggest that the process of building a female phenotype begins earlier in development than the one of building a male phenotype. Later developmental stages had more male-biased than female- biased genes. A similar shift from female- to male-bias in gene expression during development was found in *Nasonia* jewel wasps, where little male-biased expression was detected until the pupal stage, during the activation of spermatogenesis. Similar to *Timema*, the shift was interpreted as a different developmental timing of the two sexes (Rago et al. 2020). In *Timema*, male-biased genes were also expressed in a relatively stage-specific manner, in contrast to a more constant expression of female-biased genes. This further supports the idea that *Timema* individuals first develop along the female trajectory, i.e., that the female phenotype is the "default" in *Timema*, and may indicate greater pleiotropy of female-biased genes. Additional support for this interpretation comes from the lower sequence divergence rates of female-biased than male-biased genes, implicating stronger selective constraints on female- than male-biased genes. In addition, we observed that genes with greater sex-bias have faster sequence divergence rates. This is largely due to relaxed purifying selection, with positive selection contributing little to the accelerated evolutionary rate of sex-biased genes. These findings are consistent with the idea that sex-biased genes evolve from genes with few evolutionary constraints and that are relatively "dispensable" (Catalan et al. 2018; Mank and Ellegren 2009).

Sex-biased genes in *Timema* hatchlings were enriched for processes related to oogenesis. Moreover, one of the most consistently and strongly female-biased genes across development was annotated as vitellogenin receptor. In insects, vitellogenin receptor transfers yolk protein precursors into the oocytes and is necessary for oocyte and early embryo development (Cho and Raikhel 2001; Raikhel and Dhadialla 1992). The role of these processes in *Timema* hatchlings remain to be investigated, but vitellogenin receptor expression may indicate a very early onset of oocyte development in *Timema*, consistent with studies in other stick insects (Taddei et al. 1992). Sex-biased genes in juvenile and adult stages were not enriched for processes obviously related to sexual traits. However, some processes such as pigmentation and chemosensory/olfactory behavior could have a sex-related role. Pigmentation is a sexually dimorphic trait in *Timema* (Sandoval 2008), while chemosensory and olfactory behaviors are important for mate recognition and mating (Nosil et al. 2007; Schwander et al. 2013). We also checked the expression of two key genes involved in insect sex-determination pathways: *transformer* and *doublesex*. In holometabolous insects, *transformer* acts as a splicing regulator of *doublesex*, a sex differentiation master switch gene (Geuverink and Beukeboom 2014). The *doublesex-transformer* role in sex-differentiation is conserved among Diptera, Coleoptera and Hymenoptera (Verhulst et al. 2010; Wexler et al. 2019), and likely play the same role in sex differentiation in hemimetabolous insects (Zhuo et al. 2018; Wexler et al. 2019). In *T. californicum*, we found that *doublesex* was expressed in all three developmental stages, but its expression was too low to examine sex-bias. *Transformer* is not annotated in the available *T. californicum* genome; a *transformer-2* homolog is annotated but did not feature sex-bias at any of the three developmental stages. As such, whether or not these classic sex-determining genes influence sexual differentiation in *Timema* is unclear, and requires future studies.

We hypothesized that the dynamics of sex biased gene expression would be strongly affected by hemimetabolous vs holometabolous development in insects, with a gradual increase of sex-biased gene expression during development in the former and an abrupt increase at the adult stage in the latter. Hemimetabolous insects such as *T. californicum* have multiple nymphal stages that progressively resemble the adult stage, together with a gradual increase in sexual dimorphism. On the other hand, a holometabolous insect like *D. melanogaster* has more monomorphic larval stages and pupae, with no resemblance to the sexually dimorphic adult stage. The change in sexually dimorphic gene expression across development indeed mirrored these different developmental patterns, with the proportion of sex-biased genes increasing gradually in *T. californicum* as sexual dimorphism became more pronounced, whereas sexually dimorphic gene expression increased abruptly at the adult stage in *D. melanogaster*. Whether this pattern holds generally for other species of hemi- and holometabolous species is unclear as our study examined only one species from each developmental type. Thus, any generalizations will have to await further data from a broader range of species.

Although the change in sexually dimorphic gene expression across development fits with our expectations, we were surprised to find a much higher proportion of sex-biased genes in *D. melanogaster* than in *T. californicum* overall. This difference is clearest at the adult stage when most of the expressed genes in *D. melanogaster* were sex-biased (84%), compared to only 20% in *T. californicum*. Similar to *Drosophila*, other holometabolous insects also featured sex-bias for more than half of the genes expressed at the adult stage (Baker et al. 2011; Rago et al. 2020), while all studied hemimetabolous insects had a much smaller proportion of sex-biased genes (< 10%) (Pal and Vicoso 2015). Why there is such a difference in the prevalence of sex-biased genes between species with different developmental strategies is still an open question. One potential explanation is that the proportion of sex-biased genes at the adult stage may be less constrained under holo- than hemimetabolous development. For example, the complete reorganization of cells and tissues during metamorphosis in holometabolous insects may allow for more drastic phenotypic changes between the sexes, while incomplete metamorphosis constrains the evolution of distinct sexual phenotypes. Data on additional species and specific tissues rather than whole bodies are required to confirm that this difference is a general phenomenon and not simply due idiosyncrasies of the few species yet investigated. Holometabolous insects studied are often established lab-models, with high fecundity, and may thus be characterized by comparatively large gonads, which would result in large proportions of sex-biased genes in adults. By contrast, all hemimetabolous insects studied for sex-biased expression are non-model species. However, the choice of model species is unlikely to be the sole explanation for the different amount of sex bias in holo- and hemimetabolous species. Indeed, in the cricket *Gryllus bimaculatus* and in *Timema* stick insects, even the most sexually differentiated tissue (gonads) feature sex-bias of

fewer than 30% of genes (Parker et al. 2019; Whittle et al. 2020), suggesting that extensive differences are not completely driven by large gonads. Finally, while whole body analysis such as we have performed here provides a window into ontogeny, it will necessarily miss tissue specific regulation of sex-biased gene expression (Montgomery and Mank 2016). Future studies should therefore study sex-biased gene expression during development by examining a panel of different tissues or cell types.

Overall, our results describe the dynamics of sex-biased gene expression during development in a hemimetabolous insect. Generating sexually dimorphic phenotypes is a developmental process, and we show that dynamics of sex-biased gene expression mirror this development with sex-biased genes being added gradually during development, and with the majority of genes sex-biased at early stages remaining sex-biased in later stages.

DATA AVAILABILITY

Data are available online: *Timema californicum* raw reads have been deposited in SRA under PRJNA678950 bioproject, with accession codes SRR13084978-SRR13085001 (Supplementary Table 9). *Timema californicum* mapped read counts are provided in Supplementary Table 13 and fold changes in Supplementary Table 14. *Drosophila melanogaster* mapped read counts are provided in Supplementary Table 15.

REFERENCES

Alexa A, Rahnenfuhrer J (2010) topGO: enrichment analysis for gene ontology. R package version 2.26.0.

Alexa A, Rahnenführer J, Lengauer T (2006) Improved scoring of functional groups from gene expression data by decorrelating GO graph structure. Bioinformatics 22(13):1600–1607

Anders S, Pyl PT, Huber W (2014) HTSeq—a Python framework to work with high-throughput sequencing data. Bioinformatics 31(2):166–169

Andrews S (2010) FastQC: A Quality Control Tool for High Throughput Sequence Data [Online]. Available online at: http://www.bioinformatics.babraham.ac.uk/projects/fastqc/

Baker DA, Nolan T, Fischer B, Pinder A, Crisanti AA, Russell S (2011) A comprehensive gene expression atlas of sex- and tissue- specificity in the malaria vector, *Anopheles gambiae*. BMC Genom 12(296):12

Benjamini Y, Hochberg Y (1995) Controlling the false discovery rate: a practical and powerful approach to multiple testing. J R Stat Soc 57(1):289–300

Bolger AM, Lohse M, Usadel B (2014) Trimmomatic: a flexible trimmer for Illumina sequence data. Bioinformatics 30(15):2114–2120

Catalan A, Macias-Munoz A, Briscoe AD (2018) Evolution of sex-biased gene expression and dosage compensation in the eye and brain of *Heliconius* butterflies. Mol Biol Evol 35(9):2120–2134

Chen H, Boutros PC (2011) VennDiagram: a package for the generation of highly-customizable Venn and Euler diagrams in R. BMC Bioinforma 12(1):35

Chen S, Yang P, Jiang F, Wei Y, Ma Z, Kang L (2010) De novo analysis of transcriptome dynamics in the migratory locust during the development of phase traits. PLoS one 5(12):e15633

Chen Y, Lun AT, Smyth GK (2016) From reads to genes to pathways: differential expression analysis of RNA-Seq experiments using Rsubread and the edgeR quasi-likelihood pipeline. F1000Res 5:1438

Cho K-H, Raikhel AS (2001) Organization and developmental expression of the mosquito vitellogenin receptor gene. Insect Mol Biol 10(5):465–474

Cohen J (1988) Statistical power analysis Jbr the behavioral. Sciences Hillsdale (NJ): Lawrence Erlbaum Associates: 18–74.

Currie-Fraser E, Shah P, True S (2010) Data analysis using GeneMapper® v4.1: comparing the newest generation of GeneMapper software to legacy Genescan® and Genotyper® Software. J Biomol Tech 21(3 Suppl):S31–S31

Davydov II, Salamin N, Robinson-Rechavi M (2019) Large-scale comparative analysis of codon models accounting for protein and nucleotide selection. Mol Biol Evol 36(6):1316–1332

Dobin A, Davis CA, Schlesinger F, Drenkow J, Zaleski C, Jha S et al. (2013) STAR: ultrafast universal RNA-seq aligner. Bioinformatics 29(1):15–21

Ellegren H, Parsch J (2007) The evolution of sex-biased genes and sex-biased gene expression. Nat Rev Genet 8(9):689–698

Faircloth BC (2008) Msatcommander: detection of microsatellite repeat arrays and automated, locus-specific primer design. Mol Ecol Resour 8(1):92–94

Geuverink E, Beukeboom LW (2014) Phylogenetic distribution and evolutionary dynamics of the sex determination genes *doublesex* and *transformer* in Insects. Sex Dev 8(1-3):38–49

Gramates LS, Marygold SJ, Santos GD, Urbano JM, Antonazzo G, Matthews BB et al. (2017) FlyBase at 25: looking to the future. Nucleic Acids Res 45(D1):D663–D671

Grath S, Parsch J (2012) Rate of amino acid substitution is influenced by the degree and conservation of male-biased transcription over 50 myr of *Drosophila* evolution. Genome Biol Evol 4(3):346–359

Hale MC, Xu P, Scardina J, Wheeler PA, Thorgaard GH, Nichols KM (2011) Differential gene expression in male and female rainbow trout embryos prior to the onset of gross morphological differentiation of the gonads. BMC Genom 12(1):404

Haynes W (2013) "Benjamini–Hochberg method". In: Dubitzky W, Wolkenhauer O, Cho K-H, Yokota H (eds) Encyclopedia of Systems Biology. Springer New York, New York, NY, p 78–78

Ingleby FC, Ilona F, Morrow EH (2015) Sex-biased gene expression and sexual conflict throughout development. Cold Spring Harb Lab Press 7:a017632

Ingleby FC, Webster CL, Pennell TM, Flis I, Morrow EH (2016) Sex-biased gene expression in *Drosophila melanogaster* is constrained by ontogeny and genetic architecture. bioRxiv https://www.biorxiv.org/content/10.1101/034728v1.abstract

Jaron KS, Parker DJ, Anselmetti Y, Van PT, Bast J, Dumas Z et al. (2022) Convergent consequences of parthenogenesis on stick insect genomes. Sci Adv 8(8):eabg3842

Khila A, Abouheif E, Rowe L (2012) Function, developmental genetics, and fitness consequences of a sexually antagonistic trait. Science 336(6081):585–589

Kim S (2015) ppcor: an R package for a fast calculation to semi-partial correlation coefficients. Commun Stat Appl Methods 22(6):665–674

Kolde R (2018) *Pheatmap: Pretty Heatmaps*, R package version 1.0.12

Lande R (1980) Sexual dimorphism, sexual selection, and adaptation in polygenic characters. Evolution 34(2):292–305

Liu J, Robinson-Rechavi M (2018) Developmental constraints on genome evolution in four bilaterian model species. Genome Biol Evol 10(9):2266–2277

Lowe R, Gemma C, Rakyan VK, Holland ML (2015) Sexually dimorphic gene expression emerges with embryonic genome activation and is dynamic throughout development. BMC genomics 16(1):295

Magnusson K, Mendes AM, Windbichler N, Papathanos PA, Nolan T, Dottorini T et al. (2011) Transcription regulation of sex-biased genes during ontogeny in the malaria vector *Anopheles gambiae*. PLoS One 6(6):e21572

Mank JE (2017) The transcriptional architecture of phenotypic dimorphism. Nat Ecol Evol 1(1):6

Mank JE, Ellegren H (2009) Are sex-biased genes more dispensable? Biol Lett 5 (3):409–412

Mank JE, Nam K, Brunstrom B, Ellegren H (2010) Ontogenetic complexity of sexual dimorphism and sex-specific selection. Mol Biol Evol 27(7):1570–1578

Martin M (2011) Cutadapt removes adapter sequences from high-throughput sequencing reads. EMBnet J 17(1):10–12

McCarthy DJ, Chen Y, Smyth GK (2012) Differential expression analysis of multifactor RNA-Seq experiments with respect to biological variation. Nucleic Acids Res 40 (10):4288–4297

Montgomery SH, Mank JE (2016) Inferring regulatory change from gene expression: the confounding effects of tissue scaling. Mol Ecol 25(20):5114–5128

Nosil P, Crespi BJ, Gries R, Gries G (2007) Natural selection and divergence in mate preference during speciation. Genetica 129(3):309

Pal A, Vicoso B (2015) The X chromosome of hemipteran insects: conservation, dosage compensation and sex-biased expression. Genome Biol Evol 7 (12):3259–3268

Paris M, Villalta JE, Eisen MB, Lott SE (2015) Sex bias and maternal contribution to gene expression divergence in *Drosophila* blastoderm Embryos. PLOS Genet 11 (10):e1005592

Parker DJ, Bast J, Jalvingh K, Dumas Z, Robinson-Rechavi M, Schwander T (2019) Sex-biased gene expression is repeatedly masculinized in asexual females. Nat Commun 10(1):4638

Parker DJ, Jaron KS, Dumas Z, Robinson-Rechavi M, Schwander T (2022) X chromosomes show relaxed selection and complete somatic dosage compensation across Timema stick insect species. bioRxiv https://www.biorxiv.org/content/10.1101/2021.11.28.470265v2

Perry JC, Harrison PW, Mank JE (2014) The ontogeny and evolution of sex-biased gene expression in *Drosophila melanogaster*. Mol Biol Evol 31(5):1206–1219

Rago A, Werren JH, Colbourne JK (2020) Sex biased expression and co-expression networks in development, using the hymenopteran *Nasonia vitripennis*. PLoS Genet 16(1):e1008518

Raikhel A, Dhadialla T (1992) Accumulation of yolk proteins in insect oocytes. Annu Rev Entomol 37(1):217–251

Robinson MD, McCarthy DJ, Smyth GK (2009) edgeR: a bioconductor package for differential expression analysis of digital gene expression data. Bioinformatics 26(1):139–140

Sandoval CP (1993). Geographic, ecological and behavioral factors affecting spatial variation in color or morphfrequency in the walking-stick. *Timema cristinae*. Ph.D. diss. Univ. of California, Santa Barbara, CA

Sandoval CP (2008) Differential visual predation on morphs of *Timema cristinae* (Phasmatodeae:Timemidae) and its consequences for host range. Biol J Linn Soc 52(4):341–356

Schwander T, Crespi BJ (2009) Multiple direct transitions from sexual reproduction to apomictic parthenogenesis in *Timema* stick insects. Evolution 63(1):84–103

Schwander T, Crespi JB, Gries R, Gries G (2013) Neutral and selection-driven decay of sexual traits in asexual stick insects. Proc R Soc B Biol Sci 280(1764):20130823

Shi L, Zhang Z, Su B (2016) Sex biased gene expression profiling of human brains at major developmental stages. Sci Rep 6:21181

Supek F, Bosnjak M, Skunca N, Smuc T (2011) REVIGO summarizes and visualizes long lists of gene ontology terms. PLoS One 6(7):e21800

Taddei C, Chicca M, Maurizii MG, Scali V (1992) The germarium of panoistic ovarioles of *Bacillus rossius* (Insecta Phasmatodea): Larval differentiation. Invertebr Reprod Dev 21(1):47–56

Team 2019 R (2019) RStudio: integrated development environment for R. Boston, MA 770(394):165–171. http://www.rstudio.com/

Verhulst EC, van de Zande L, Beukeboom LW (2010) Insect sex determination: it all evolves around *transformer*. Curr Opin Genet Dev 20(4):376–383

Vickery VR, Sandoval CP (2001) Descriptions of three new species of *Timema* (Phasmatoptera: Timematodea: Timematidae) and notes on three other species. *Journal of Orthoptera*. Research 10(1):53–61

Wang M, Zhao Y, Zhang B (2015) Efficient test and visualization of multi-set intersections. Sci Rep 5:16923

Weigmann K, Klapper R, Strasser T, Rickert C, Technau G, Jäckle H et al. (2003) FlyMove- a new way to look at development of *Drosophila*. Trends Genet 19 (6):310–311

Wexler J, Delaney EK, Belles X, Schal C, Wada-Katsumata A, Amicucci MJ et al. (2019) Hemimetabolous insects elucidate the origin of sexual development via alternative splicing. eLife 8:e47490

Whittle CA, Kulkarni A, Extavour CG (2020) Sex-biased genes expressed in the cricket brain evolve rapidly. bioRxiv https://www.biorxiv.org/content/10.1101/2020.07.07.192039v2.full

Wickham H (2016) ggplot2: elegant graphics for data analysis. Springer-Verlag, New York, NY

Yanai I, Benjamin H, Shmoish M, Chalifa-Caspi V, Shklar M, Ophir R et al. (2004) Genome-wide midrange transcription profiles reveal expression level relationships in human tissue specification. Bioinformatics 21(5):650–659

Zhao M, Zha X-F, Liu J, Zhang W-J, He N-J, Cheng D-J et al. (2011) Global expression profile of silkworm genes from larval to pupal stages: toward a comprehensive understanding of sexual differences. Insect Sci 18(6):607–618

Zhuo J-C, Hu Q-L, Zhang H-H, Zhang M-Q, Jo SB, Zhang C-X (2018) Identification and functional analysis of the doublesex gene in the sexual development of a hemimetabolous insect, the brown planthopper. Insect Biochem Mol Biol. 102: 31–42

ACKNOWLEDGEMENTS

This study was supported by Swiss National Science Foundation Grant 31003A_182495. Version 6 of this preprint has been peer-reviewed and recommended by Peer Community In Evolutionary Biology (https://doi.org/10.24072/pci.evolbiol.100135).

AUTHOR CONTRIBUTIONS

JD, DJP, TS, and MRR designed the study. JD conducted the analyses, with input from DJP, TS and MRR. JD curated the data. ZD conducted the lab work with assistance of JD. JD wrote the manuscript with DJP and TS, with input from all authors.

FUNDING

Open access funding provided by University of Lausanne.

COMPETING INTERESTS

TS and MRR are recommenders for PCI. The authors declare no competing interests.

ADDITIONAL INFORMATION

Supplementary information The online version contains supplementary material available at https://doi.org/10.1038/s41437-022-00536-y.

Correspondence and requests for materials should be addressed to Jelisaveta Djordjevic or Darren James Parker.

Reprints and permission information is available at http://www.nature.com/reprints

Publisher's note Springer Nature remains neutral with regard to jurisdictional claims in published maps and institutional affiliations.

Chapter 2

Unresolved sexual conflict during early development in the stick insect *Timema poppense*?

Jelisaveta Djordjevic[1], Darren J Parker[2], Marjorie Labédan[1], Tanja Schwander[1]

[1]Department of Ecology and Evolution, University of Lausanne, 1015 Lausanne.

[2]School of Natural Sciences, Brambell Building, Bangor University, Bangor, LL57 2UW, United Kingdom.

Corresponding authors: jelisaveta.djordjevic@unil.ch; tanja.schwander@unil.ch

Manuscript in preparation

Abstract

Males and females experience divergent selective pressures for certain traits, due to different fitness optima in each sex for those traits. When trait changes increase fitness in one sex but lower the fitness in opposite sex, sexual conflict arises. When sexual conflict occurs over gene expression levels, sex-biased expression of genes emerges and resolves or partially resolves such conflicts. Despite predictions that sexual conflict, and therefore sex-biased gene expression, is most prominent in the adult stage, when sexual dimorphism is fully expressed, little is known about the dynamics of sexual conflict and sex-biased gene expression throughout development and across tissues. In this study, we investigated tissue-specific sex-biased gene expression across post-embryonic development, from one-day-old hatchlings to the adult stage, in two closely related *Timema* stick insect species with sexual (*T. poppense*) or parthenogenetic reproduction (*T. douglasi*). In parthenogenetic species where male phenotypes are absent, sexual conflict is eliminated, such that genes that were previously under conflict in sexual species may shift their expression levels towards a female optimum. Our findings reveal extensive differences in the amount of sex-biased gene expression across developmental stages and between somatic and reproductive tissues. Somatic tissues have low sex-bias overall with a small increase at the adult stage, while reproductive tissue have extensive sex-biased gene expression from the first instar and throughout development until the adult stage. Notably, sexual and parthenogenetic females exhibit the greatest differences at the earliest developmental stages (in all tissues), with reproductive tracts showing the largest proportion of differentially expressed genes. Half of the latter are also sex-biased in sexual species in the first instar and we observe feminization and demasculinization patterns of sex-biased genes in parthenogenetic species, suggesting a situation of unresolved sexual conflict early in the development of the reproductive tissue. Our results show that sexual conflict and sex biased gene expression vary strikingly across development and tissues and that unresolved conflicts may be confined to specific developmental stages of tissues with strongly sex-specific functions.

Introduction

Males and females have often diverged fitness optima for traits, leading to opposing selective pressures on these traits in the two sexes (Arnqvist and Rowe 2005). This is known as sexual antagonism, or sexual conflict (Ellegren and Parsch 2007). In the case of gene expression levels, such conflict over optimal expression levels can drive the evolution of sex-biased genes. These genes are characterized by different levels of expression in the two sexes, and would thus reflect resolved or partially resolved sexual conflict over gene expression levels (Parsch and Ellegren 2013).

Although sexual conflict is predicted to be the strongest at the adult stage (Chippindale, et al. 2001; Rice and Chippindale 2001; Cox and Calsbeek 2009) when sexual dimorphism is completely manifested, little is known about how sexual conflict and sex-biased gene expression vary over ontogeny. Recent studies suggest that sex-biased gene expression is dynamic during development, and the extent of the bias depends on the analyzed tissue (Ingleby, et al. 2015). Thus, in *Timema* stick insects and *Nasonia* wasps, analyses of whole bodies show a general increase in sex-bias during development, mirroring the gradual increase of morphological sexual dimorphism (Rago, et al. 2020; Djordjevic, et al. 2022). Reproductive tracts in *Drosophila melanogaster* flies have a consistent sex-bias of approximately half of the genes from 3rd instar larvae to the adult stage (Perry, et al. 2014), while mammalian somatic organs show little sex-bias during development with an increase around sexual maturity (Rodríguez-Montes, et al. 2023). These findings suggest that resolved but perhaps also unresolved sexual conflict over optimal gene expression is present during development, and that its extent varies depending on the levels of sexual dimorphism of tissue functions.

Two recent studies, one in *Timema* stick insects and one in *Artemia* brine shrimp, probed for the presence of unresolved conflicts over gene expression levels by studying how genes with sex biased expression change in expression patterns upon the loss of sex in parthenogenetic species (Parker, et al. 2019; Huylmans, et al. 2021). Since the male phenotype is not produced in parthenogenetic species, sexual conflict is eliminated, thus genes that were under unresolved conflict over gene expression levels

in sexual species should shift their expression levels toward the female optimum. However, contrary to the predictions of having feminized expression in parthenogenetic females due to relaxed sexually antagonistic selection, parthenogenetic females were masculinized in both studies, i.e. had reduced expression of female-biased and greater expression of male-biased genes. In the stick insects, this was explained as most likely the result of the decay of female sexual traits, rather than the release of intralocus sexual conflict, while masculinization was a general trend in brine shrimp in both sexual and parthenogenetic species. However, because both studies focused on adults only it remains possible that conflict occurs earlier in development and that different trajectories of sex-biased genes expression would be observed in pre-adult stages in parthenogenetic females.

Here we examine the developmental gene expression patterns in two closely related stick insect species, *Timema poppense* and *T. douglasi*. *T. poppense* reproduces sexually, whereas *T. douglasi* reproduces parthenogenetically (Schwander, et al. 2013). In *Timema,* there are no sex-specific genome regions (XX:XO sex determination; Schwander and Crespi, 2009), meaning that differences between sexes stem solely from differential gene expression and other regulatory changes. Using the two *Timema* species, we investigated in depth the dynamics of sex-biased gene expression across somatic tissues, including the brain, legs, guts, and antennas, as well in the reproductive tracts. We sequenced RNA from those tissues, across multiple developmental stages starting from the 1st nymphal until the adult stage, whereby the ontogeny of *Timema* males and females consists of six and seven distinct developmental stages, respectively. Firstly, we explore sex-biased gene expression within the sexual species, the consistency of sex-bias across development, genomic distribution of sex-biased genes, and gene networks associated with different tissues. This is followed by an examination of how sex-biased genes differ in expression between sexual and parthenogenetic females and whether we can identify instances of unresolved sexual conflict. Finally, we also provide a detailed gene expression comparison between sexual and parthenogenetic females, across tissues and development.

Material and Methods

Insect husbandry

First instars were derived from eggs laid by captive-bred individuals initially collected in California in 2017. Therefore, our primary objective was to acquire samples from five distinct tissues (reproductive tracts and four somatic tissues) for each of seven developmental stages in sexual and parthenogenetic females (nymphal stages 1-6 and adults) and six stages in sexual males (nymphal stages 1-5 and adults; see Supplemental Table S1).

Upon hatching, insects were reared in petri dishes containing *Ceanothus* plant cuttings enveloped in moist cotton. They were nurtured until they reached a specific developmental stage, at which point they were dissected upon molting. To track molting, we applied red acrylic paint to the thoraxes after each molt and checked daily for individuals lacking the paint. Prior to dissection, the insects were anesthetized using CO_2.

From each developmental stage, we dissected the brain, antennae, legs, and guts. Initially, we only dissected reproductive tracts from the 4th stage onwards, as we encountered difficulties in unequivocally identifying reproductive tissues in earlier stages. After enhancing our dissection techniques, we were able to identify and dissect gonad tissues at earlier stages, and consequently, we included reproductive tract samples from newly hatched individuals (1st nymphal stage) at a later date.

During the dissection process, tissues were carefully placed into Eppendorf tubes containing ceramic beads and rapidly flash-frozen before being stored at -80°C for approximately one-third of the dissections. For the remaining dissections, due to laboratory closures associated with the pandemic, tissues were preserved in RNA later (Qiagen) before being stored at -80°C. Finally, we did not obtain any adult females in this study and therefore used adult tissue samples from females collected from the same populations but which were dissected and sequenced for another project (Parker et al in prep). In total, we obtained one to four replicates per sex and tissue at every developmental stage as detailed in (Supplemental Table S1).

RNA extraction and sequencing

To each tissue-containing tube, 1 mL of TRIzol solution was added. Tissue homogenization was carried out using the Precellys Evolution tissue homogenizer (Bertin Technologies). Subsequently, 200 µL of chloroform was added to each sample, followed by vortexing for 15 seconds. The samples were then subjected to centrifugation at 12,000 revolutions per minute (rpm) at 4°C for 25 minutes. The upper phase, which contains the RNA, was transferred to a fresh 1.5 mL tube along with the addition of 650 µL isopropanol and 1 µL of Glycogen blue (GlycoBlue™ Coprecipitant). The samples were vortexed and placed at -20°C overnight. Samples were then centrifuged for 30 minutes at 12,000 rpm at 4°C. The liquid supernatants were removed, and the RNA pellet underwent two washes using 80% and 70% ethanol. Each wash was followed by a 5-minute centrifugation step at 12,000 rpm. Finally, the RNA pellet was resuspended in nuclease-free water and quantified using a fluorescent RNA-binding dye (QuantiFluor RNA System) and a nanodrop (DS-11 FX).

Library preparation using NEBNext (New England BioLabs) and sequencing on an Illumina NovaSeq 6000 platform with 100 bp paired-end sequencing (~45 million reads per sample on average) was outsourced to a sequencing facility (Fasteris, Geneva).

Quality control, mapping and counting

RNAseq reads were quality trimmed with trimmomatic (Bolger, et al. 2014) (v. 0.39, options: ILLUMINACLIP:AllIllumina-PEadapters.fa:3:25:6 LEADING:9 TRAILING:9 SLIDINGWINDOW:4:15). Any reads that were less than 80 bp long following trimming were discarded along with the corresponding read pair. Reads were then mapped to the *T. poppensis* genome from (Parker *et al*, in prep) with STAR (Dobin, et al. 2013) (v 2.7.8a) with default settings except for the addition of two-pass mapping (--twopassMode Basic). Read counts were then obtained using HTseq (Anders, et al. 2014) (v.011.2, options: --order=pos --type=exon --idattr=gene_id --stranded=reverse).

Differential gene expression analyses

We assessed differential gene expression between the sexes using edgeR v.3.42.4 (Robinson, et al. 2009; McCarthy, et al. 2012) in R Statistical Software v. 4.3.1 (Team 2023). The analyses employed a negative binomial distribution-based generalized linear model and TMM normalization to determine p-values for gene count similarities among experimental groups. Data were analyzed separately for each tissue at each developmental stage (and only if at least two replicates per sex were available for given stage and tissue, see Supplemental Table S1).

We filtered out genes with low counts, requiring a gene to be expressed in the majority of male or female libraries, dependent on the number of replicates per sex (i.e., at least three libraries for four or more replicates, and two libraries for three replicates), with an expression level above 0.5 CPM.

Differential gene expression between sexes was examined using a generalized linear model with a quasi-likelihood F-test (Chen, et al. 2016). Multiple testing was corrected using the Benjamini-Hochberg method (Benjamini and Hochberg 1995) with a 5% significance level. Genes with significantly higher expression in males were considered male-biased, genes with higher expression in females were labeled female-biased, and genes with no significant differential expression were categorized as unbiased. Genes were further classified into categories depending on the strength of bias into; slight (< 2 FC), strong (> 2 FC), or sex-limited (i.e., not expressed in opposite sex). To visualize the overlap of sex-biased genes between developmental stages we used ggVennDiagram by ggplot2 v.3.4.4 (Wickham 2016).

Because the X chromosome is hypothesized to be a hotspot for sexually antagonistic genes (Rice 1984; Gibson, et al. 2002) we further compared the proportion of sex-biased genes (i.e. male-biased and female-biased) on autosomes and on the X chromosome(s).

Gene Co-expression Networks

We conducted gene co-expression network analyses using the Weighted Gene Co-expression Network Analysis (WGCNA) (Langfelder and Horvath 2008). The dataset included all *T. poppense* samples (i.e. both sexes, all tissues and developmental stages). We removed genes that had less than 50 counts in

total across samples. Following the recommendations by the WGCNA tutorial, we normalized the expression across samples using the variance stabilizing function (vst) from deSeq2. We used hierarchical clustering to identify outlier samples, and excluded them for gene network building and modules identification (Supplemental Figure S7). Soft thresholding (power parameter set to 6) was applied to enhance the preservation of strong pairwise correlations. The co-expression networks were constructed with a focus on both positive and negative correlations among genes, considering negatively correlated nodes as not connected (signed network). Modules of highly interconnected genes were detected, ensuring a minimum module size of 30 genes. The dendrogram height for module merging was set at 0.25. The Topological Overlap Matrix (TOM) was computed and saved for subsequent analysis. We visualized modules association with traits (samples), by plotting a module eigengenes heatmap.

Functional enrichment analysis

We performed Gene Ontology (GO) enrichment analysis using TopGO v.2.54.0 (Alexa and Rahnenfuhrer 2023), on sex-biased genes identified with edgeR (as described earlier), as well as on genes associated with each module. Genes were functionally annotated by comparing the longest isoform of each gene to NCBI's nr *Drosophila melanogaster* database (taxa id: 7227) using BlastP via Blast2GO (Götz, et al. 2008) within OmicsBox (Bioinformatics 2019) (v.3.1.2) with default options. Interproscan (OmicsBox default settings) was then run and merged with the BLAST results to obtain GO terms. Node size was set to ten, indicating the inclusion of only GO terms with annotations for at least 10 genes. Term enrichment was assessed using a weighted Kolmogorov-Smirnov-like statistical test, equivalent to the gene set enrichment analysis (GSEA) method, which considers all genes without applying an arbitrary threshold (Alexa and Rahnenführer 2009). The "elim" algorithm was applied, considering the Gene Ontology hierarchy, prioritizing the assessment of the most specific GO terms before evaluating more general ones. Our analysis specifically focused on gene sets within the Biological Processes (BP) category of GO. Terms were deemed significant if the p-value was below 0.05.

Expression differences between sexual and parthenogenetic females

We called differential gene expression between sexual and parthenogenetic females as described above for males and females of the sexual species. Next, to investigate whether genes with sex-biased expression in the sexual species (*T. poppense*) exhibited increased or decreased expression levels in parthenogenetic females, we compared expression levels for those genes between sexual and parthenogenetic females. We only used tissues and developmental stages with at least 20 sex-biased genes for these comparisons and used Wilcoxon rank sum tests to compare genes categorized as female-biased and male-biased, relative to genes with no sex-bias. To account for multiple testing, we applied False Discovery Rate (FDR) correction to the p-values obtained.

A large fraction of gene expression differences between species are caused by drift and are unlikely to be functionally relevant (Whitehead and Crawford 2006; Catalán, et al. 2019). To investigate expression differences between sexual and parthenogenetic females with likely functional consequences, we assessed differential gene expression for the subset of genes in modules associated with specific tissues. We thus repeated differential gene expression analysis between sexual and parthenogenetic females in the reproductive tract, gut, brain, and antennae for the subset of genes found in modules associated with each of these tissues and quantified the fraction of genes in each module with significant expression differences.

Results

As expected, a PCA based on global RNA-seq data from the dissected *T. poppense* tissues clusters biological replicates by tissue, for both sexes and across all developmental stages (Supplemental Figure S1). Within reproductive tracts, male samples from the 2nd nymphal to the adult stages group together, and are distinct from samples stemming from 1st nymphal stage male and all female stages (Supplemental Figure S2). Somatic tissues do not separate by sex, but by developmental stage, and generally separate into three groups; 1st nymphal stage, all other nymphal stages and adult stages (Supplemental Figure S2).

Sex-biased gene expression

Somatic and reproductive tissues differ in their dynamics of sex-biased gene expression during development. Somatic tissues have few sex-biased genes across all developmental stages, generally with an increase at the adult stage (Figure 1). The brain has the lowest percentage of sex-biased genes, ranging between 0 and 0.02 % across development, and without an increase at the adult stage (Figure 1). In guts, the percentage of sex- biased gene expression ranges between 0 and 0.4%, and in legs between 0 and 0.5%. Antennae had the greatest sex-bias, with 10 % of genes being sex-biased at the adult stage. We further tested which biological processes sex-biased genes were enriched for. Sex-biased genes are enriched for metabolic processes associated with physiological and molecular roles of associated tissue (Supplemental Figure S3).

Because the X chromosome is expected to accumulate sexually-antagonistic genes (Rice 1984; Gibson, et al. 2002), we further examined the distribution of sex-biased genes on the X chromosome versus autosomes. In antennae from adults, the X is significantly enriched for female-biased (Fisher's exact test, padj < 0.01) and depleted for male-biased genes (Fisher's exact test, padj < 0.01). By contrast, in legs, the X is enriched for both female and male-biased genes at the 3rd nymphal stage (Fisher's exact test male-biased; padj.= 0.015, female-biased; padj.< 0.01). Sex-biased genes in the gut do not have a differential distribution between the X and autosomes, for neither male- or female-biased genes.

Reproductive tract

In the reproductive tract at the 1st nymphal stage, 5651 (44%) of the expressed genes show sex-biased expression, with 28% of them displaying strong sex bias, characterized by a fold change (FC) > 2 (adjusted p-value <0.05) (Figure 1). At the 4th nymphal stage, 6619 (45%) of the genes exhibit sex-biased expression, with 39% of them displaying strong sex bias (FC > 2) (adjusted p-value <0.05) (Figure 1). At the adult stage, 7748 (54%) of the genes are sex biased, with 46% of them exhibiting strong sex bias (FC > 2) (adjusted p-value <0.05).

At the 1st nymphal stage 24.2% of the sex-biased genes are female biased, whereas 20% are male-biased. In later stages, there are more male-biased genes compared to female-biased ones. Specifically, at the 4th nymphal stage, 25.4% are male-biased and 19.4% are female-biased. In the adult stage, this trend continues with 30% of male-biased genes and 23.4% of female-biased genes. The vast majority of male-biased and female-biased genes are stage specific (Figure 3). Only 278 (4%) male-biased genes remain male-biased in all three stages, while 748 (12%) remain female-biased (Figure 3).

We then examined the distribution of sex-bias on autosomes and the X chromosome, in order to test for the enrichment of sex-biased genes on the X (Figure 2 and Supplemental Figure S4). Because *T. poppense* males silence their X chromosome during meiosis in germ cells (Chapter 3), the majority of X-linked genes are female- biased, 62% at 4th nymphal and 66% at adult stage (Figure 2). At the first nymphal stage when X is not silenced in males (Chapter 3), we detect 12 % of genes on the X with male-bias and 29.5% female-biased. We find a significant enrichment of female-biased genes on X chromosome (Fisher's exact test, $p_{adj.} = 0.007$), and significant depletion of male-biased genes on the X (Fisher's exact test, $p_{adj.} < 0.01$) in the first nymphal stage.

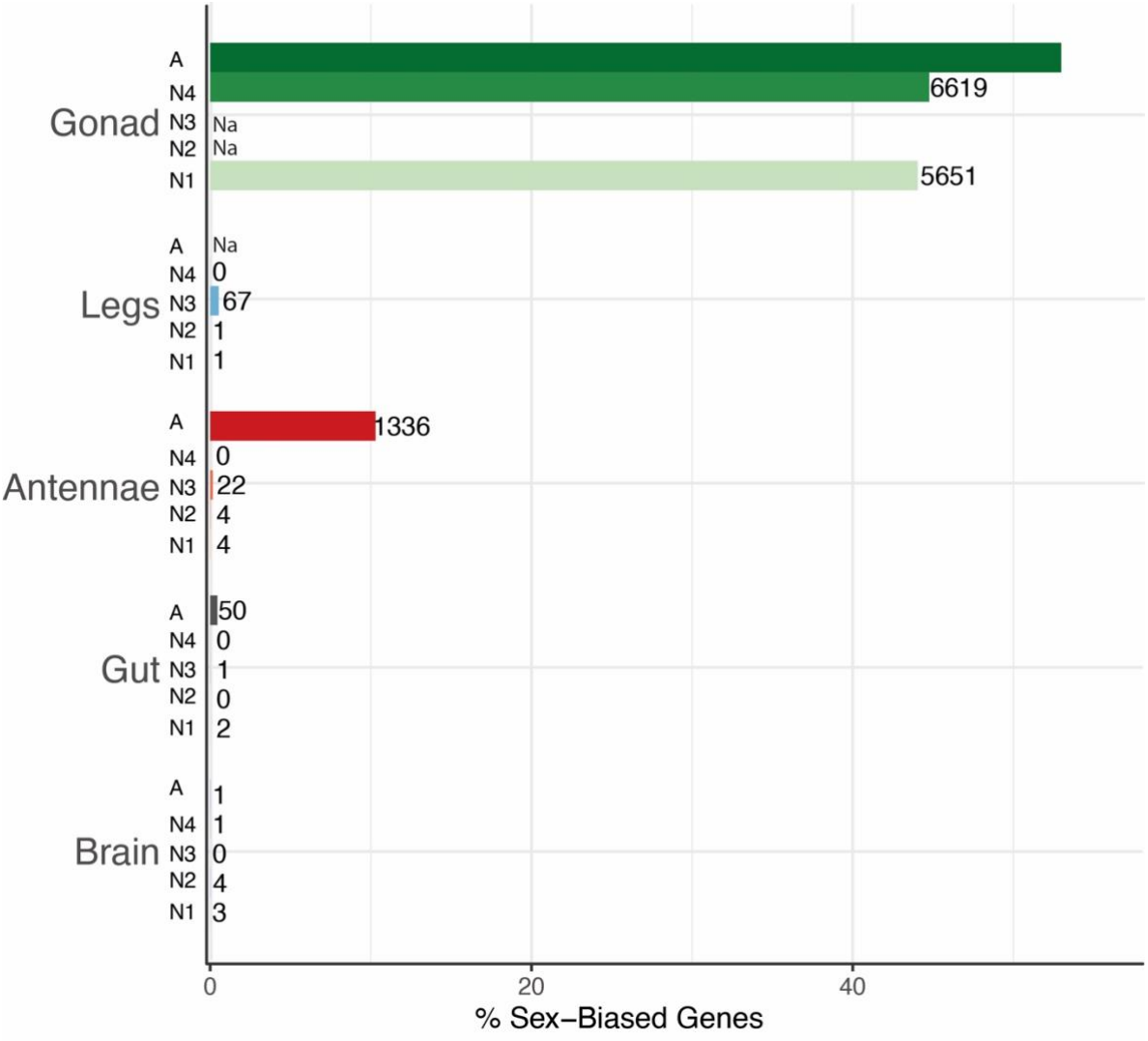

Figure 1. The percentage of sex-biased genes in somatic and reproductive tissues throughout development. The number of sex-biased genes is indicated next to each bar, with tissues color-coded (green-gonad, blue-legs, red-antennae, grey-gut, violet-brain) and shaded based on developmental stages from Nymphal stage 1 (N1) to Adult stage (A). The average number of expressed genes across tissues and developmental stages is 12,937 ± 824.35 (mean ± SD). Developmental stages are denoted as A (adult) and [N1-N4] (1st to 4th nymphal).

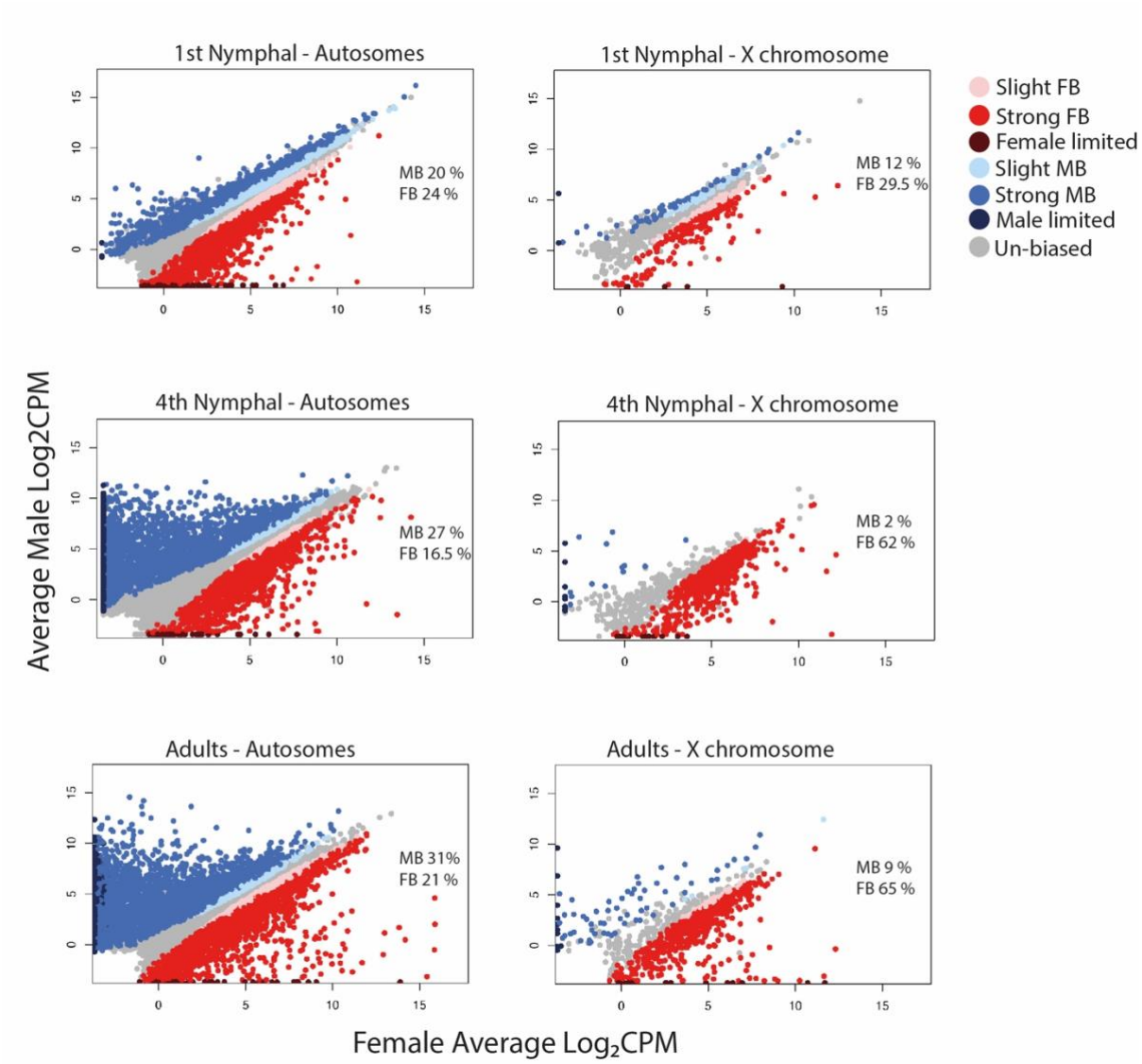

Figure 2. Sex-biased gene expression in the reproductive tract for three developmental stages. Panels on the left show expression on the autosomes, and right-side panels show expression on the X-chromosome. Genes are classified into categories depending on the strength of the sex-bias, slight female or male biased genes < 2 FC, strong female or male biased genes > 2 FC, female or male limited genes, have 0 expression the opposite sex, and un-biased genes are not significantly differentially expressed.

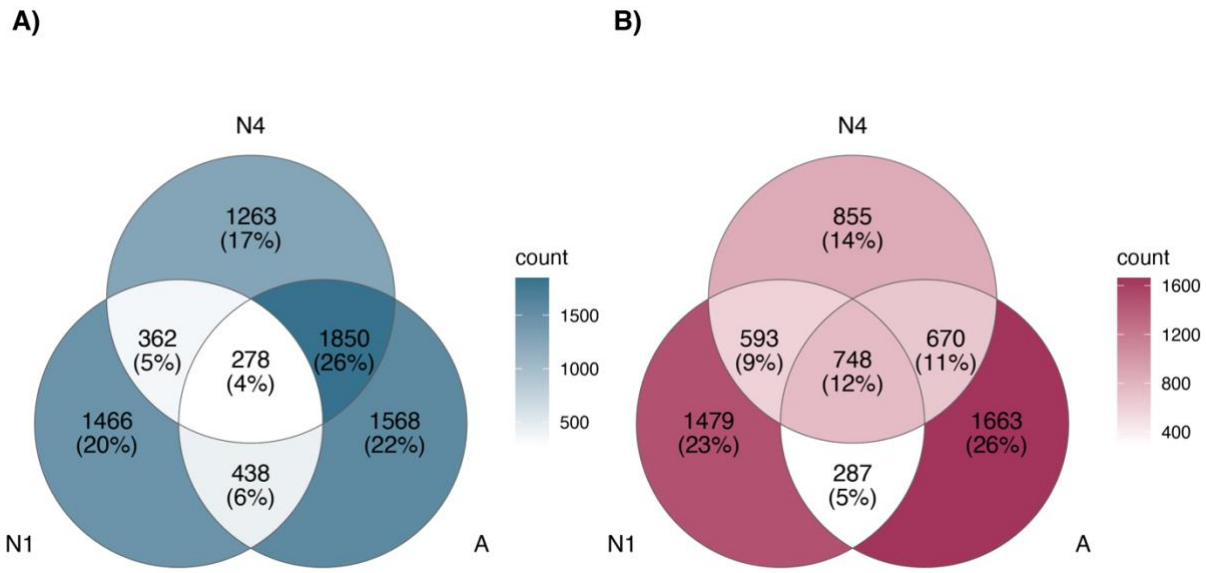

Figure 3. Venn diagrams showing the overlap of sex-biased genes from the reproductive tract between developmental stages A) Male-biased genes B) Female-biased genes

Gene networks and modules

A total of 20,176 genes, spanning developmental stages, somatic and reproductive tissues, and both sexes of *T. poppense*, were utilized to construct gene networks. In Figure 4, module-trait relationships are visualized through a module eigengenes heatmap, revealing 13 distinct modules, with varying sizes ranging from 33 to 4,065 genes. Eleven modules are associated with specific tissues (modules 3, 6, 7, 9: gonads, 2: gut, 1: brain, 10: antennae, 8: legs, 4,12: antennae and legs, 5: brain and gonad). Module 0 consists of genes that could not be clustered into any of the modules. Notably, Modules 7, 3, and 9 exhibit sex-specific associations, being linked to the female-adult reproductive tract, male reproductive tract (from the 4th nymphal stage onwards), and the male-adult reproductive tract, respectively. Module 12 is also linked to male-adult legs; however, it is worth noting that no samples from female-adult legs were available for analysis (see "insect husbandry" method section).

We further tested which biological processes the genes in each module were enriched for. The functional enrichment detected for each module supports the expected physiological and molecular roles of each tissue (Figure 5). For example, module 1, which is associated with brain samples (Figure

4), is enriched for “neuropeptide signaling pathway”, “neuron recognition”, and “neuromuscular synaptic transmission”. Module 2, associated with gut samples, is enriched for “transmembrane transport” and “metabolism of carbohydrates and proteins” (Figure 5).

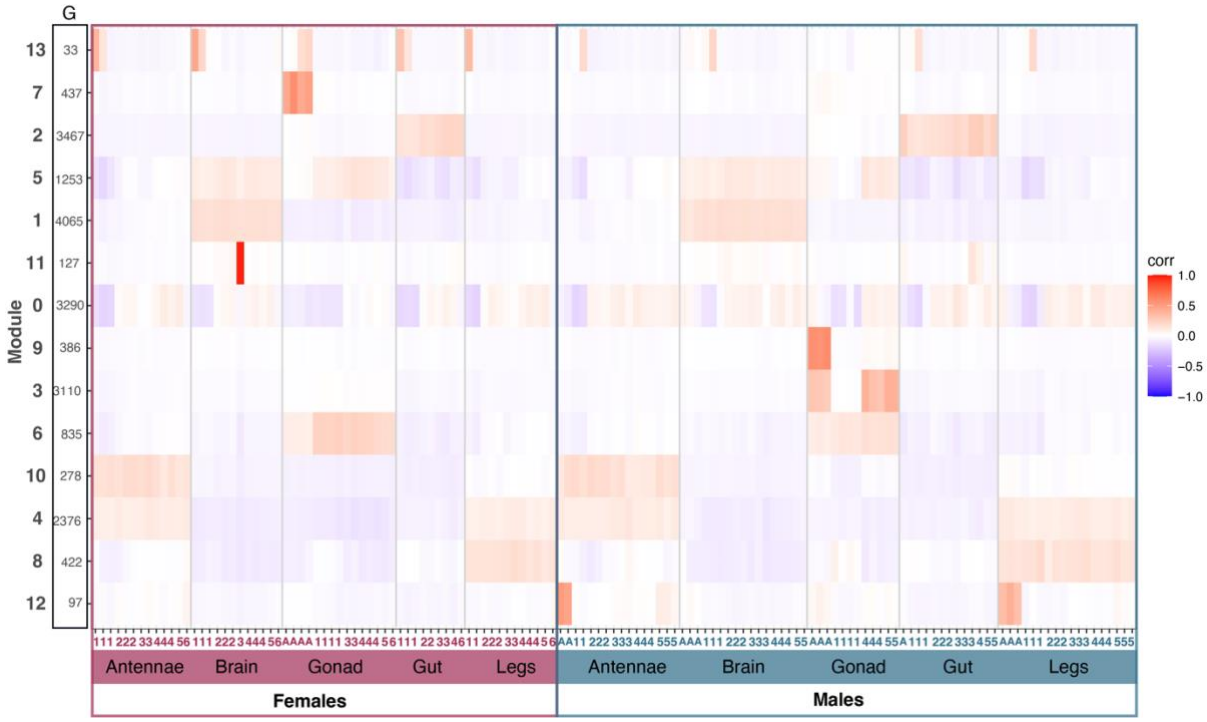

Figure 4. Module-tissue association heatmap of module eigengenes. Red shading depicts positive correlations, while blue shading depicts negative ones. Each row represents a module (labeled from 0-13), the column “G” shows the number of genes in each module. Each column is a sample, nymphal stages are marked with numbers from 1 to 6, and the adult stage with A. Light grey vertical lines separate tissues.

Module 1
GO:0007218 neuropeptide signaling pathway
GO:0045433 male courtship behavior, veined wing generated song production
GO:0019932 second-messenger-mediated signaling
GO:0016079 synaptic vesicle exocytosis
GO:0030154 cell differentiation
GO:0008038 neuron recognition
GO:1900073 regulation of neuromuscular synaptic transmission
GO:0051129 negative regulation of cellular component organization
GO:0042254 ribosome biogenesis
GO:0042391 regulation of membrane potential

Module 2
GO:0055085 transmembrane transport
GO:0005975 carbohydrate metabolic process
GO:0006508 proteolysis
GO:0097037 heme export
GO:0070588 calcium ion transmembrane transport
GO:0009615 response to virus
GO:0006826 iron ion transport
GO:0044281 small molecule metabolic process
GO:1901566 organonitrogen compound biosynthetic process
GO:0001700 embryonic development via the syncytial blastoderm

Module 3
GO:0003341 cilium movement
GO:0010996 response to auditory stimulus
GO:0000226 microtubule cytoskeleton organization
GO:0035356 intracellular triglyceride homeostasis
GO:0009615 response to virus
GO:0006919 activation of cysteine-type endopeptidase activity involved in apoptotic process
GO:0009612 response to mechanical stimulus
GO:0030011 maintenance of cell polarity
GO:0009744 response to sucrose
GO:0007005 mitochondrion organization

Module 4
GO:0040003 chitin-based cuticle development
GO:0006570 tyrosine metabolic process
GO:0009615 response to virus
GO:0048513 animal organ development
GO:0035336 long-chain fatty-acyl-CoA metabolic process
GO:0007591 molting cycle, chitin-based cuticle
GO:0008592 regulation of Toll signaling pathway
GO:0042335 cuticle development
GO:0048856 anatomical structure development
GO:0018958 phenol-containing compound metabolic process

Module 5
GO:0035356 intracellular triglyceride homeostasis
GO:0009408 response to heat
GO:0050896 response to stimulus
GO:0006357 regulation of transcription by RNA polymerase II
GO:0006302 double-strand break repair
GO:0007111 meiosis II cytokinesis
GO:0015074 DNA integration
GO:0031123 RNA 3'-end processing
GO:0006261 DNA-templated DNA replication
GO:0006139 nucleobase-containing compound metabolic process

Module 6
GO:0006364 rRNA processing
GO:0006261 DNA-templated DNA replication
GO:0009987 cellular process
GO:0022402 cell cycle process
GO:0006351 DNA-templated transcription
GO:0006974 cellular response to DNA damage stimulus
GO:0070925 organelle assembly
GO:0031570 DNA integrity checkpoint signaling
GO:0006325 chromatin organization
GO:0009880 embryonic pattern specification

Module 7
GO:0008610 lipid biosynthetic process
GO:0008202 steroid metabolic process
GO:0035336 long-chain fatty-acyl-CoA metabolic process
GO:0015074 DNA integration
GO:0009057 macromolecule catabolic process
GO:0009410 response to xenobiotic stimulus
GO:0006805 xenobiotic metabolic process
GO:0071466 cellular response to xenobiotic stimulus
GO:0006915 apoptotic process
GO:1901362 organic cyclic compound biosynthetic process

Module 8
GO:0051146 striated muscle cell differentiation
GO:0051050 positive regulation of transport
GO:0040003 chitin-based cuticle development
GO:0043408 regulation of MAPK cascade
GO:0009416 response to light stimulus
GO:0071214 cellular response to abiotic stimulus
GO:0007099 centriole replication
GO:0048646 anatomical structure formation involved in morphogenesis
GO:0030003 intracellular monoatomic cation homeostasis
GO:1902533 positive regulation of intracellular signal transduction

Module 9
GO:0006508 proteolysis
GO:0040018 positive regulation of multicellular organism growth
GO:0043266 regulation of potassium ion transport
GO:0045752 positive regulation of Toll signaling pathway
GO:0007586 digestion
GO:0009101 glycoprotein biosynthetic process
GO:0006486 protein glycosylation
GO:0043413 macromolecule glycosylation
GO:0070085 glycosylation
GO:0009100 glycoprotein metabolic process

Module 10
GO:0007610 behavior
GO:0050912 detection of chemical stimulus involved in sensory perception of taste
GO:0042742 defense response to bacterium
GO:0009615 response to virus
GO:0009260 ribonucleotide biosynthetic process
GO:0009141 nucleoside triphosphate metabolic process
GO:0006220 pyrimidine nucleotide metabolic process
GO:0006221 pyrimidine nucleotide biosynthetic process
GO:0016052 carbohydrate catabolic process
GO:0019637 organophosphate metabolic process

Module 11
GO:0006479 protein methylation
GO:0016482 cytosolic transport
GO:0016197 endosomal transport
GO:0007218 neuropeptide signaling pathway
GO:0022416 chaeta development
GO:0007186 G protein-coupled receptor signaling pathway
GO:0097659 nucleic acid-templated transcription
GO:0006351 DNA-templated transcription
GO:0032774 RNA biosynthetic process
GO:0040003 chitin-based cuticle development

Module 12
GO:0040003 chitin-based cuticle development
GO:0043252 sodium-independent organic anion transport
GO:0046552 photoreceptor cell fate commitment
GO:0007111 meiosis II cytokinesis
GO:0006629 lipid metabolic process
GO:0007498 mesoderm development
GO:0001752 compound eye photoreceptor fate commitment
GO:0042706 eye photoreceptor cell fate commitment

Module 13
GO:0035046 pronuclear migration
GO:0015980 energy derivation by oxidation of organic compounds
GO:0006091 generation of precursor metabolites and energy
GO:0016053 organic acid biosynthetic process
GO:0046394 carboxylic acid biosynthetic process
GO:0006310 DNA recombination
GO:0006631 fatty acid metabolic process
GO:0044283 small molecule biosynthetic process
GO:0032787 monocarboxylic acid metabolic process
GO:0044237 cellular metabolic process

Figure 5. Functional enrichment of genes associated with each module. A list of the 10 most significantly enriched GO terms is indicated. For every module, each GO term ID is followed by the description of the term.

Differential gene expression between sexual and parthenogenetic females

Sexual and parthenogenetic females generally feature strongly differentiated gene expression at the first nymphal and adult stages, and very similar expression throughout intermediate nymphal stages (Figure 6). This is the case for both somatic and reproductive tissues. Specifically, at the 1st nymphal stage, differential gene expression ranges between 13.4 and 39.6% for brain, gut, and reproductive tract, while legs and antennae have 0.8 and 0.4% of differentially expressed genes (DEG) respectively. Later nymphal stages feature very few DEGs, ranging between 0.1 and 1.2%. At the adult stage there is an increase with percentages of DEGs between 3.2 and 17.2%.

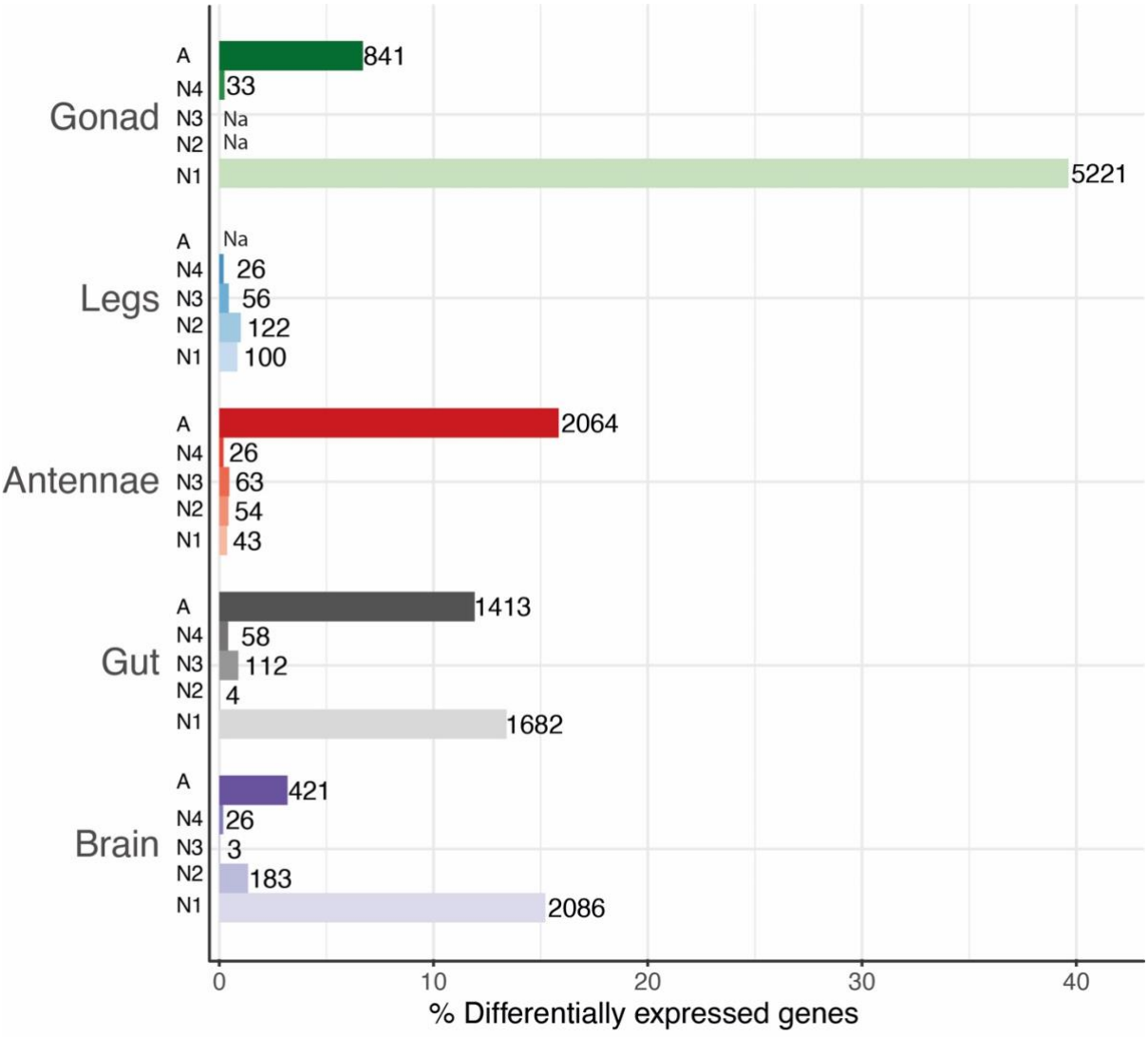

Figure 6. Percentage of the differentially expressed genes between sexual and parthenogenetic females in somatic and reproductive tissues, throughout development. The number of differentially expressed genes is indicated next to each bar, with tissues color-coded (green-gonad, blue-legs, red-antennae, grey- gut, violet- brain) and shaded based on developmental stages from Nymphal stage 1 (N1) to Adult stage (A). Average number of expressed genes across tissues and developmental stages: 12967 ± 711.7 (mean ± SD). Developmental stages are denoted as A (adult) and [N1-N4] (1st to 4th nymphal).

To investigate whether the considerable expression differences between sexual and parthenogenetic females at the hatchling and adult stages were likely associated with functional divergences, we focused on the subset of genes in tissue-associated modules. Thus, we repeated the differential gene expression analyses between sexual and parthenogenetic females for the gene modules associated with the

reproductive tract, gut, antennae and brain (see Figure 7). In modules associated with gonads, 40% of genes are differentially expressed between sexual and parthenogenetic females at the first nymphal stage in gonad tissue. A much smaller percentage of genes are differentially expressed in gonad tissues of adult females (4.5%), as well in the different modules associated with somatic tissues (1.9-19.2%; Figure 7 and Supplemental Figure S5).

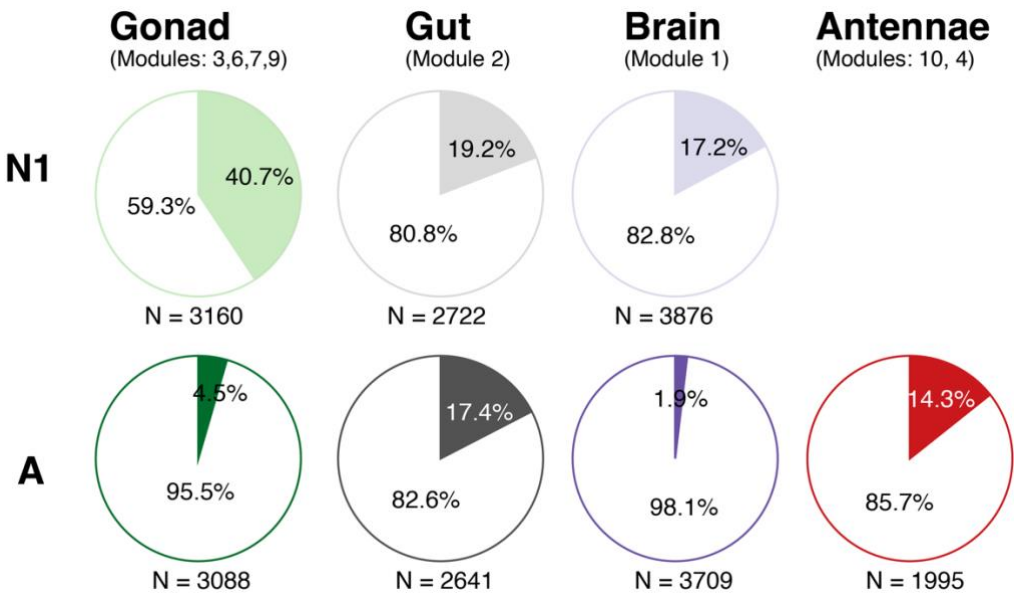

Figure 7. Pie charts showing percentages of differentially expressed genes (shaded parts) between sexual and parthenogenetic females among the genes from modules associated with specific tissues, at two developmental stages: N1- 1st nymphal and A- adult stage.

Finally, we examined differences between sexual and parthenogenetic females for genes with sex-biased expression in the sexual species (*T. poppense*). In the reproductive tract, 1st nymphal stage parthenogenetic females are characterized by feminized gene expression: they have higher expression of female-biased genes, and lower expression of male-biased genes than sexual females (Figure 8A). In 4th nymphal and adult stage, we record opposite shifts in sex-biased gene expression, i.e. masculinization: higher expression of male-biased genes and lower expression of female biased genes in parthenogenetic females (Figure 8A). At the first nymphal stage, there is further considerable overlap between sex-biased genes and genes differentially expressed between sexual and parthenogenetic

females, with 46 % of the latter also sex-biased in the sexual species (Figure 8B). The 4th nymphal and adult stages feature less overlap (Figure 8B). Finally, similarly to the pattern observed in reproductive tracts at the 4th nymphal and adult stages, parthenogenetic females show masculinization of expression in somatic tissues compared to sexually reproducing females (Supplemental Figure S6).

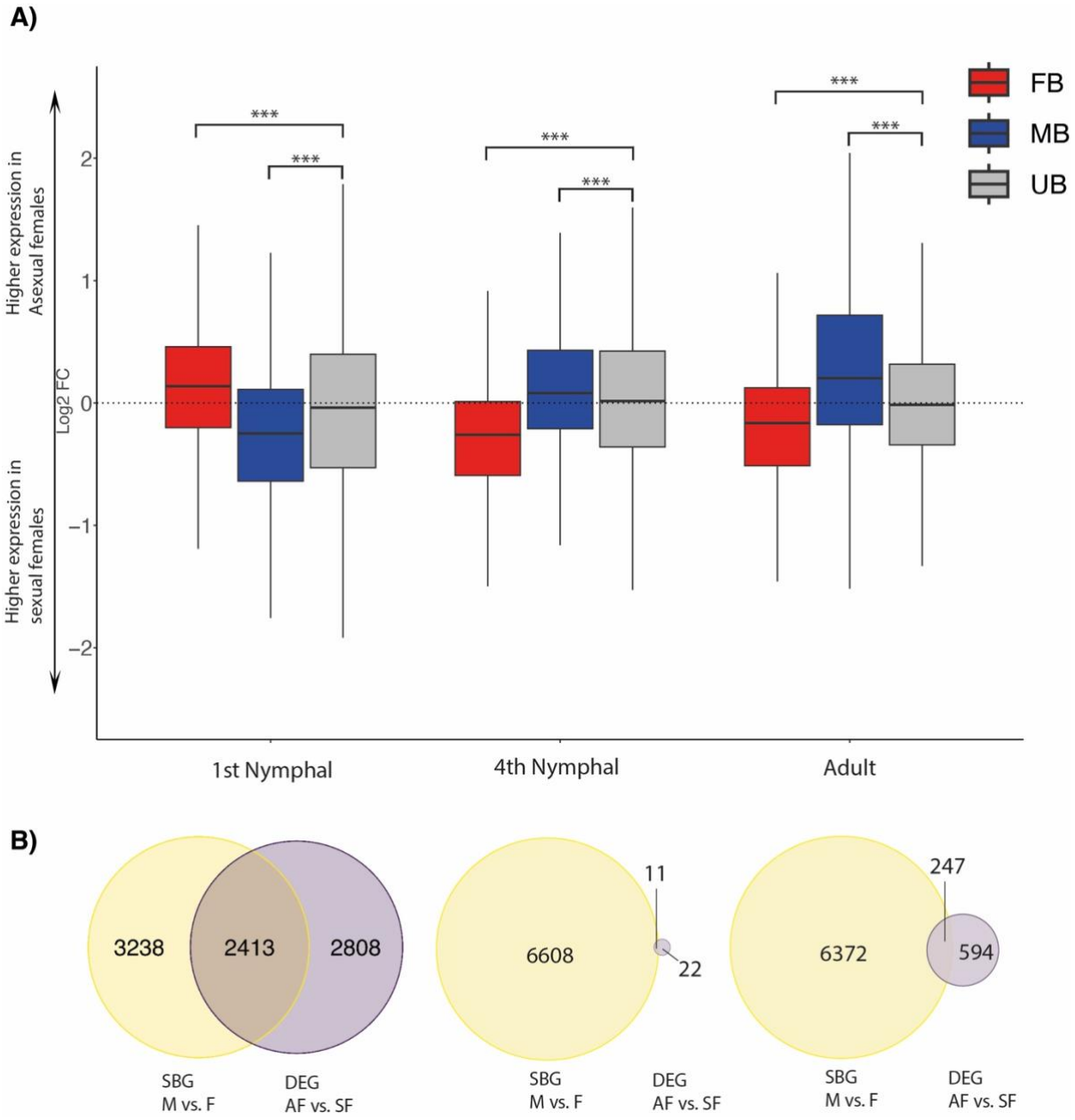

Figure 8. A) Shifts in expression levels of sex-biased genes between sexual and parthenogenetic females across development (in reproductive tracts). Three gene categories are depicted with different colors; female-biased in red, male-biased in blue, and un-biased in grey. Boxplots represent the median, lower and upper quartiles, and whiskers the minimum and maximum values (in the limit of 1.5x interquartile range). All comparisons between gene categories at each developmental stage yielded

statistically significant results, as indicated by adjusted p values from Wilcoxon rank sum tests, with *** denoting p < 2e-16. B) Venn-diagrams showing overlaps between sex-biased genes identified in sexual species, and differentially expressed genes between sexual and parthenogenetic females in reproductive tracts.

Discussion

The mechanisms by which sexually dimorphic phenotypes are achieved during development, as well as which tissues and developmental stages predominantly contribute to sexual dimorphism, remain insufficiently investigated. In this study, we investigated the patterns of gene expression in sexual *Timema poppense* as well as in its closely related parthenogenetic sister species *T. douglasi*, throughout post-embryonic development, and across various somatic and reproductive tissues. Our analyses in the sexual species revealed variations in the extent of sex bias between somatic and reproductive tissues. Overall, there was very little sex-bias in somatic tissues across development, and extensive bias in the reproductive tract already at the 1st nymphal stage. The amount of sex-bias in the reproductive tract was high (44-54%) and relatively stable throughout development, with only little increase at the adult stage. This dynamic is similar to the fly *Drosophila melanogaster* where ~50 % of the genes were sex-biased from the third larval stage, to the adult stage (Perry, et al. 2014).

However, in contrast to *Drosophila*, where sex-biased genes largely remain the same during development, we observe the opposite pattern in *Timema*, with a minority of sex-biased genes being shared across development. This might be partially driven by a larger gap between developmental stages analyzed in *Timema* compared to *Drosophila*, where three consecutive stages were analyzed. Another reason might be that in *Timema*, different sets of genes are involved in different processes at every stage, resulting in lower overlap between three stages. For example, large difference between 1st nymphal and 4th and adult stages in males most likely stems from the onset of meiosis and spermatogenesis in 4th nymphal stage (Chapter 3).

We previously reported little sex-biased gene expression in the 1st nymphal stage of *T. californicum* (whole-body analyses), a closely related species of *T. poppense* (Djordjevic, et al. 2022). However, our current study shows that little sexual differentiation is only the case for somatic tissues, while the reproductive tract is highly sexually differentiated. Because gonads represent a very small portion of cells at the 1st nymphal stage, they have little effect on sex-biased gene expression at the whole-body level. Furthermore, the gradual increase in sex-biased gene expression over development we observed in *T. californicum* was a result of gonads gradually increasing in relative size.

The degree of sex-biased gene expression underlying morphological, behavioral and physiological differences between the sexes in *T. poppense* varies between somatic tissues. Among somatic tissues, the brain exhibited the lowest percentage of sex-biased genes. Even at the adult stage, only 0.05% of expressed genes displayed sex bias in this tissue. Likewise, low levels of sex-bias gene expression in brain were also observed in crickets, fruit flies, and mammals (mice, rats, and rabbits) (Huylmans and Parsch 2015; Whittle, et al. 2021; Rodríguez-Montes, et al. 2023). The brain is a complex organ involved in processing a diverse range of information, detected by olfactory, gustatory and visual receptors. Sex-biased gene expression may differ depending on the brain region associated with a given trait, but putative differences might be masked in bulk sequencing of the entire brain (Harrison, et al. 2012). For example, female pheromones are detected by males to find a mate (Shorey 1973). Hence, the antennal lobe, associated with antennae olfactory receptors, may display sex bias, but the relative size of the lobe may be too small for affecting brain-level expression patterns. In addition, sex-biased gene expression of few pleiotropic genes may induce behavioral and morphological differences between sexes. For instance, the gene *fruitless* in *Drosophila* controls development of sexually-dimorphic neural circuits, which underlie behavioral differences such as courtship in males (Ruta, et al. 2010; Yamamoto and Koganezawa 2013).

Remarkably, the antennae emerged as the most sexually dimorphic among somatic tissues, with 10% of expressed genes displaying sex bias, albeit exclusively in the adult stage. Insect antennae are sensory organs (Hansson and Stensmyr 2011), playing a crucial role in detecting and processing environmental cues, including pheromones (Breer 1997), which are often involved in communication and mating behaviors. The extensive sex-biased gene expression observed in antennae during the adult

stage aligns with their sex-specific behavioral roles in these processes. Antennae in nymphal stages feature little sex -bias, with the olfactory functions (e.g., detecting food, or avoid predators) likely being similar in both sexes during juvenile development.

The gut featured a slightly higher degree of sex bias than the brain, with 0.4% of genes exhibiting sex-biased expression at the adult stage. Despite being reared on same diet during the course of the experiment, the sex-biased gene expression we observe could be related to sex-linked variation in metabolism. This idea is supported by sex-biased genes from the gut being enriched for processes such as carbohydrate metabolism, carbohydrate transport, or lipid transport. In *Drosophila*, there are indeed sex differences in the intestinal carbohydrate metabolism. These represent a physiological adaptation for different reproductive needs, such as sperm maturation versus oogenesis (Hudry, et al. 2019). Nevertheless, sex-biased genes in the gut could also be an adaptation to sex-specific diets. In *T. cristinae*, there is a sexual dimorphism in mandibule shape, which might be associated with differential feeding niches between sexes (Roy, et al. 2013).

The X chromosome is hypothesized to accumulate sexually antagonistic genes (Rice 1984; Oliver and Parisi 2004; Connallon and Knowles 2005). It is present in females two-thirds of the time, unlike autosomes that are equally transmitted in both sexes. Consequently, the selection pressure on X chromosome may favor accumulation of dominant female-beneficial alleles, as well as recessive alleles beneficial to males that are masked in females (Vicoso and Charlesworth 2009b). Because sex-biased genes are assumed to represent resolved or partially resolved sexual conflict, the genomic distribution of sex-biased genes is expected to be non-random (Ellegren and Parsch 2007; Meisel, et al. 2012), and typically, female-biased genes are enriched on the X, while male-biased genes are depleted (Parisi, et al. 2003; Meisel, et al. 2012; Perry, et al. 2014). Depletion of male-biased genes on the X is not completely understood. Different factors could contribute to the observed pattern, including the prevention of the accumulation of male-biased genes on the X due to the sexually antagonistic selection, meiotic-sex chromosome inactivation (MSCI), and dosage compensation (Meisel, et al. 2012). Our results in *Timema* allow us to exclude some of the factors. First, we show that male-biased genes are consistently underrepresented on the X chromosome in reproductive tracts, across development, while female-biased genes are consistently enriched on the X. In the 4th nymphal and adult stages, this is

because of MSCI in males during meiosis (Chapter 3), resulting in almost all genes being female-biased on the X. However, in the first nymphal stage, the X in males is transcriptionally active, MSCI did not start, and genes on the X are hyperrepressed to achieve complete dosage compensation. At this stage we still find a depletion of male-biased genes on the X. This suggests that most likely there is selection for the accumulation of female- biased genes on the X, at least in the reproductive tract.

Parthenogenetic *Timema* species produce female only offspring, and do not reproduce with males. Because selection acts only on females, sexual conflict is absent. Comparisons between sexual and parthenogenetic females can thus be used to infer potential expression changes due to the disappearance of sexual conflict (Parker, et al. 2019).

If sexual conflict constrains gene expression levels in sexual females, the expectation is that gene expression levels in parthenogenetic females would show feminization patterns, because expression toward the female optima (Parker, et al. 2019). However, a previous test of this hypothesis in *Timema* sexual and parthenogenetic stick insects revealed an overall masculinization of gene expression in parthenogenetic females. This was likely due to the decay of many sexual traits in parthenogenetic females, which would result in decreased expression of many female-biased genes and thus mask any putative signals from released antagonism. Consistent with this previous study, we also observed masculinization in somatic tissues across development. However, we found the opposite pattern in the 1st nymphal stage in reproductive tracts. At this stage, parthenogenetic females showed feminized gene expression (increased expression of female-biased and decreased expression of male-biased). This suggests that unresolved sexual conflict may be strongest at this stage and would not be masked by effects of sexual trait decay. Indeed, we do not expect to observe sexual trait decay in 1st instar gonads in *Timema* as early oogenesis processes are likely the same in parthenogenetic and sexual females. Only later processes differ, when parthenogenetic females undergo gamete duplication to produce diploid eggs (Jaron, et al. 2020; Larose, et al. 2023). Sexual conflict over gene expression in early gonads may remain unresolved because at this early stage the reproductive tracts have yet to differentiate between the sexes. As development proceeds the reproductive tracts become more differentiated in terms of morphology, function and gene expression profile. In this case the opportunity to resolve sexual conflict may be greater than at earlier stages, resulting in less unresolved sexual

conflict in adult tissues. This would be specific to the reproductive tract, as at the adult stage this tissue has very different morphology and function in each sex and could almost be considered as two separate tissues. In line with this idea, nearly half of the genes showing differential expression between sexual and parthenogenetic females are also sex-biased in sexual species, reinforcing the notion that changes are influenced by the absence of sexual conflict. Finally, expression differences in 1st instar gonads between sexual and parthenogenetic females are likely associated with functional consequences, since many changes in gene expression happen to genes in reproductive tract modules.

Overall, we find that the differences in gene expression between sexual and parthenogenetic females are more extensive than the differences between the sexes in somatic tissues, particularly during the earliest nymphal stage. Among tissues, the reproductive tract is the most differentiated one, with 40% of genes differentially expressed between sexual and parthenogenetic females at the earliest nymphal stage. Moreover, we observe a consistent pattern across tissues: substantial differential gene expression in the first nymphal stage when comparing sexual and parthenogenetic females, followed by little differences in the subsequent nymphal stages, and a final increase in amount of differentially expressed genes at the adult stage. Future studies, involving multiple sexual and parthenogenetic sisters' pairs should decipher which evolutionary forces drive these differences at 1st nymphal stage.

Conclusion

The dynamics of sex-biased gene expression differs extensively between somatic and reproductive tissues in *Timema poppense*. Somatic tissues have minimal sex-bias across development with an increase at the adult stage in only one of the tissues (antennae), while reproductive tracts show extensive differences from early development. Sexual and parthenogenetic females differ the most in gene expression at 1st nymphal stage and in particular in the reproductive tract. At this stage, parthenogenetic females showed feminization of gene expression in the reproductive tract, suggesting an unresolved sexual conflict in early gonads of the sexual species. This supports that sexual conflict can occur earlier in development, and is often overlooked by focusing only on adult stages.

Supplemental Material - Chapter 2

Supplemental Table S1. Final number of replicates for males (M), females (F) and asexual females (Asex F), per stage and tissue that passed quality control.

	Adult			Nymphal 1			Nymphal 2			Nymphal 3			Nymphal 4			Nymphal 5			Nymphal 6		
Tissue	Asex F	F	M	Asex F	F	M	Asex F	F	M	Asex F	F	M	Asex F	F	M	Asex F	F	M	Asex F	F	M
Antennae	4	4	4	3	3	2	3	3	3	3	2	3	2	3	3	4	1	3	1	1	0
Brain	4	4	4	3	3	3	3	3	3	3	2	3	2	3	3	4	1	2	1	1	0
Gonads	4	4	3	4	4	4	0	0	0	3	2	1	2	3	3	3	1	3	1	1	0
Guts	4	4	4	3	3	3	3	3	3	3	2	3	2	2	3	2	0	2	1	1	0
Legs	0	0	0	3	3	3	3	3	3	3	2	3	2	3	3	4	1	3	1	1	0

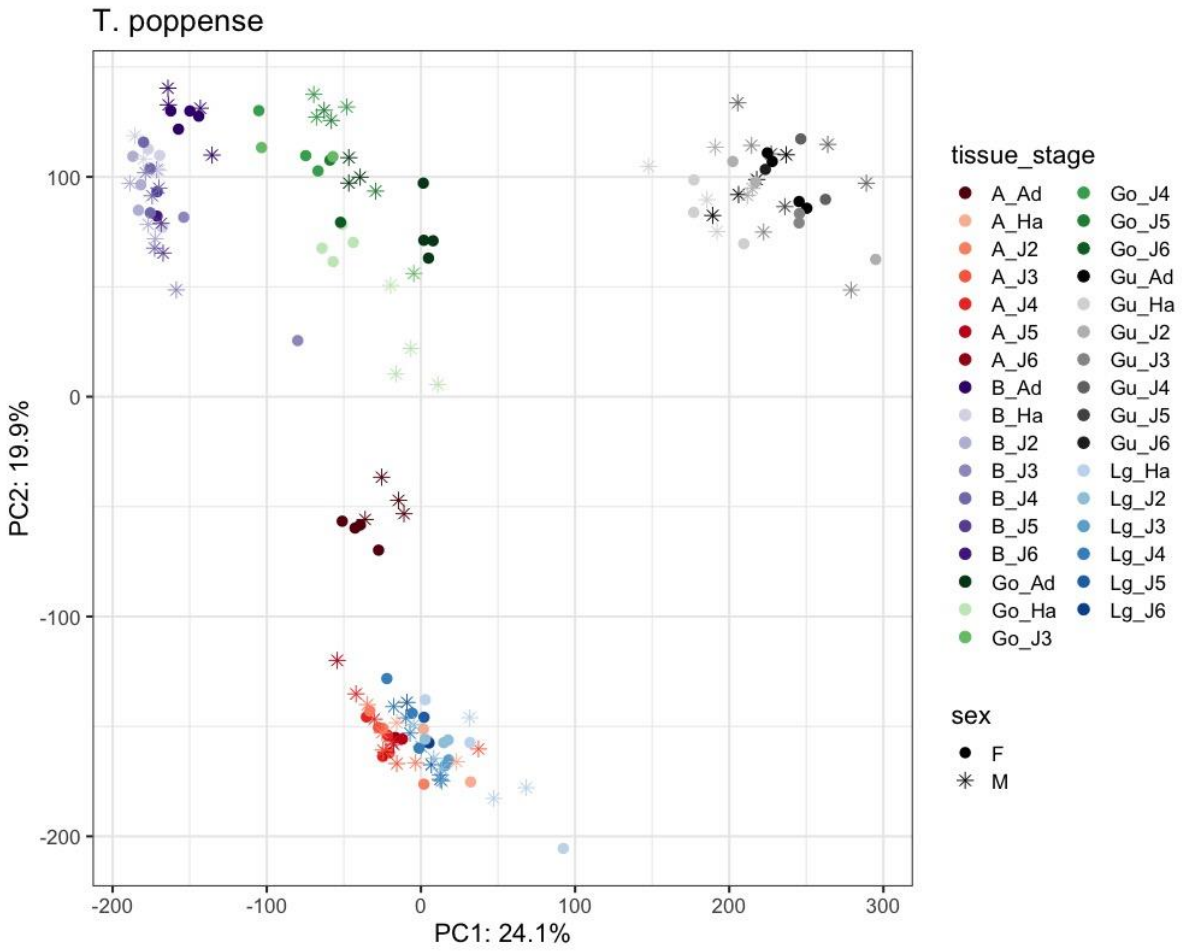

Supplemental Figure S1. PCA plot of all *T. poppense* RNA-seq samples. Different tissues are depicted with different colors, and each color corresponds to the age of sample (lighter shading- younger, darker shading older). Antennae (A), brain (B), gonad, guts and legs are depicted with red, purple, green, grey and blue, respectively. Females (F) are represented with circles, while males (M) are shown with stars.

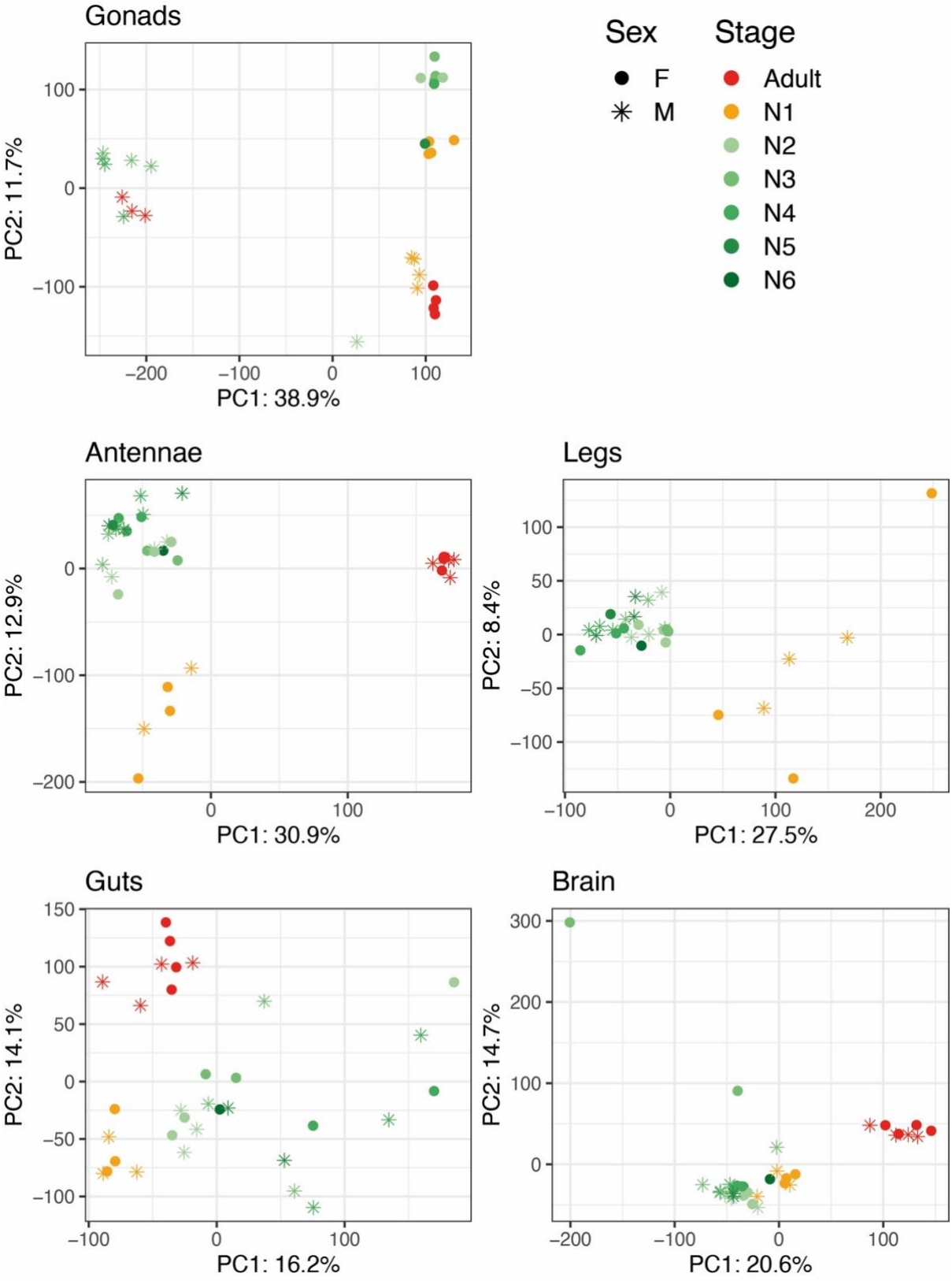
Gonads
PC2: 11.7%
PC1: 38.9%
Sex
F
M
Stage
Adult
N1
N2
N3
N4
N5
N6
Antennae
PC2: 12.9%
PC1: 30.9%
Legs
PC2: 8.4%
PC1: 27.5%
Guts
PC2: 14.1%
PC1: 16.2%
Brain
PC2: 14.7%
PC1: 20.6%

Supplemental Figure S2. PCA plots of *T. poppense* RNA-seq samples from each tissue (Reproductive tract, Legs, Antennas, Guts, and Brain). The 1st nymphal stage is depicted in orange, the adult stage in red, while other nymphal stages are depicted in shades of green, from light to darker matching the age. Males (M) are represented with stars, and females (F) with circles.

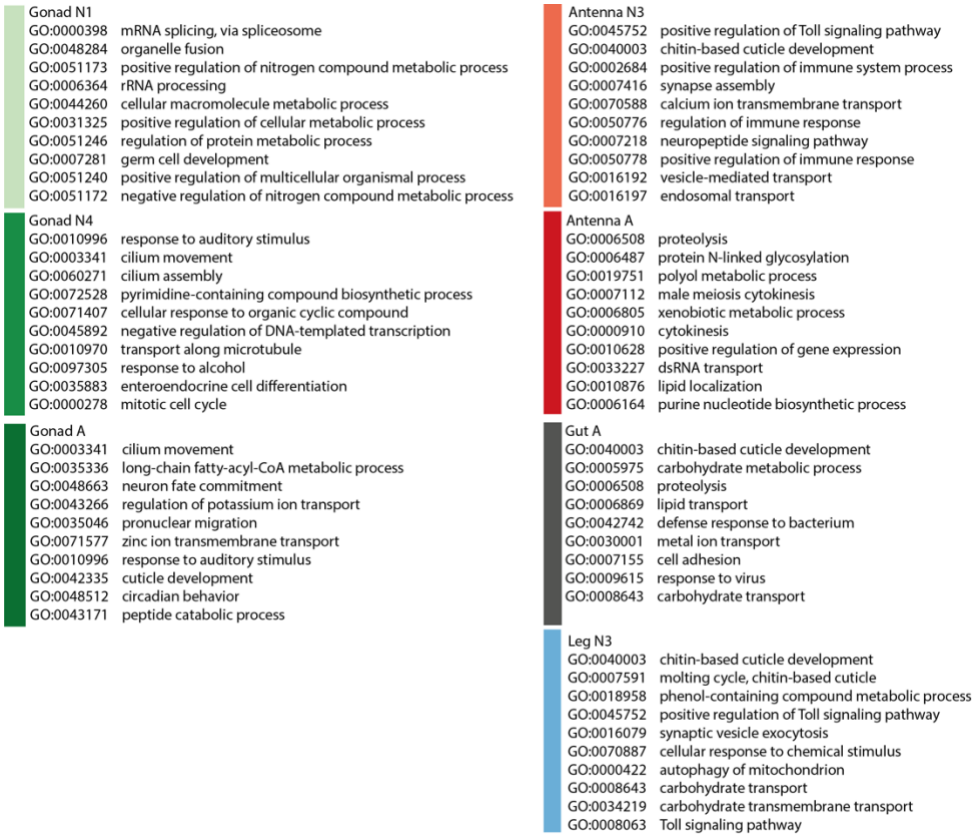

Supplemental Figure S3. Go term enrichment of sex-biased genes for different tissues and developmental stages

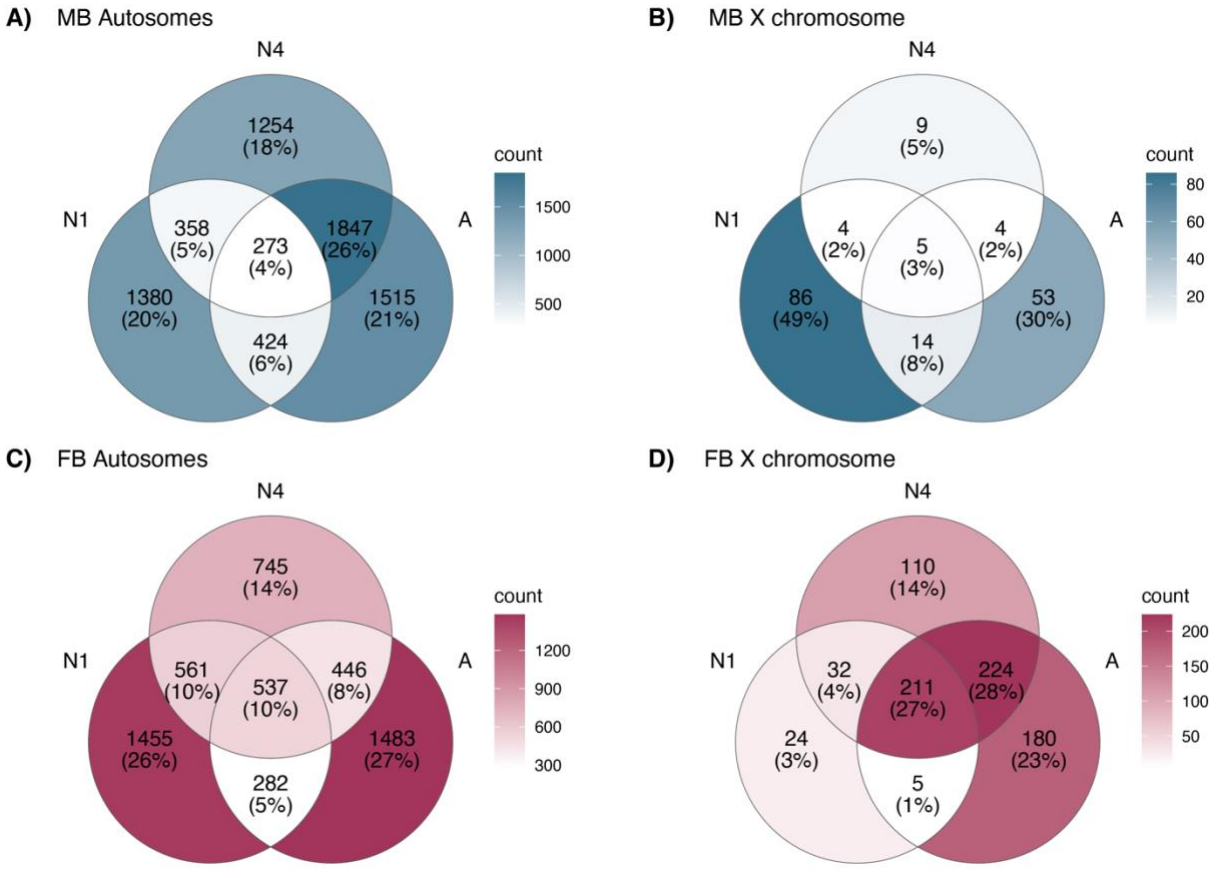

Supplemental Figure S4. Venn diagrams showing the overlap of sex-biased genes in the reproductive tract across different developmental stages (A) male-biased genes on autosomes and on the X chromosome (B) and Female-biased genes on autosomes (C) and on the X chromosome (D)

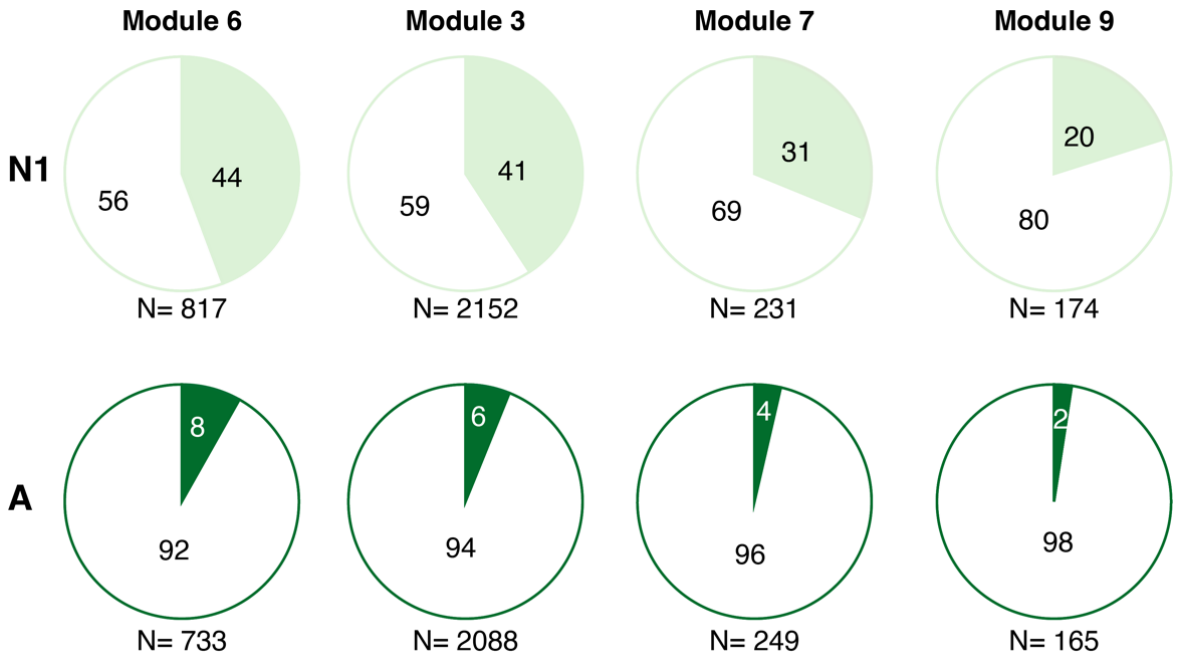

Supplemental Figure S5. Pie charts showing percentages of differentially expressed genes (shaded parts) between sexual and parthenogenetic females in four modules associated with gonads at two developmental stages: N1- 1st nymphal and A- adult stage. The number of expressed genes in each module (N) is noted below every pie chart.

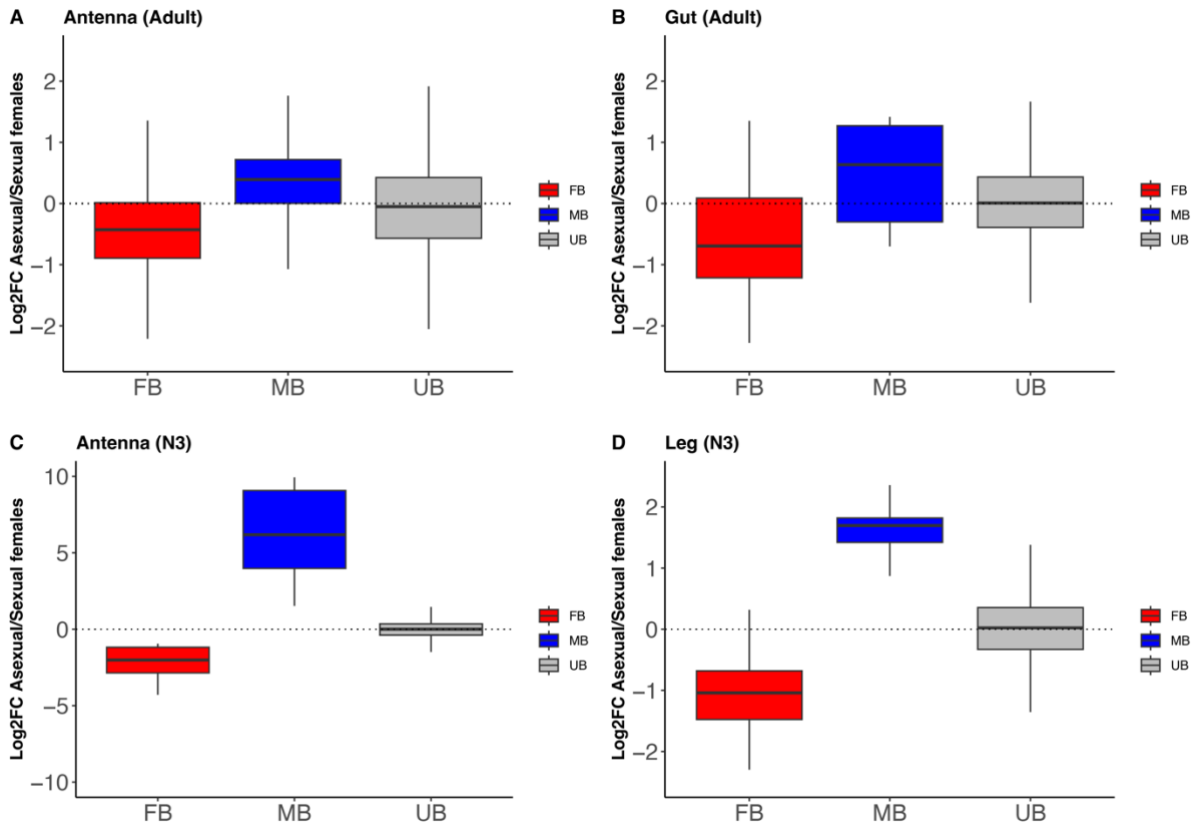

Supplemental Figure S6. Shifts in expression levels of sex-biased genes between sexual and asexual females in; A) Antennae- adult stage, B) Gut- adult stage C) Antennae- 3rd nymphal stage and D) Leg- third nymphal stage. Three gene categories are depicted with different colors; female-biased in red, male-biased in blue, and un-biased in grey. Positive values indicate greater expression in parthenogenetic females, negative values indicate greater expression in sexual females. Boxplots represent the median, lower and upper quartiles, and whiskers the minimum and maximum values (in the limit of 1.5x interquartile range). All comparisons between gene categories at each developmental stage yielded statistically significant results, as indicated by adjusted p values from Wilcoxon rank sum tests, with $p < 0.01$.

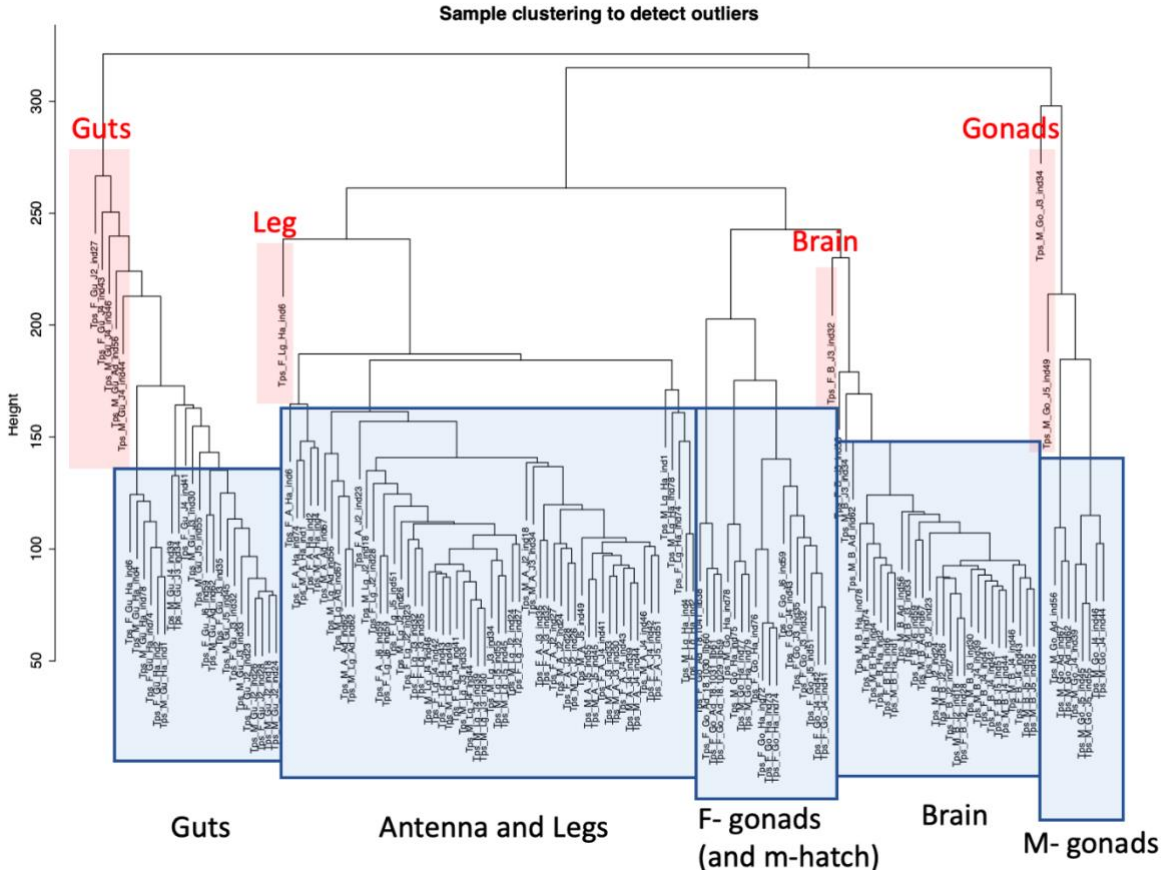

Supplemental Figure 7. Hierarchical clustering of RNA-seq samples to detect outliers (highlighted in red). Those samples were excluded for gene network and modules identification (see material and methods).

Chapter 3

Dynamics of X chromosome hyper-expression and inactivation in male tissues during stick insect development

Jelisaveta Djordjevic[1], William Toubiana[1], Marjorie Labédan[1], Zoé Dumas[1], Darren J Parker[2], Tanja Schwander[1]

[1]Department of Ecology and Evolution, University of Lausanne, 1015 Lausanne.

[2]School of Natural Sciences, Brambell Building, Bangor University, Bangor, LL57 2UW, United Kingdom.

Corresponding authors: jelisaveta.djordjevic@unil.ch; tanja.schwander@unil.ch

Manuscript in preparation

Abstract

Dosage compensation balances the gene expression levels of sex chromosomes between males and females. In *Timema* stick insects, females have two X chromosome copies, while males have only one X (XX:X0 sex determination). Using tissue-specific RNAseq data throughout insect development, we show that X-linked expression in stick insects is equalized between the sexes via hyper-expression of the single X in males in somatic tissues and results in complete dosage compensation. Complete dosage compensation is also present in male gonads at the first nymphal stage, when germ cells have not yet entered meiosis I. In later nymphal stages, X-linked expression is strongly reduced, and immunolabeling and silencing histone mark profiling reveal that this reduction is caused by meiotic X-chromosome inactivation in the male germline. Our findings support the idea that meiotic X-chromosome inactivation protects un-synapsed chromosomes from damaging effects synapsed chromosomes are not exposed to.

Introduction

In species where sex is determined by differentiated sex chromosomes, sex chromosome copy number differs between males and females. For example, in X0 and XY systems, males have only one copy of each gene located on the X chromosome, while females have two. Because gene copy number generally correlates with expression levels (Stingele, et al. 2012) the expression level of X-linked genes in males is expected to be half that of autosomal genes, and half that of the same genes in females. However, selection can act on the regulation of expression in a sex-specific manner, and potentially restore balanced expression levels in the heterogametic sex (Ohno 1967; Straub and Becker 2007; Mank 2013).

Selection for balanced expression of genes on sex chromosomes tends to result in increased expression of genes located on the single copy chromosome in the heterogametic sex, a process known as dosage compensation (Ohno 1967; Gupta, et al. 2006; Nguyen and Disteche 2006). Thus, in many species with XO or XY sex chromosome systems, X-linked genes in males are upregulated and expressed at the same level as autosomal genes (Lucchesi 1998; Meller 2000; Vicoso and Bachtrog 2015; Hu, et al. 2022; Parker, et al. 2022). However, the mechanisms through which such dosage compensation occurs are typically unknown and vary among the few species studied in detail. Thus, in the fruit fly *Drosophila melanogaster*, the X is hyper-expressed in males, with apparently no targeted modification of X expression in females (Hamada, et al. 2005; Straub, et al. 2005). In the worm *Caenorhabditis elegans*, the expression of both X chromosome copies in females is reduced to achieve similar total expression levels as for the hyper-expressed X in males (Meyer and Casson 1986; Meyer, et al. 2004). Finally, in eutherian mammals, females inactivate one of the X chromosomes in each cell, and the single (active) X is hyper-expressed in both sexes (Lyon 1961; Nguyen and Disteche 2006).

Interestingly, in all studied XO and XY species that feature dosage compensation, the single X in males is much less expressed in the testes than in the somatic tissues (Vicoso and Bachtrog 2015; Rayner, et al. 2021; Hu, et al. 2022; Parker, et al. 2022). This is thought to be due to the presence of dosage compensation in somatic tissues and the absence of dosage compensation in the reproductive tissues, perhaps because the gene expression optima in male versus female gonads are so different that

there is no or reduced selection for balanced expression in this tissue (Vicoso and Bachtrog 2015). In addition, transcriptional silencing of the X because of meiotic sex chromosome inactivation (MSCI) can specifically reduce the expression levels of X-linked genes in the testes of some species (Turner 2007; Namekawa and Lee 2009).

Beyond the specific case of testes in adult males, it is largely unknown whether the extent of dosage compensation varies among tissues and across development (but see (Rayner, et al. 2021) and (Kramer, et al. 2015)). Furthermore, mechanisms affecting X-linked expression and dosage compensation are only characterized for a few well-studied model organisms as mentioned above, preventing inferences of conserved versus lineage specific aspects of sex chromosome expression.

Here we fill these knowledge gaps by exploring how the extent of dosage compensation varies over development in somatic and reproductive tissues, through which mechanisms dosage compensation is achieved, as well as the potential impact of meiotic sex chromosome inactivation in the stick insect *Timema poppense*. Females of this species have two X chromosomes and males have only one (Schwander and Crespi 2009) and previous work on *Timema* stick insects showed that in adults, there is dosage compensation in heads and legs, but not in the reproductive tract (Parker, et al. 2022). However, whether the extent of dosage compensation varies among specific tissues and across development, as well as the mechanism of dosage compensation, remain unknown. We take advantage of a new chromosome-level genome assembly of *T. poppense* from Parker et al (in prep) and sequence RNA from brain, gut, antennae, leg and reproductive tract samples in males and females, across development. We then assess the expression levels of genes located on the X chromosome(s) in both sexes relative to those on the autosomes and infer whether both X copies are similarly expressed in females or whether there is evidence of silencing. Finally, we test for meiotic sex chromosome silencing (MSCI) in the male germline via immunolabeling and genome profiling for silencing histone marks, and discuss how MSCI globally affects X-linked gene expression patterns in male gonads.

Material and methods

Insect husbandry

Hatchlings were obtained from eggs laid by captive bred *T. poppense* individuals, originally collected in California in 2018. To complete development, *Timema* females have one extra molt compared to males (Djordjevic, et al. 2022), hence our aim was to obtain five different tissues (reproductive tracts and four somatic tissues) for each of seven developmental stages in females (nymphal stage 1-6, adult) and six in males (nymphal stage 1-5, adult; Supplemental Table S1). Upon hatching, insects were reared in Petri dishes containing *Ceanothus* plant cuttings wrapped in wet cotton up to a specific developmental stage and then dissected one day after molting. To identify individuals that molted, we painted the thoraxes with red acrylic paint after each molt and checked daily for individuals without the paint. Prior to dissection, the insects were anesthetized with CO_2. Brain, antennae, legs, and gut samples were obtained from each developmental stage, while the reproductive tract was collected at every stage from the 4th nymphal stage (Supplemental Table S1). We dissected reproductive tracts only starting from the 4th nymphal stage because we were originally unable to unambiguously identify gonad tissues in the earlier stages. Upon improving our dissection techniques, we were later able to identify and dissect gonad tissues at earlier stages, and we therefore secondarily added reproductive tract samples of newly hatched individuals (1st nymphal stage). During dissections, tissues were placed in Eppendorf tubes and immediately flash frozen in liquid nitrogen before storage at -80°C until extraction for approximately 1/3 of the dissections. For the remaining dissections, due to pandemic-related laboratory closures, tissues were preserved in RNA later (Qiagen) before storage at -80°C. In total, we obtained two to four replicates per sex and tissue (Supplemental Table S1).

RNA extraction and sequencing

TRIzol solution (1 mL) and a small amount of ceramic beads were added to each tube containing tissue. Samples were homogenized using a tissue homogenizer (Precellys Evolution; Bertin Technologies). Chloroform (200 µL) was added to each sample and samples were then vortexed for 15 seconds and

centrifuged for 25 minutes at 12,000 revolutions per minute (rpm) at 4°C. The upper phase containing the RNA was then transferred to a new 1.5 mL tube with the addition of isopropanol (650 µL) and Glycogen blue (GlycoBlue™ Coprecipitant; 1 µL). The samples were vortexed and placed at -20°C overnight. Samples were then centrifuged for 30 minutes at 12,000 rpm at 4°C. The liquid supernatants were removed, and the RNA pellet underwent two washes using 80% and 70% ethanol. Each wash was followed by a 5-minute centrifugation step at 12,000 rpm. Finally, the RNA pellet was resuspended in nuclease-free water and quantified using a fluorescent RNA-binding dye (QuantiFluor RNA System) and nanodrop (DS-11 FX).

Library preparation using NEBNext (New England BioLabs) and sequencing on an Illumina NovaSeq 6000 platform with 100 bp paired-end sequencing (~45 million reads per sample on average) was outsourced to a sequencing facility (Fasteris, Geneva).

Raw data quality control, mapping and read counting

RNA-seq reads were trimmed with Trimmomatic (Bolger, et al. 2014) (v. 0.39, options: ILLUMINACLIP:AllIllumina-PEadapters.fa:3:25:6 LEADING:9 TRAILING:9 SLIDINGWINDOW:4:15). Reads with a length below 80 bp were discarded. Trimmed reads were mapped to the *T. poppense* genome from (Parker *et al*, in prep) with STAR (Dobin, et al. 2013) (v 2.7.8a) with default settings except for the addition of two-pass mapping (--twopassMode Basic). Read counts were then obtained using HTseq (Anders, et al. 2014) (v.011.2, options: --order=pos --type=exon --idattr=gene_id --stranded=reverse).

Data analysis

Dosage compensation analysis

We categorized the data based on tissue and developmental stage. Subsequently, we excluded genes with low expression, specifically those that were not expressed in a minimum of three libraries when the replicate number equaled four, two libraries when the replicate number was three, and one library

when the replicate number was two in each sex. This filtering required an expression level greater than 0.5 CPM (counts per million) in males or females within the specified tissue and stage.

For the computation of RPKM values, we first obtained gene sizes using the GenomicFeatures package (Lawrence, et al. 2013) and then calculated the average RPKM values for each sex using EdgeR (Robinson, et al. 2009). Lastly, we determined the log2 RPKM ratio between the male and female average expression levels. Statistical analyses (Wilcoxon test), graphical representations of the data were performed in R (4.3.1).

Tissue specificity (Tau)

To test if the X chromosome has more tissue specific expression than the autosomes, we calculated Tau, an index of gene expression tissue specificity ranging from zero (expressed equally in all studied tissues) to one (gene expressed in only one tissue) (Yanai, et al. 2004). For these analyses we used the subset of four tissues (antenna, brain, gut and reproductive tract) and four developmental stages (1^{st}, 3^{rd}, 4^{th} nymphal and the adult stage) for which we had data for both sexes (see Supplemental Table S1). Using median expression RPKM values, we calculated Tau for the 12 longest scaffolds (corresponding to the 12 chromosomes of *T. poppense*), where scaffold 3 is the X chromosome (Parker *et al*, in prep). We visualized the results with ggplot2 (v. 3.3.2) (Wickham 2016).

Variant calling on RNA-seq data

To determine if both X chromosome copies are expressed in females, we calculated coverage depth for heterozygous sites located on X-linked transcripts, expecting to observe equal depth of the two alleles in case of similar expression of both X chromosome copies. First, we performed variant calling on RNA-seq data following the pipeline proposed in (Brouard and Bissonnette 2022). The aligned reads were processed using GATK tools (McKenna, et al. 2010), with "SplitNCigarReads" to split reads that span splice junctions, and "MarkDuplicates" to remove PCR duplicates. After preprocessing, variant calling is performed using GATK's HaplotypeCaller.

Immunolabeling of X chromosomes

In order to determine the presence of meiotic cells as well as X heterochromatinization and transcriptional activity in male gonads, we performed double immunolabeling of SMC3_488 (#AB201542, AbCam) as a marker of cohesin axes (this allows for the assessment of synapsis progression, and hence, cell cycle) and either H3K9ME (#AB8898, AbCam; which labels silencing heterochromatin marks) or RNA polymerase II phosphorylated at serine 2 (p-RNApol-II (ab193468, AbCam); an indicator of transcription). Gonads from 1st nymphal and 4th nymphal males were dissected in 1X PBS, then fixed in paraformaldehyde (2%) and Triton X-100 (0.1%) solution for 15 minutes. Gonads were then squashed on slides coated with poly-L-lysine, and flash frozen in liquid nitrogen. Slides were incubated in PBS 1x for 20 minutes at room temperature, then blocked with a BSA 3% solution (prepared by dissolving 3g of BSA in 100mL of PBS 1X) for 20 minutes. Slides were then incubated overnight at 4°C in a humid chamber with the primary (p-RNA-Pol II or H3K9), diluted in BSA 3% (1:100), and washed 3x for 5 minutes in PBS 1X. The secondary antibody, anti-rabbit Alexa 594 (711-585-152, Jackson), diluted in BSA 3% (1:100), was applied, and samples were incubated for 45 minutes at room temperature. Further washes were conducted as described above, followed by an extended 10-minute wash in PBS 1X, and by blocking using a 5% Normal Rabbit Serum (NRS) solution (X090210-8, Agilent Technology) (1.5uL NRS in 28.5uL PBS 1x) for 30 minutes at room temperature. Another 5-minute wash in PBS 1x was performed to remove excess blocking solution. Samples were then incubated with the labeled antibody SMC3_488 (#AB201542, AbCam) at a 1:100 dilution for 1 hour at room temperature, followed by a final series of washes and staining with DAPI (D9542, Sigma-Aldrich) for 3 minutes at room temperature. The final washing step of 5 minutes in PBS 1x was performed before mounting the samples for subsequent imaging.

ChIP-sequencing to reveal heterochromatin marks

To profile silencing histone modifications on the X chromosome in male gonad tissue, we conducted ChIP-sequencing using H3K9me (Methylation of histone H3 at lysine-9), a histone variant generally associated with heterochromatic silencing, and which marks the silenced X chromosome in male mouse spermatogenesis (Khalil, et al. 2004; Ernst, et al. 2019). We dissected male gonads and immediately

froze them in liquid nitrogen. A similar protocol was applied for female somatic tissues, involving the dissection and flash-freezing of all internal organs except the gut and gonads. For chromatin preparations, frozen tissues were homogenized by cryogenic grinding (CryoMill; Retsch GmbH) using a specific regimen (2x 60 s, 25 Hz, resting 30 s, 5 Hz), transferred to a 15-ml Falcon tube, and subsequently subjected to rotation at room temperature for 12 minutes in a cross-linking solution composed of 50 mM Hepes (pH 7.9), 1 mM EDTA (pH 8), 0.5 mM EGTA (pH 8), 100 mM NaCl, and 1% formaldehyde. The cross-linking reaction was stopped by pelleting nuclei for 2 min at 2000g, followed by rotation for 10 minutes in a stop solution containing PBS, 125 mM glycine, and 0.01% Triton X-100. Nuclei were then subjected to washing steps in solution A [10 mM Hepes (pH 7.9), 10 mM EDTA (pH 8), 0.5 mM EGTA (pH 8), and 0.25% Triton X-100] and solution B [10 mM Hepes (pH 7.9), 1 mM EDTA (pH 8), 0.5 mM EGTA (pH 8), 0.01% Triton X-100, and 200 mM NaCl]. This was followed by a sonication step in 100 µl of radioimmunoprecipitation assay (RIPA) buffer [10 mM tris-HCl (pH 8), 140 mM NaCl, 1 mM EDTA (pH 8), 1% Triton X-100, 0.1% SDS, 0.1% sodium deoxycholate, and 1× complete protease inhibitor cocktail] in AFA microtubes in a Covaris S220 sonicator for 5 min with a peak incident power of 140 W, a duty cycle of 5%, and 200 cycles per burst. Sonicated chromatin was centrifuged to pellet insoluble material and snap-frozen.

ChIP was carried out using 5 µl of H3K9me (#AB8898, AbCam) incubated overnight at 4°C with half of the prepared chromatin sample (10 ul of the same chromatin preparation was used as input control, see below). Protein A Dynabeads (50 µl; Thermo Fisher Scientific, 100-01D and 100-03D) were added for 3 hours at 4°C, and subsequently washed for 10 min each once with RIPA, four times with RIPA with 500 mM NaCl, once in LiCl buffer [10 mM tris-HCl (pH 8), 250 mM LiCl, 1 mM EDTA, 0.5% IGEPAL CA-630, and 0.5% sodium deoxycholate], and twice in TE buffer [10 mM tris-HCl (pH 8) and 1 mM EDTA]. DNAs of the ChIP sample and the input control were then purified by ribonuclease digestion, proteinase K digestion, reversal of cross-links at 65°C for 6 hours, and elution from a QIAGEN MinElute PCR purification column. The purified DNA (ChIP and input) was then processed at the Lausanne Genomic Technologies Facility for library preparation using the NEBNext Ultra II DNA Library Prep Kit for Illumina and 150-bp paired-end sequencing on an Illumina HiSeq 4000.

ChIP and input reads were trimmed using trimmomatic (v0.39). The reads were then mapped to the reference genome using the BWA-MEM algorithm v0.7.17 (-c 1000000000). Chimeric reads were removed using SA:Z tags, and PCR duplicates were eliminated with Picard tools (v2.26.2). Mean coverage was computed for ChIP and input reads within non-overlapping 10 kb windows across all scaffolds using BEDTools (v2.30.0) and normalized by the number of mapped reads in each library.

Results and Discussion

Complete dosage compensation across male somatic tissues and developmental stages

In *Timema* stick insects, males carry a single X chromosome copy (X0), while females have two copies (XX) (Schwander and Crespi 2009). In all four somatic tissues examined (guts, brains, antennae, legs), males feature complete dosage compensation. This is revealed by similar ratios of male to female expression for autosomal and X-linked genes (Figure 1A; Supplemental Table S2). Additionally, gene expression levels are relatively constant along the single male X (Supplemental Figure S1). This indicates that dosage compensation is achieved through a global mechanism that affects the entire chromosome (rather than through regulating individual genes) as is the case in other insects (Larschan, et al. 2011; Gu and Walters 2017).

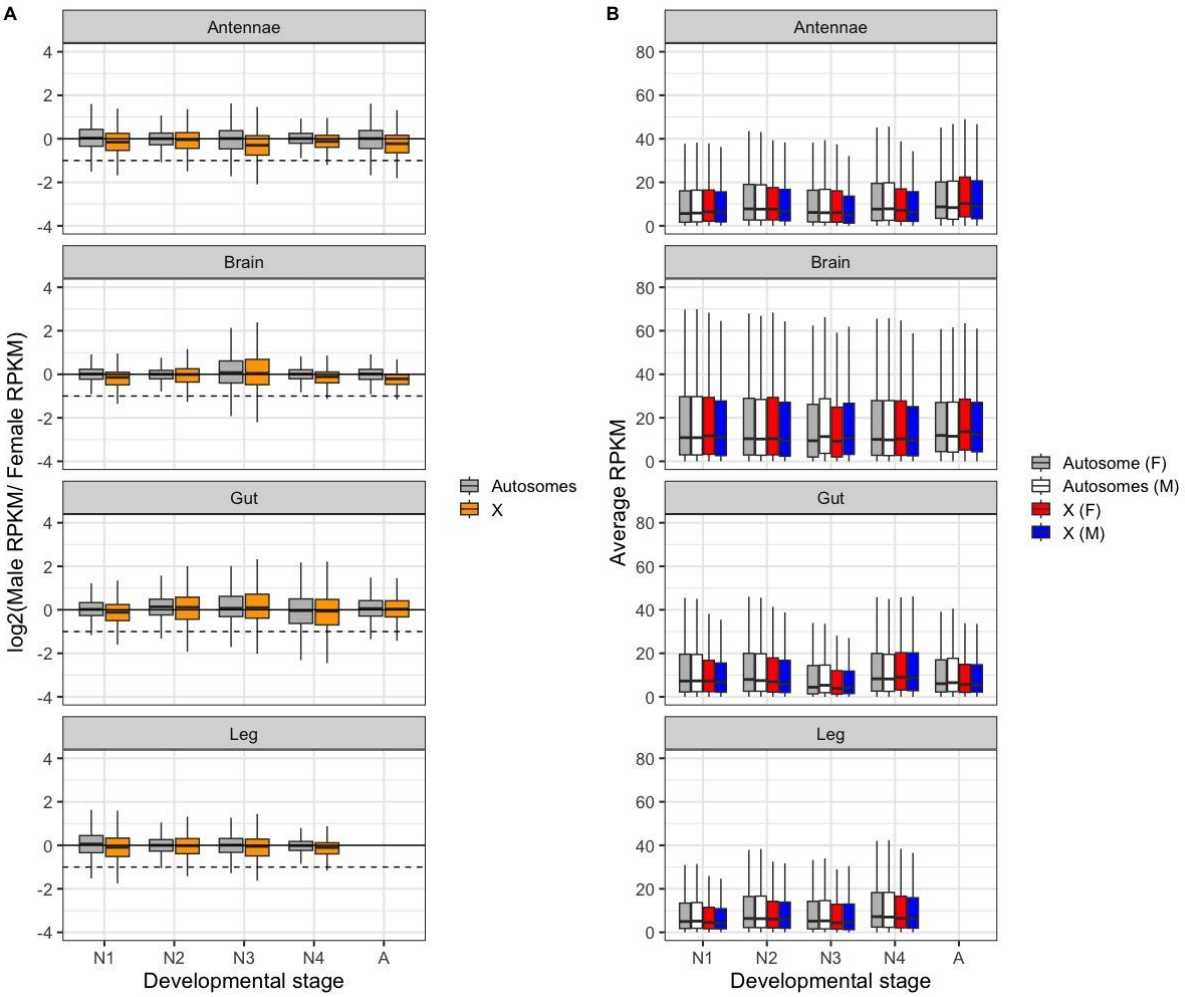

Figure 1. Complete dosage compensation in male somatic tissues throughout development

A) Log2 of male to female expression ratio for the X (orange) and autosomes (grey) in somatic tissues along development. Dashed lines represent a two-fold reduction in expression in males (as expected if there was no dosage compensation). See Supplemental Figure S2 for individual rather than pooled autosomes **B)** Average expression levels (RPKM values) of genes located on the autosomes and X in females (grey and red) and in males (white and blue) in somatic tissues along development. Boxplots depict the median, the lower and upper quartiles, while the whiskers represent the minimum and maximum values, within 1.5x the interquartile range. See Supplemental Figure S3 for individual rather than pooled autosomes.

Complete dosage compensation is typically used to refer to cases where X-linked and autosomal genes have equal expression in males (Gu and Walters 2017). In *T. poppense*, although

dosage compensation results in similar X-wide expression levels in males and females (Figure 1A), X-linked genes generally have lower expression than autosomal genes in somatic tissues. Importantly, this is not solely the case for males (as would be expected under incomplete upregulation of the single X in males), but also for females (Figure 1B; Supplemental Table S3). It can be argued that complete dosage compensation should refer to situations where the single X is transcribed at a level comparable to the ancestral levels for two X copies, prior to X chromosome formation (i.e., when the X chromosome would have been an autosome; (Gu and Walters 2017). However, the X chromosome in stick insects has been conserved for at least 120 mya (Parker, et al. 2022; Stuart, et al. 2023) and shares most of its content with the X chromosome in other insect orders, which split over 450 mya (Toups and Vicoso 2023) meaning that such ancestral transcription levels cannot be inferred.

Why X-linked genes are overall less expressed than autosomal genes in *Timema* remains as an open question. A likely explanation is that there is an upper limit to how much the transcriptional activity of a haploid X can be increased, which would favor the movement of highly expressed genes from the X to autosomes (Vicoso and Charlesworth 2009a; Hurst, et al. 2015). A limit to the maximal transcriptional activity of a haploid chromosome is notably believed to explain X chromosome gene contents and reduced expression levels in therian mammals (Vicoso and Charlesworth 2009a; Hurst, et al. 2015) and *Drosophila* fruit flies (Argyridou and Parsch 2018). Support for a similar explanation in *Timema* stems from the tissue-specificity of X- linked genes. Along with lower levels of expression, the X chromosome in mammals has higher tissue specificity than autosomes (Hurst, et al. 2015), because highly expressed genes generally have broader expression (Pessia, et al. 2014; Hurst, et al. 2015). Similar to mammals, we find on average higher tissue specificity of X-linked than autosomal genes in both male and female *Timema* (Wilcoxon test, $p_{\text{adj (females)}}$= 3.5e-11, $p_{\text{adj (males)}}$= 2.3e-08; Figure 2; see also Supplemental Figure S4 and Supplemental Table S5).

Lastly, X chromosome degradation could also contribute to lower expression of X-linked as compared to autosomal genes, similar to patterns reported for genes on the Y chromosomes in some species (Bachtrog 2013). The X chromosome has a reduced effective population size as compared to autosomes, as a consequence of reduced copy numbers and the lack of X recombination in males, which leads to the accumulation of deleterious mutations in *Timema* (Parker, et al. 2022).

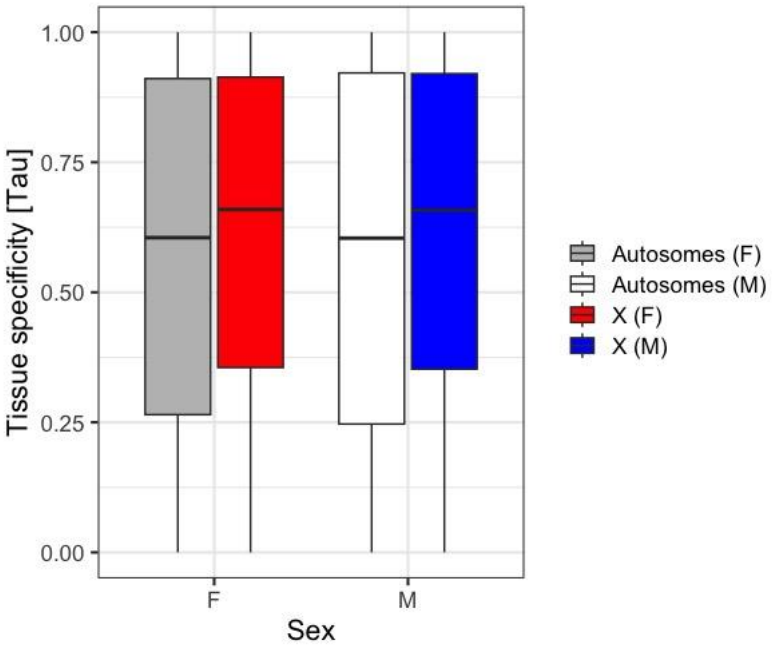

Figure 2. X-linked genes are more tissue-specific in their expression than autosomal genes. Tissue specificity of expression for genes on the X chromosome in males (blue box) and females (red box), compared to autosomal genes (white and gray boxes), calculated across four tissues. Boxes depict the median, the lower and upper quartiles, while the whiskers represent the minimum and maximum values, within 1.5x the interquartile range. Note that this pattern is not solely driven by averaging values across 11 autosomes or gene expression in gonads (Supplemental Figure S4).

Females express both X copies

Dosage compensation mechanisms equalize X-linked expression between males and females. This can be achieved by only changing expression in males, females, or by changing expression in both sexes. In all species studied thus far, the single X in males is hyper-expressed, but X-linked expression in females varies (reviewed in (Straub and Becker 2007; Gu and Walters 2017)). Thus, the X is hyper-expressed in males, with either no change to X expression in females (*D. melanogaster* system), reduced expression of both X chromosome copies in females (*C. elegans* system), or with females inactivating one of the X chromosomes in each cell, and the single (active) X is hyper-expressed in both sexes (therian mammal system). To develop insights into the regulation of X-linked expression in stick insect females, we studied whether one or both X chromosomes were expressed in each studied tissue, and

whether expression was biased towards one or was equal for both copies. To this end, we analyzed coverage depth of the two alleles at heterozygous sites at X linked transcripts in each female, separately for each tissue. Both alleles at heterozygous sites are present at equal frequencies in all females, indicating similar expression of both X chromosome copies at the level of each tissue (Figure 3A). Similarly, we do not detect a clear signature of silencing histone modifications on the female X (H3K9me marks; Figure 3B). Together, these findings suggest that *Timema* stick insect females do not inactivate one of their X chromosome copies.

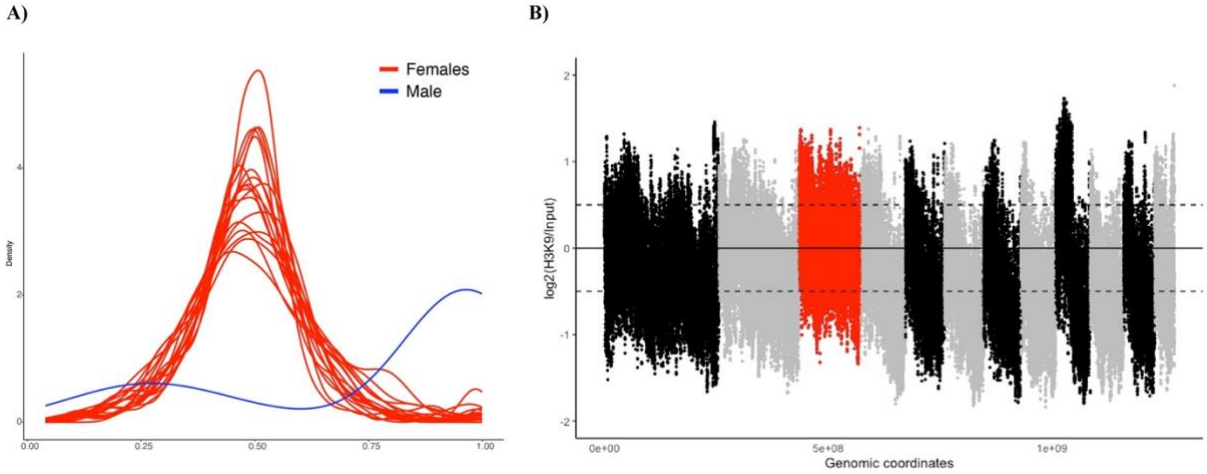

Figure 3. No evidence for dosage compensation mechanisms affecting X-linked expression in females. **A)** Distribution of coverage depths ratios for heterozygous sites on X-linked transcripts in females (red) and one male sample (blue) (used to illustrate the expected pattern for expression of a single X). **B)** H3K9me histone marks as inferred via ChIP-Seq along the genome for female somatic tissues. Different autosomes are distinguished by gray and black, the X chromosome is depicted in red.

Early presence and later absence of dosage compensation in the male reproductive tract

The patterns of X-linked expression in *Timema* male reproductive tracts differ strikingly from those observed in somatic tissues. During the first nymphal stage, there is complete dosage compensation in the reproductive tract, similar to somatic tissues (Figure 4A, B, C). However, from the 4th nymphal stage, there is a strong reduction of X-linked expression in males, relatively constant along the length of the X (Supplemental Figure S6), and which persists throughout development and until the adult stage (Figure 4). We first hypothesized that dosage compensation might be active during early gonad

development in the first nymphal stage because the tissue was not yet strongly sexually differentiated. However, this is not the case as the degree of gonadal sexual differentiation (as measured from sex biased gene expression) is relatively constant throughout development. Already 44% of the genes in gonads show sex-biased expression at the first nymphal stage, as compared to 45% at the 4th nymphal stage or 53% in adults (Supplemental Table S4; Djordjevic et al Chapter 2).

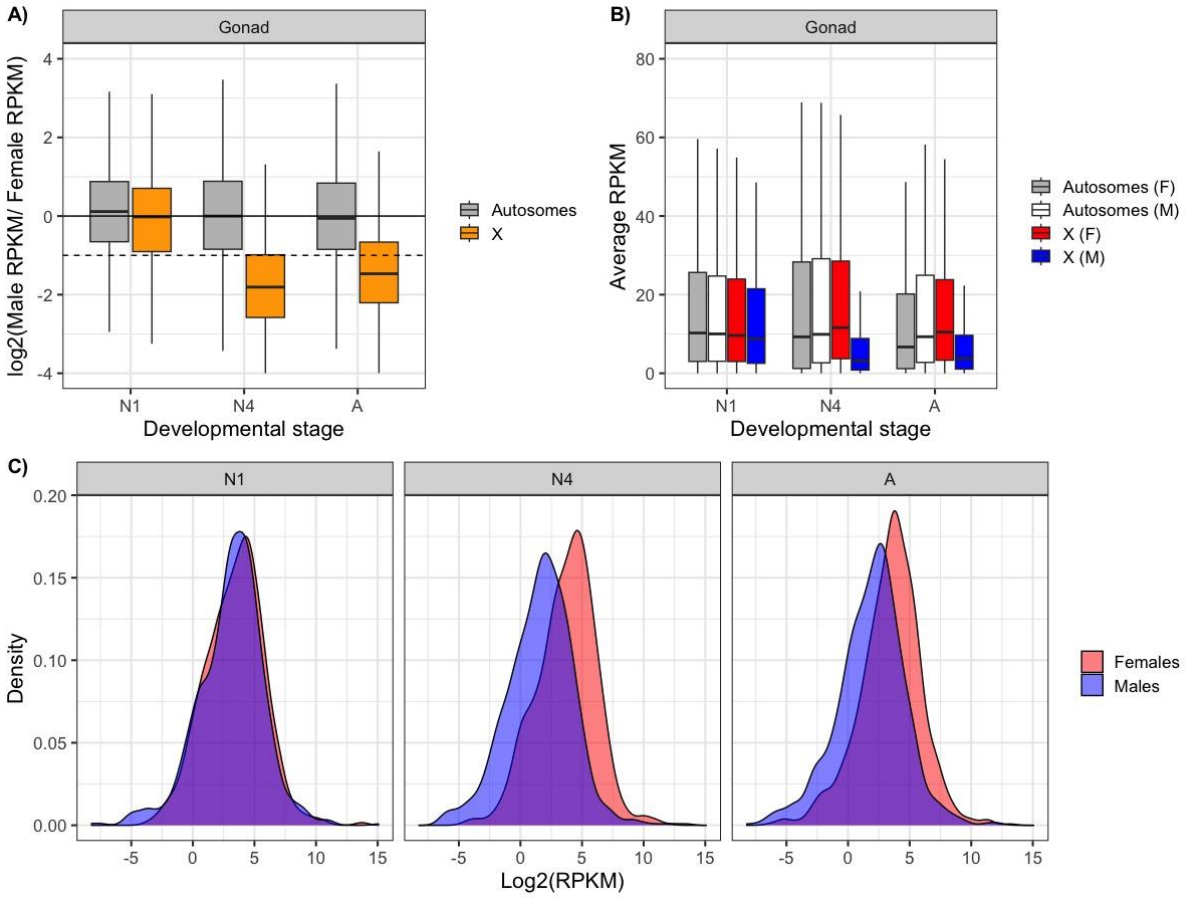

Figure 4. Absence of dosage compensation in male reproductive tracts at 4th nymphal and adult stages. **A)** Log_2 of male to female expression ratio for the X chromosome (orange) and autosomes (gray) at three developmental stages (N1- 1st nymphal, N4- 4th nymphal and A- adult stage) in the reproductive tract. See Supplemental Figure S5 for individual rather than pooled autosomes. **B)** Average expression levels (RPKM values) of genes located on the autosomes and X in females (gray and red boxes) and in males (white and blue) at three developmental stages. Boxplots depict the median, the lower and upper quartiles, while the whiskers represent the minimum and maximum values, within 1.5x the interquartile range. See Supplemental Figure S5 for individual rather than pooled autosomes. **C)** Distribution of

expression levels for X-linked genes in males (blue) and females (red) (overlapping ranges are indicated in purple).

Next, we evaluated whether the strong reduction of X-linked expression from the 4th nymphal stage was caused by meiotic X-chromosome inactivation (MSCI), as is well described in therian mammals (Turner 2015). Indeed, the extent of the reduction significantly exceeds the two-fold reduction expected in the absence of dosage compensation (Wilcoxon signed rank test with continuity correction; 4th nymphal stage: V = 77366, p-value < 2.2e-16, adult stage: V = 150046, p-value < 2.2e-16) indicating other mechanisms are affecting the expression of X linked genes in male gonads (Figure 4A, B). Immunolabeling of gonad tissue from adult and 4th nymphal stage males corroborate the transcriptional inactivity of the X chromosome. The X chromosome in male meiotic cells is visible in DAPI stainings as highly condensed ("heteropycnotic"; Figure 5), similar to other insects (Viera, et al. 2021). It also lacks a RNApol-II signal, a marker for transcriptional activity, in otherwise transcriptionally active meiotic cells (Figure 5). We then also performed immunolabelling of meiotic cells for silencing histone modifications (using an H3K9me antibody) and profiled the corresponding molecular marks in the genome using ChIP-seq based on male gonad tissue. As expected, the X has a strong H3K9 signal (Figure 6 A, B) and the corresponding H3K9me marks are enriched all along the male X (Figure 6 C), suggesting that the silencing of the X is achieved via histone modifications (Figure 6).

The patterns of MSCI in stick insects are in stark contrast to what is known about X chromosome expression in spermatocytes of *D. melanogaster*. Indeed, MSCI does not occur in *D. melanogaster*, as revealed by transcriptional profiling of *D. melanogaster* testis (Mahadevaraju, et al. 2021; Witt, et al. 2021; Raz, et al. 2023), similar RNA polymerase activity on the X and autosomes (Anderson, et al. 2023), and lack of enrichment of silencing histone modifications on the X in the male germline (Anderson, et al. 2023). As such, MSCI in stick insects shares many similarities with MSCI as described in mammals and birds (Schoenmakers, et al. 2009) but none with the more closely related fly species.

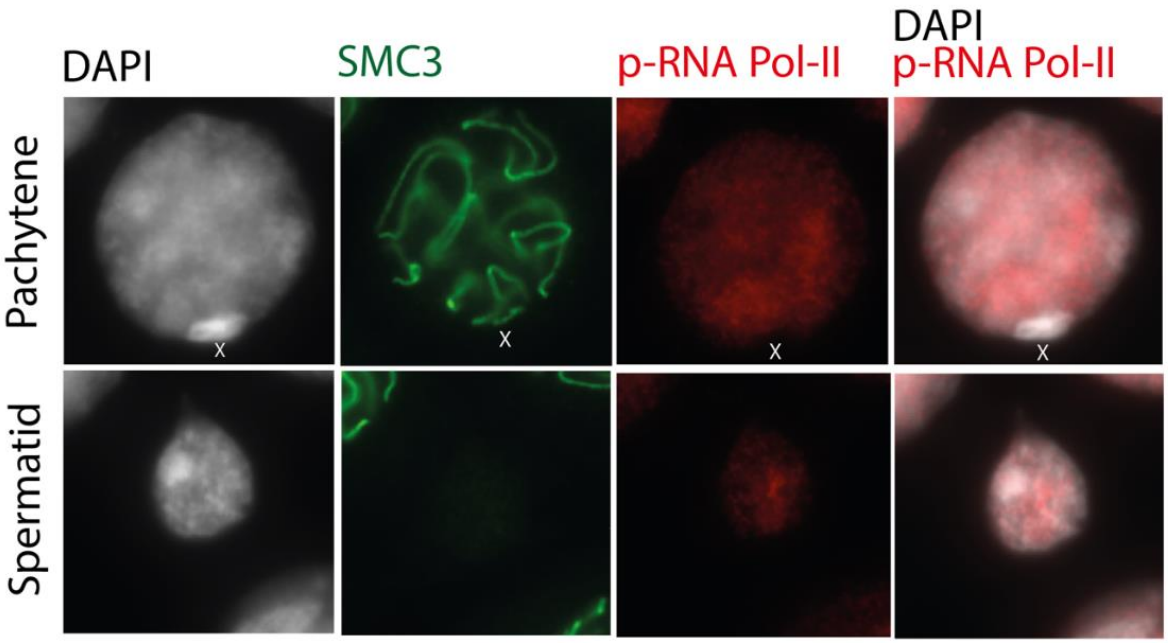

Figure 5. No transcriptional activity of the X chromosome in meiosis DAPI, SMC3, p-RNA Pol-II stainings applied to germ cell squashes of 4th nymphal stage males. Shown are two cells at different stages in meiosis for illustration. The X in each image indicates the location of the X chromosome.

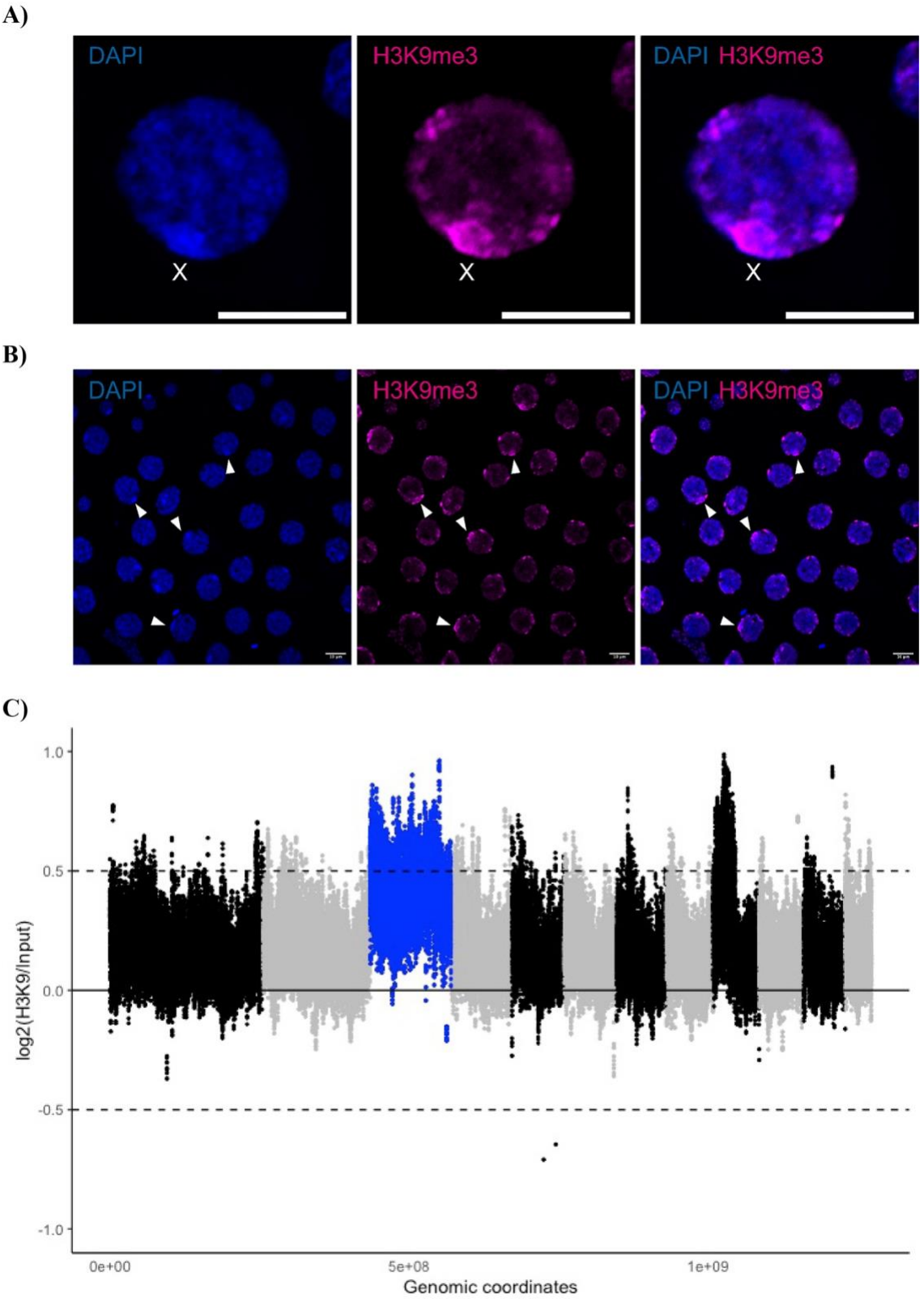

Figure 6. Enrichment of the H3K9me marks on the X chromosome in adult male testes

A, **B**) DAPI (blue) and H3K9me3 (magenta) applied to cells from male adult gonad squashes, **A**) single germ cell, with X indicating the location of the X chromosome, scale bar (10um) **B**) Many germ cells,

with arrows pointing to the X chromosome **C**) Log2 ratio of H3K9me to input ChIP-Seq data along the genome. The X chromosome is depicted in blue, while autosomes are depicted in black or grey.

At least three, mutually non-exclusive hypotheses have been proposed for the evolution of MSCI. Under the first hypothesis, inactivation would have evolved to protect un-synapsed chromosomes from damaging effects such as ectopic exchanges, non-homologous recombination, and unrepaired double-strand breaks (McKee and Handel 1993). The second hypothesis suggests that MSCI is advantageous because it prevents meiotic expression of selfish genetic elements, including sex-ratio distorters (Kelly and Aramayo 2007; Meiklejohn and Tao 2010). Finally, the third hypothesis proposes that MSCI is driven by sexually antagonistic effects of X-linked genes (Wu and Xu 2003). Because the X spends more time in females than in males, it can accumulate female-beneficial genes with detrimental effects in males (Vicoso and Charlesworth 2006). It might then be advantageous to reduce or eliminate X-expression in the late stages of spermatogenesis (Wu and Xu 2003).

The presence of MSCI in stick insects as we document here and lack thereof in *D. melanogaster* supports the first hypothesis. A key difference between male meiosis in *Timema* stick insects and *D. melanogaster* is that meiosis is achiasmatic in *Drosophila* males (McKee, et al. 1992) but chiasmatic in *Timema* (Parker, et al. 2022). The evolution of a completely achiasmatic meiosis in males means that all chromosomes, not only hemizygous sex chromosomes, would be exposed to damaging effects in the absence of synapsis. Such a situation should generate strong selection for sheltering mechanisms not linked to hemizygosity (McKee and Handel 1993).

An association between achiasmy and lack of sex chromosome inactivation is supported by a survey of older cytogenetic data in insects (McKee and Handel 1993). Chiasmatic insects, including; Orthoptera, Dictyoptera and Heteroptera, typically show sex chromosome morphologies during male meiosis that likely reflect heterochromatization, while many (though not all) achiasmatic insects do not. This pattern is consistent with the idea that achiasmatic insects evolved from ancestral, chiasmatic forms with sex chromosome inactivation; some achiasmatic groups have subsequently lost sex chromosome inactivation while others have retained it (McKee and Handel 1993).

Independently of the causes underlying the evolution of MSCI, the contrasting X-expression patterns in reproductive tracts in male hatchlings versus 4th nymphal stage likely reflect the start of meiosis I. Thus, in hatchlings where dosage compensation is complete (Figure 4A), cell divisions would be largely mitotic (spermatogonia stage). MSCI would start in cells entering meiosis I, resulting in the X-linked expression pattern we observe in reproductive tracts at the 4th nymphal stage (Figure 4A). In accordance with these interpretations, observation of cells from 4th nymphal stage testes reveal the presence of many meiotic cells, whereas we could not find a single meiotic cell in squashes from testis of male hatchlings (Supplemental Figure S7). Finally, it appears that X-linked expression is somewhat elevated in reproductive tracts of adult males as compared to those of 4th nymphal stage males (Figure 4A). This is most likely due to the larger portion of somatic tissues in adult male reproductive tracts, most notably accessory glands, which are very small in all nymphal stages but well developed in adults (Jelisaveta Djordjevic, personal observation). Such a pattern is known to also occur in *Caenorhabditis elegans*, where the X is completely silenced in germ cells and changes in X-linked expression during development are caused by changes in the ratio of somatic to germ cells (Kelly, et al. 2002; Deng, et al. 2011; Gu and Walters 2017). More generally, the observation of reduced X-expression in male gonads without investigation of associated mechanism is typically interpreted as lack of dosage compensation in this tissue (Vicoso and Bachtrog 2015; Gu, et al. 2017; Hu, et al. 2022; Parker, et al. 2022). However, as we observe in *Timema*, dosage compensation in males may well be ubiquitous across tissues and developmental stages in many species, and reduced X-expression patterns would solely be driven by MSCI.

Conclusion

Dosage compensation by upregulation of the single X in males consistently occurs in somatic tissues across development in *Timema poppense*. By contrast, male X-expression in the reproductive tract is dynamic. It starts with complete dosage compensation in the first nymphal stage, when spermatogonia have not yet entered meiosis I, and is followed by X inactivation in later nymphal stages when most gonadal cells are undergoing meiotic divisions. We suggest that absence of dosage in testes is solely because of X chromosome inactivation during meiosis in germ cells.

Supplemental Material- Chapter 3

Supplemental Tables

	Adult		Nymphal 1		Nymphal 2		Nymphal 3		Nymphal 4	
Tissue	F	M	F	M	F	M	F	M	F	M
Antennae	4	4	3	2	3	3	2	3	3	3
Brain	4	4	3	3	3	3	2	3	3	3
Gonads	4	3	4	4	0	0	0	0	3	3
Guts	4	4	3	3	3	3	2	3	2	3
Legs	0	0	3	3	3	3	2	3	3	3

Supplemental Table S1. Number of replicates per sex, for every developmental stage and tissue

stage	group1	group2	p.format	tissue
N1	Autosomes	X_chromosome	8.10E-15	Antennae
N3	Autosomes	X_chromosome	< 2e-16	Antennae
A	Autosomes	X_chromosome	< 2e-16	Antennae
N2	Autosomes	X_chromosome	0.0019	Antennae
N4	Autosomes	X_chromosome	< 2e-16	Antennae
N1	Autosomes	X_chromosome	3.10E-14	Gut
N3	Autosomes	X_chromosome	0.81	Gut
N2	Autosomes	X_chromosome	0.048	Gut
N4	Autosomes	X_chromosome	0.038	Gut
A	Autosomes	X_chromosome	0.119	Gut
N1	Autosomes	X_chromosome	4.80E-11	Leg
N3	Autosomes	X_chromosome	9.10E-05	Leg
N2	Autosomes	X_chromosome	0.015	Leg
N4	Autosomes	X_chromosome	4.60E-14	Leg
N1	Autosomes	X_chromosome	<2e-16	Brain
N3	Autosomes	X_chromosome	0.575	Brain
A	Autosomes	X_chromosome	<2e-16	Brain
N2	Autosomes	X_chromosome	0.025	Brain
N4	Autosomes	X_chromosome	<2e-16	Brain

Supplemental Table S2. Results of Wilcoxon tests where the ratio of male to female average RPKM values were compared between autosomes and the X chromosome within every developmental stage and somatic tissue. The column "stage" indicates the developmental stage; N1-N4 (1st to 4th nymphal

stage), A- adult stage, the column “tissue” the different tissues Column; “p.format”- fdr correction of p-values for multiple testing using the Benjamini & Hochberg method (Benjamini and Hochberg 1995).

stage	group1	group2	p.format	tissue
A	Autosomes_F	X_chromosome_F	0.03347	Antennae
A	Autosomes_F	Autosomes_M	0.6899	Antennae
A	Autosomes_F	X_chromosome_M	0.28741	Antennae
A	X_chromosome_F	Autosomes_M	0.02686	Antennae
A	X_chromosome_F	X_chromosome_M	0.01837	Antennae
A	Autosomes_M	X_chromosome_M	0.36216	Antennae
N4	Autosomes_F	X_chromosome_F	0.01953	Antennae
N4	Autosomes_F	Autosomes_M	0.37115	Antennae
N4	Autosomes_F	X_chromosome_M	4.80E-05	Antennae
N4	X_chromosome_F	Autosomes_M	0.00663	Antennae
N4	X_chromosome_F	X_chromosome_M	0.19624	Antennae
N4	Autosomes_M	X_chromosome_M	8.00E-06	Antennae
N2	Autosomes_F	X_chromosome_F	0.05908	Antennae
N2	Autosomes_F	Autosomes_M	0.67496	Antennae
N2	Autosomes_F	X_chromosome_M	0.00026	Antennae
N2	X_chromosome_F	Autosomes_M	0.08587	Antennae
N2	X_chromosome_F	X_chromosome_M	0.17806	Antennae
N2	Autosomes_M	X_chromosome_M	0.00051	Antennae
N3	Autosomes_F	X_chromosome_F	0.22076	Antennae
N3	Autosomes_F	Autosomes_M	0.49011	Antennae
N3	Autosomes_F	X_chromosome_M	7.80E-07	Antennae
N3	X_chromosome_F	Autosomes_M	0.34885	Antennae
N3	X_chromosome_F	X_chromosome_M	0.00592	Antennae
N3	Autosomes_M	X_chromosome_M	5.10E-06	Antennae
N1	Autosomes_F	X_chromosome_F	0.41249	Antennae
N1	Autosomes_F	Autosomes_M	0.00749	Antennae
N1	Autosomes_F	X_chromosome_M	0.41654	Antennae
N1	X_chromosome_F	Autosomes_M	0.92076	Antennae
N1	X_chromosome_F	X_chromosome_M	0.18314	Antennae
N1	Autosomes_M	X_chromosome_M	0.06545	Antennae
N1	Autosomes_F	X_chromosome_F	0.00158	Gut
N1	Autosomes_F	Autosomes_M	0.10553	Gut
N1	Autosomes_F	X_chromosome_M	6.00E-06	Gut
N1	X_chromosome_F	Autosomes_M	0.00015	Gut
N1	X_chromosome_F	X_chromosome_M	0.25817	Gut
N1	Autosomes_M	X_chromosome_M	2.00E-07	Gut
N4	Autosomes_F	X_chromosome_F	0.92544	Gut

N4	Autosomes_F	Autosomes_M	0.07545	Gut
N4	Autosomes_F	X_chromosome_M	0.07073	Gut
N4	X_chromosome_F	Autosomes_M	0.56423	Gut
N4	X_chromosome_F	X_chromosome_M	0.20523	Gut
N4	Autosomes_M	X_chromosome_M	0.25729	Gut
N2	Autosomes_F	X_chromosome_F	7.60E-07	Gut
N2	Autosomes_F	Autosomes_M	0.38691	Gut
N2	Autosomes_F	X_chromosome_M	2.30E-09	Gut
N2	X_chromosome_F	Autosomes_M	1.30E-07	Gut
N2	X_chromosome_F	X_chromosome_M	0.38866	Gut
N2	Autosomes_M	X_chromosome_M	2.20E-10	Gut
N3	Autosomes_F	X_chromosome_F	1.10E-06	Gut
N3	Autosomes_F	Autosomes_M	8.10E-08	Gut
N3	Autosomes_F	X_chromosome_M	0.00122	Gut
N3	X_chromosome_F	Autosomes_M	9.80E-13	Gut
N3	X_chromosome_F	X_chromosome_M	0.18544	Gut
N3	Autosomes_M	X_chromosome_M	3.80E-08	Gut
A	Autosomes_F	X_chromosome_F	9.00E-05	Gut
A	Autosomes_F	Autosomes_M	0.13749	Gut
A	Autosomes_F	X_chromosome_M	0.00013	Gut
A	X_chromosome_F	Autosomes_M	4.80E-06	Gut
A	X_chromosome_F	X_chromosome_M	0.90971	Gut
A	Autosomes_M	X_chromosome_M	7.60E-06	Gut
N4	Autosomes_F	X_chromosome_F	0.10405	Leg
N4	Autosomes_F	Autosomes_M	0.33953	Leg
N4	Autosomes_F	X_chromosome_M	0.00063	Leg
N4	X_chromosome_F	Autosomes_M	0.22252	Leg
N4	X_chromosome_F	X_chromosome_M	0.18551	Leg
N4	Autosomes_M	X_chromosome_M	0.0027	Leg
N2	Autosomes_F	X_chromosome_F	0.14464	Leg
N2	Autosomes_F	Autosomes_M	0.49108	Leg
N2	Autosomes_F	X_chromosome_M	0.00302	Leg
N2	X_chromosome_F	Autosomes_M	0.24054	Leg
N2	X_chromosome_F	X_chromosome_M	0.25593	Leg
N2	Autosomes_M	X_chromosome_M	0.00733	Leg
N3	Autosomes_F	X_chromosome_F	0.12741	Leg
N3	Autosomes_F	Autosomes_M	0.76636	Leg
N3	Autosomes_F	X_chromosome_M	0.01095	Leg
N3	X_chromosome_F	Autosomes_M	0.09981	Leg
N3	X_chromosome_F	X_chromosome_M	0.43813	Leg
N3	Autosomes_M	X_chromosome_M	0.0083	Leg
N1	Autosomes_F	X_chromosome_F	0.14473	Leg
N1	Autosomes_F	Autosomes_M	0.04366	Leg

N1	Autosomes_F	X_chromosome_M	0.00191	Leg
N1	X_chromosome_F	Autosomes_M	0.02297	Leg
N1	X_chromosome_F	X_chromosome_M	0.20916	Leg
N1	Autosomes_M	X_chromosome_M	8.80E-05	Leg
A	Autosomes_F	X_chromosome_F	0.0605	Brain
A	Autosomes_F	Autosomes_M	0.4587	Brain
A	Autosomes_F	X_chromosome_M	0.1901	Brain
A	X_chromosome_F	Autosomes_M	0.0313	Brain
A	X_chromosome_F	X_chromosome_M	0.016	Brain
A	Autosomes_M	X_chromosome_M	0.3082	Brain
N4	Autosomes_F	X_chromosome_F	0.4743	Brain
N4	Autosomes_F	Autosomes_M	0.86	Brain
N4	Autosomes_F	X_chromosome_M	0.0403	Brain
N4	X_chromosome_F	Autosomes_M	0.4343	Brain
N4	X_chromosome_F	X_chromosome_M	0.3154	Brain
N4	Autosomes_M	X_chromosome_M	0.0355	Brain
N2	Autosomes_F	X_chromosome_F	0.3723	Brain
N2	Autosomes_F	Autosomes_M	0.9969	Brain
N2	Autosomes_F	X_chromosome_M	0.0155	Brain
N2	X_chromosome_F	Autosomes_M	0.3741	Brain
N2	X_chromosome_F	X_chromosome_M	0.2555	Brain
N2	Autosomes_M	X_chromosome_M	0.0157	Brain
N3	Autosomes_F	X_chromosome_F	0.0285	Brain
N3	Autosomes_F	Autosomes_M	< 2e-16	Brain
N3	Autosomes_F	X_chromosome_M	0.0637	Brain
N3	X_chromosome_F	Autosomes_M	1.20E-10	Brain
N3	X_chromosome_F	X_chromosome_M	0.0027	Brain
N3	Autosomes_M	X_chromosome_M	0.011	Brain
N1	Autosomes_F	X_chromosome_F	0.7118	Brain
N1	Autosomes_F	Autosomes_M	0.986	Brain
N1	Autosomes_F	X_chromosome_M	0.0364	Brain
N1	X_chromosome_F	Autosomes_M	0.7191	Brain
N1	X_chromosome_F	X_chromosome_M	0.0654	Brain
N1	Autosomes_M	X_chromosome_M	0.0353	Brain

Supplemental Table S3. Results of Wilcoxon tests where average RPKM values were compared for autosomal and X-linked genes for each sex and within each developmental stage and somatic tissue (indicated in the "Tissue" column). The "Stage" column denotes the developmental stage, with N1-N4 representing the 1st to 4th nymphal stages and A indicating the adult stage. **Columns: Group1 and Group2:** Specify the groups being compared, with colored cells highlighting the comparisons of

interest. **"p.format":** Represents the false discovery rate (FDR) corrected p-values, utilizing the Benjamini & Hochberg method for multiple testing.

	N1 (%)	N4 (%)	A (%)
MB	2544 (19.8)	3753 (25.4)	4330 (30)
FB	3107 (24.2)	2866 (19.4)	3418 (23.4)
SB	5651 (44.1)	6619 (45)	7748 (53)
T	12830	14790	14626

Supplemental Table S4. Sex-biased gene counts during reproductive tract development at N1 (1st nymphal), N4 (4th nymphal), and A (adult) stages. It includes MB (male-biased), FB (female-biased), SB (total sex-biased genes), and T (total expressed genes) categories, with percentages in brackets. Differential gene expression between the sexes was assessed using a generalized linear model with a quasi-likelihood F-test (Chen, et al. 2016) in edgeR v.3.42.4 (Robinson, et al. 2009; McCarthy, et al. 2012) in each of the three developmental stages.

variable	group1	group2	p.format
Females	Tps_LRv5b_scf1	Tps_LRv5b_scf2	0.00787
Females	Tps_LRv5b_scf1	Tps_LRv5b_scf3	< 2e-16
Females	Tps_LRv5b_scf1	Tps_LRv5b_scf4	0.00132
Females	Tps_LRv5b_scf1	Tps_LRv5b_scf5	0.00012
Females	Tps_LRv5b_scf1	Tps_LRv5b_scf6	0.22259
Females	Tps_LRv5b_scf1	Tps_LRv5b_scf7	0.10729
Females	Tps_LRv5b_scf1	Tps_LRv5b_scf8	0.00318
Females	Tps_LRv5b_scf1	Tps_LRv5b_scf9	0.18078
Females	Tps_LRv5b_scf1	Tps_LRv5b_scf10	0.00112
Females	Tps_LRv5b_scf1	Tps_LRv5b_scf11	4.70E-11
Females	Tps_LRv5b_scf1	Tps_LRv5b_scf12	0.11296
Females	Tps_LRv5b_scf2	Tps_LRv5b_scf3	3.40E-08
Females	Tps_LRv5b_scf2	Tps_LRv5b_scf4	0.43516
Females	Tps_LRv5b_scf2	Tps_LRv5b_scf5	0.16298
Females	Tps_LRv5b_scf2	Tps_LRv5b_scf6	0.38374
Females	Tps_LRv5b_scf2	Tps_LRv5b_scf7	0.60092
Females	Tps_LRv5b_scf2	Tps_LRv5b_scf8	0.38869
Females	Tps_LRv5b_scf2	Tps_LRv5b_scf9	0.0024
Females	Tps_LRv5b_scf2	Tps_LRv5b_scf10	1.60E-06
Females	Tps_LRv5b_scf2	Tps_LRv5b_scf11	4.40E-05
Females	Tps_LRv5b_scf2	Tps_LRv5b_scf12	0.90298
Females	Tps_LRv5b_scf3	Tps_LRv5b_scf4	1.60E-05

Females	Tps_LRv5b_scf3	Tps_LRv5b_scf5	0.00047
Females	Tps_LRv5b_scf3	Tps_LRv5b_scf6	3.10E-08
Females	Tps_LRv5b_scf3	Tps_LRv5b_scf7	4.20E-07
Females	Tps_LRv5b_scf3	Tps_LRv5b_scf8	0.00015
Females	Tps_LRv5b_scf3	Tps_LRv5b_scf9	8.50E-12
Females	Tps_LRv5b_scf3	Tps_LRv5b_scf10	< 2e-16
Females	Tps_LRv5b_scf3	Tps_LRv5b_scf11	0.42835
Females	Tps_LRv5b_scf3	Tps_LRv5b_scf12	3.40E-05
Females	Tps_LRv5b_scf4	Tps_LRv5b_scf5	0.53249
Females	Tps_LRv5b_scf4	Tps_LRv5b_scf6	0.14825
Females	Tps_LRv5b_scf4	Tps_LRv5b_scf7	0.26394
Females	Tps_LRv5b_scf4	Tps_LRv5b_scf8	0.88165
Females	Tps_LRv5b_scf4	Tps_LRv5b_scf9	0.00082
Females	Tps_LRv5b_scf4	Tps_LRv5b_scf10	4.20E-07
Females	Tps_LRv5b_scf4	Tps_LRv5b_scf11	0.00163
Females	Tps_LRv5b_scf4	Tps_LRv5b_scf12	0.49576
Females	Tps_LRv5b_scf5	Tps_LRv5b_scf6	0.05178
Females	Tps_LRv5b_scf5	Tps_LRv5b_scf7	0.09907
Females	Tps_LRv5b_scf5	Tps_LRv5b_scf8	0.69919
Females	Tps_LRv5b_scf5	Tps_LRv5b_scf9	0.00019
Females	Tps_LRv5b_scf5	Tps_LRv5b_scf10	6.00E-08
Females	Tps_LRv5b_scf5	Tps_LRv5b_scf11	0.01288
Females	Tps_LRv5b_scf5	Tps_LRv5b_scf12	0.23798
Females	Tps_LRv5b_scf6	Tps_LRv5b_scf7	0.81434
Females	Tps_LRv5b_scf6	Tps_LRv5b_scf8	0.13891
Females	Tps_LRv5b_scf6	Tps_LRv5b_scf9	0.03726
Females	Tps_LRv5b_scf6	Tps_LRv5b_scf10	0.00038
Females	Tps_LRv5b_scf6	Tps_LRv5b_scf11	1.70E-05
Females	Tps_LRv5b_scf6	Tps_LRv5b_scf12	0.62415
Females	Tps_LRv5b_scf7	Tps_LRv5b_scf8	0.2336
Females	Tps_LRv5b_scf7	Tps_LRv5b_scf9	0.02975
Females	Tps_LRv5b_scf7	Tps_LRv5b_scf10	0.00021
Females	Tps_LRv5b_scf7	Tps_LRv5b_scf11	7.80E-05
Females	Tps_LRv5b_scf7	Tps_LRv5b_scf12	0.86027
Females	Tps_LRv5b_scf8	Tps_LRv5b_scf9	0.00103
Females	Tps_LRv5b_scf8	Tps_LRv5b_scf10	1.60E-06
Females	Tps_LRv5b_scf8	Tps_LRv5b_scf11	0.00668
Females	Tps_LRv5b_scf8	Tps_LRv5b_scf12	0.47339
Females	Tps_LRv5b_scf9	Tps_LRv5b_scf10	0.21877
Females	Tps_LRv5b_scf9	Tps_LRv5b_scf11	8.70E-09
Females	Tps_LRv5b_scf9	Tps_LRv5b_scf12	0.04245
Females	Tps_LRv5b_scf10	Tps_LRv5b_scf11	8.40E-14
Females	Tps_LRv5b_scf10	Tps_LRv5b_scf12	0.00053
Females	Tps_LRv5b_scf11	Tps_LRv5b_scf12	0.00161

Males	Tps_LRv5b_scf1	Tps_LRv5b_scf2	0.0167
Males	Tps_LRv5b_scf1	Tps_LRv5b_scf3	< 2e-16
Males	Tps_LRv5b_scf1	Tps_LRv5b_scf4	0.00088
Males	Tps_LRv5b_scf1	Tps_LRv5b_scf5	1.70E-05
Males	Tps_LRv5b_scf1	Tps_LRv5b_scf6	0.20824
Males	Tps_LRv5b_scf1	Tps_LRv5b_scf7	0.96411
Males	Tps_LRv5b_scf1	Tps_LRv5b_scf8	0.00149
Males	Tps_LRv5b_scf1	Tps_LRv5b_scf9	0.28751
Males	Tps_LRv5b_scf1	Tps_LRv5b_scf10	7.90E-06
Males	Tps_LRv5b_scf1	Tps_LRv5b_scf11	2.90E-09
Males	Tps_LRv5b_scf1	Tps_LRv5b_scf12	0.11008
Males	Tps_LRv5b_scf2	Tps_LRv5b_scf3	1.30E-10
Males	Tps_LRv5b_scf2	Tps_LRv5b_scf4	0.28657
Males	Tps_LRv5b_scf2	Tps_LRv5b_scf5	0.03869
Males	Tps_LRv5b_scf2	Tps_LRv5b_scf6	0.51707
Males	Tps_LRv5b_scf2	Tps_LRv5b_scf7	0.06628
Males	Tps_LRv5b_scf2	Tps_LRv5b_scf8	0.21531
Males	Tps_LRv5b_scf2	Tps_LRv5b_scf9	0.00942
Males	Tps_LRv5b_scf2	Tps_LRv5b_scf10	1.00E-08
Males	Tps_LRv5b_scf2	Tps_LRv5b_scf11	0.00023
Males	Tps_LRv5b_scf2	Tps_LRv5b_scf12	0.96537
Males	Tps_LRv5b_scf3	Tps_LRv5b_scf4	6.50E-07
Males	Tps_LRv5b_scf3	Tps_LRv5b_scf5	0.00013
Males	Tps_LRv5b_scf3	Tps_LRv5b_scf6	5.50E-10
Males	Tps_LRv5b_scf3	Tps_LRv5b_scf7	2.10E-12
Males	Tps_LRv5b_scf3	Tps_LRv5b_scf8	2.30E-05
Males	Tps_LRv5b_scf3	Tps_LRv5b_scf9	1.00E-12
Males	Tps_LRv5b_scf3	Tps_LRv5b_scf10	< 2e-16
Males	Tps_LRv5b_scf3	Tps_LRv5b_scf11	0.04983
Males	Tps_LRv5b_scf3	Tps_LRv5b_scf12	2.80E-06
Males	Tps_LRv5b_scf4	Tps_LRv5b_scf5	0.32561
Males	Tps_LRv5b_scf4	Tps_LRv5b_scf6	0.13505
Males	Tps_LRv5b_scf4	Tps_LRv5b_scf7	0.01089
Males	Tps_LRv5b_scf4	Tps_LRv5b_scf8	0.77626
Males	Tps_LRv5b_scf4	Tps_LRv5b_scf9	0.00172
Males	Tps_LRv5b_scf4	Tps_LRv5b_scf10	6.60E-10
Males	Tps_LRv5b_scf4	Tps_LRv5b_scf11	0.00993
Males	Tps_LRv5b_scf4	Tps_LRv5b_scf12	0.47344
Males	Tps_LRv5b_scf5	Tps_LRv5b_scf6	0.01845
Males	Tps_LRv5b_scf5	Tps_LRv5b_scf7	0.00083
Males	Tps_LRv5b_scf5	Tps_LRv5b_scf8	0.54719
Males	Tps_LRv5b_scf5	Tps_LRv5b_scf9	0.00011
Males	Tps_LRv5b_scf5	Tps_LRv5b_scf10	9.80E-12
Males	Tps_LRv5b_scf5	Tps_LRv5b_scf11	0.1175

Males	Tps_LRv5b_scf5	Tps_LRv5b_scf12	0.15377
Males	Tps_LRv5b_scf6	Tps_LRv5b_scf7	0.27558
Males	Tps_LRv5b_scf6	Tps_LRv5b_scf8	0.10207
Males	Tps_LRv5b_scf6	Tps_LRv5b_scf9	0.06475
Males	Tps_LRv5b_scf6	Tps_LRv5b_scf10	4.30E-06
Males	Tps_LRv5b_scf6	Tps_LRv5b_scf11	0.00016
Males	Tps_LRv5b_scf6	Tps_LRv5b_scf12	0.62107
Males	Tps_LRv5b_scf7	Tps_LRv5b_scf8	0.0091
Males	Tps_LRv5b_scf7	Tps_LRv5b_scf9	0.43994
Males	Tps_LRv5b_scf7	Tps_LRv5b_scf10	0.00059
Males	Tps_LRv5b_scf7	Tps_LRv5b_scf11	2.40E-06
Males	Tps_LRv5b_scf7	Tps_LRv5b_scf12	0.19706
Males	Tps_LRv5b_scf8	Tps_LRv5b_scf9	0.00138
Males	Tps_LRv5b_scf8	Tps_LRv5b_scf10	3.50E-09
Males	Tps_LRv5b_scf8	Tps_LRv5b_scf11	0.04051
Males	Tps_LRv5b_scf8	Tps_LRv5b_scf12	0.38504
Males	Tps_LRv5b_scf9	Tps_LRv5b_scf10	0.0189
Males	Tps_LRv5b_scf9	Tps_LRv5b_scf11	4.30E-07
Males	Tps_LRv5b_scf9	Tps_LRv5b_scf12	0.06398
Males	Tps_LRv5b_scf10	Tps_LRv5b_scf11	2.20E-15
Males	Tps_LRv5b_scf10	Tps_LRv5b_scf12	1.50E-05
Males	Tps_LRv5b_scf11	Tps_LRv5b_scf12	0.00672

Supplemental Table S5. Wilcoxon tests comparing tissue specificity [Tau], calculated across three somatic tissues, between scaffolds within each sex **("variable"**; Females, Males). **Columns: Group1 and Group2:** Specify the scaffolds being compared, with colored cells highlighting the comparisons of interest, **"p.format":** Represents the false discovery rate (FDR) corrected p-values, utilizing the Benjamini & Hochberg method for multiple testing.

Supplemental Figures

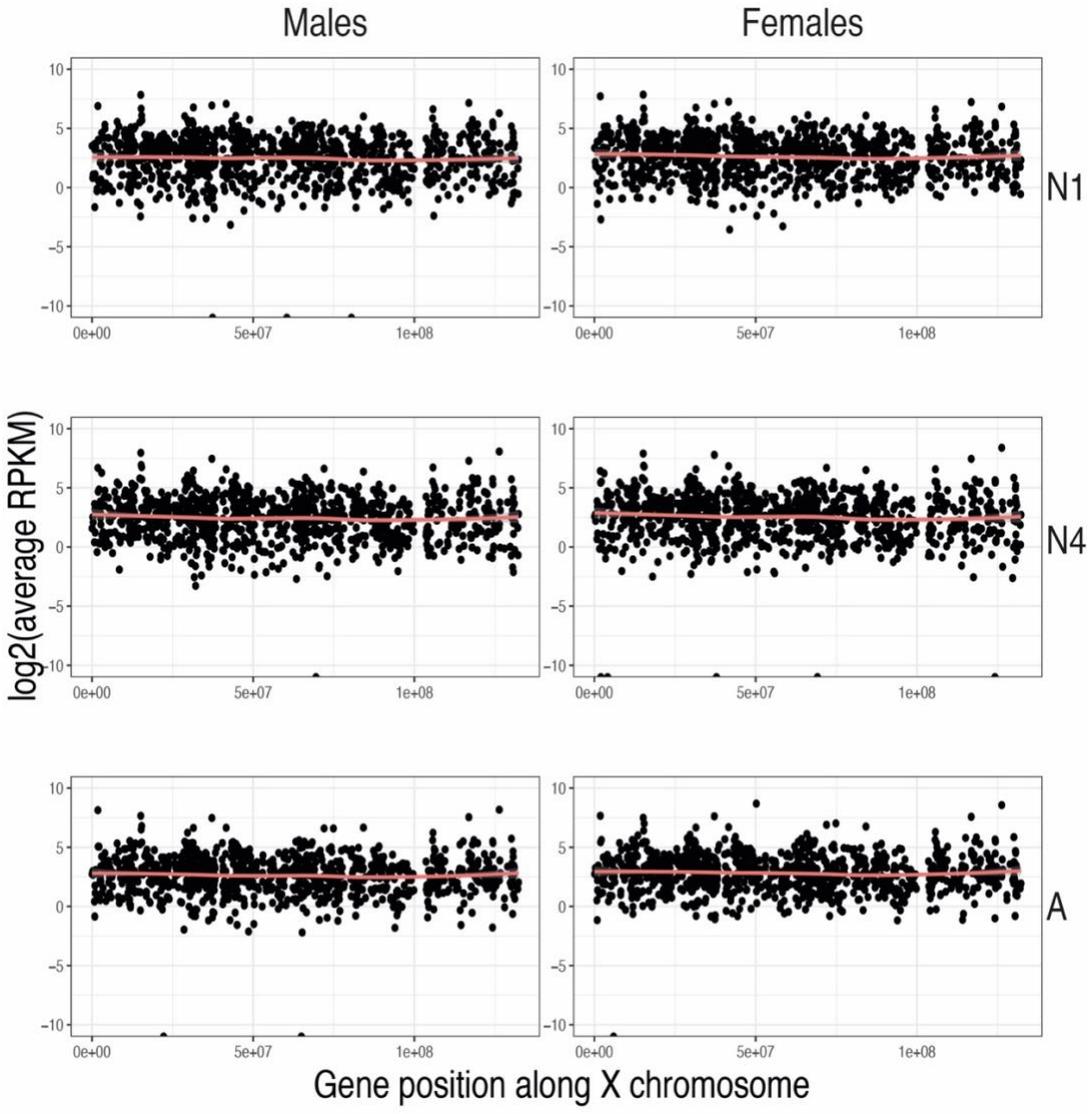

Supplemental Figure S1. Mean expression levels per gene along the X chromosome in brain somatic tissue at 1st (N1), 4th (N4) and adult (A) stages in females (left) and males (right). The line in each panel represents a loess smoothed curve.

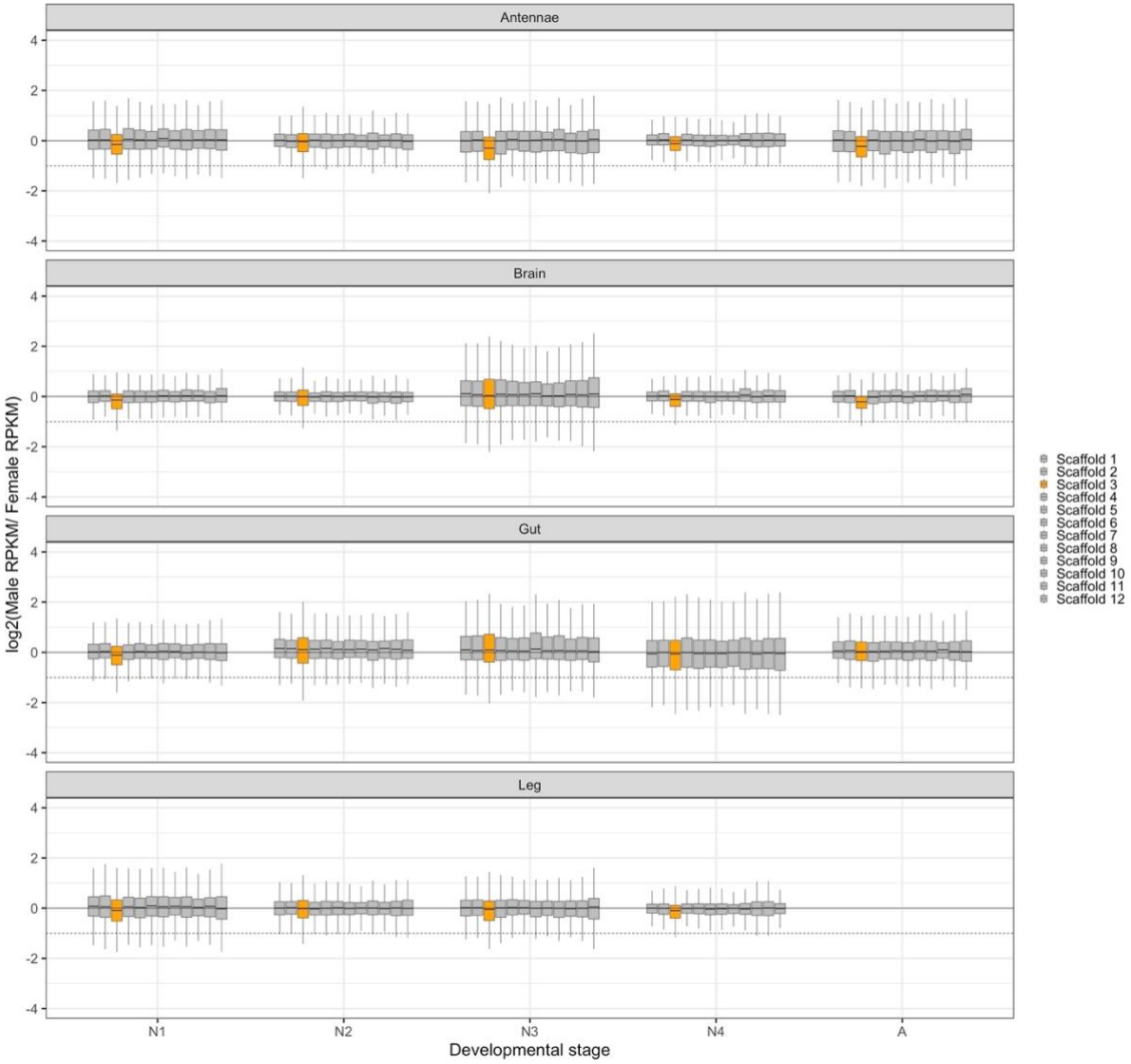

Supplemental Figure S2. Log2 of male to female expression ratio across scaffolds (representing all 12 *T. poppense* chromosomes) at five developmental stages: N1, N2, N3, N4, and A (representing the 1st to 4th nymphal stages and the adult stage, respectively). Scaffold 3, represented in orange, corresponds to the X chromosome, while autosomal scaffolds are depicted in gray. The panels, arranged from top to bottom, showcase the Log2 ratio in different somatic tissues: antenna, brain, guts, and legs. Boxplots depict the median, the lower and upper quartiles, while the whiskers represent the minimum and maximum values, within 1.5x the interquartile range.

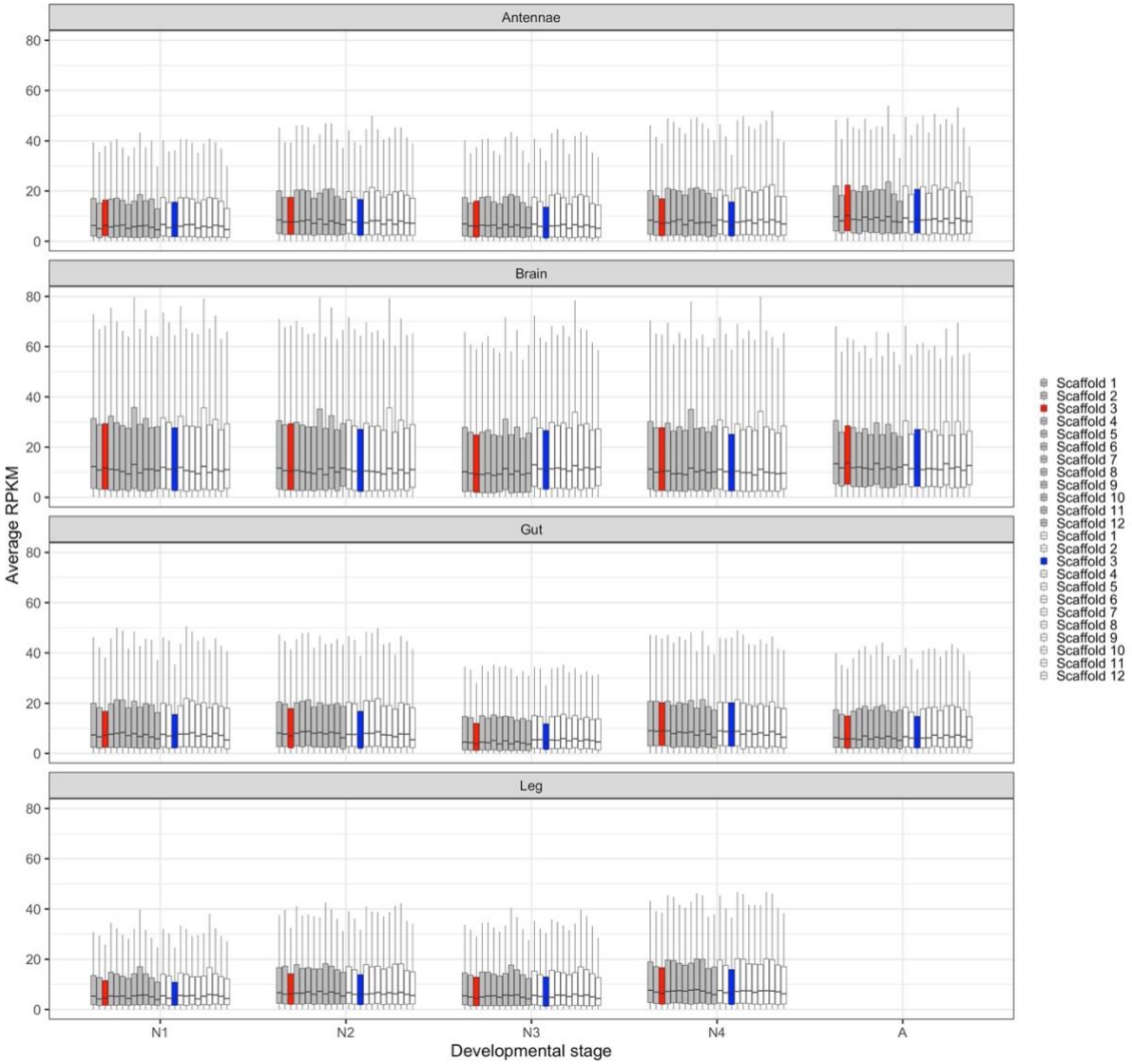

Supplemental Figure S3. Average RPKM expression levels across scaffolds in females (grey) and in males (white) along development, scaffold three corresponds to the X and is depicted in red (females) and blue (males). The panels, from top to bottom, showcase the Average RPKM in different somatic tissues: antenna, brain, guts, and legs. Boxplots depict the median, the lower and upper quartiles, while the whiskers represent the minimum and maximum values, within 1.5x the interquartile range.

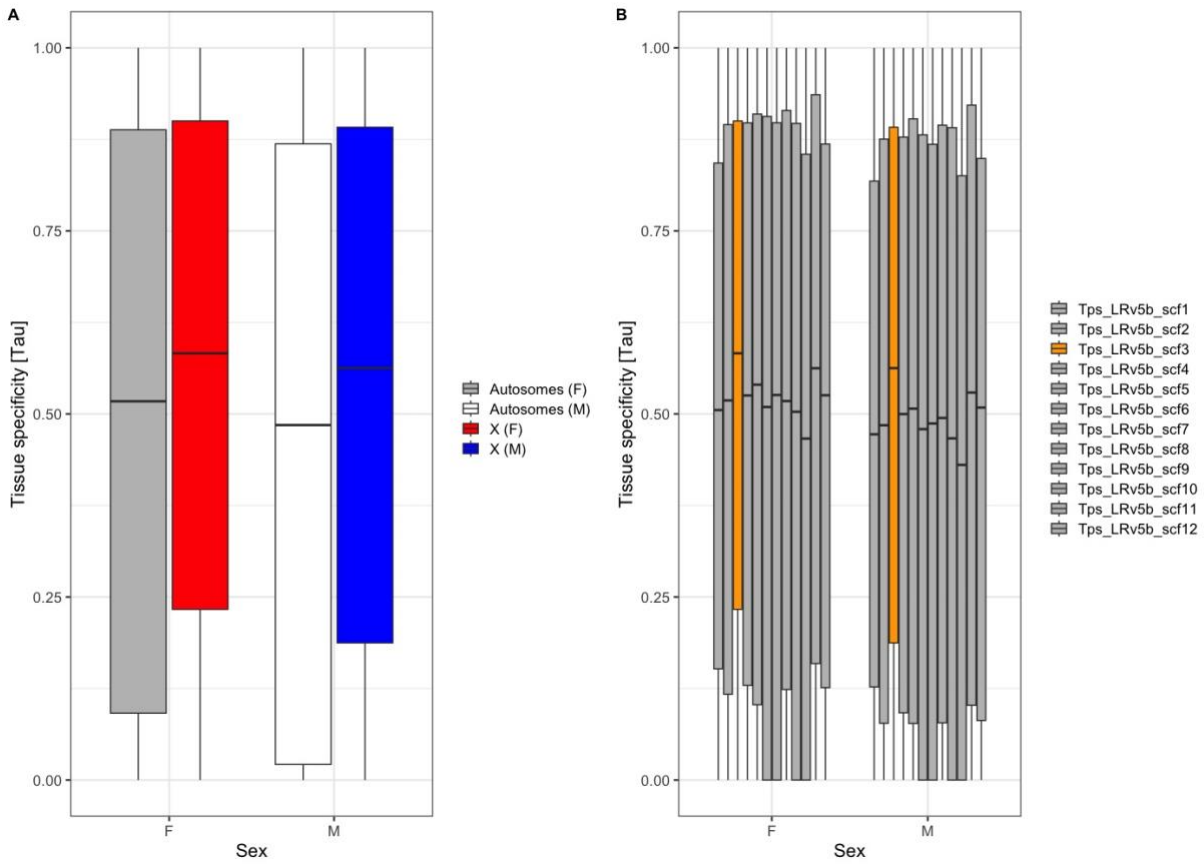

Supplemental Figure S4. A) Tissue specificity of X chromosomes in males (M) (blue box) and females (F) (red box) as compared to the autosomes (white and gray boxes), calculated across three somatic tissues. Because genes on the X are often testes or ovaries specific, we here repeated the analysis presented in the main text based on four tissues (three somatic tissues and reproductive tracts) with the three somatic tissues only, and X tissue specificity remained higher than autosomes Wilcoxon test, $p_{adj\ (females)}$= 6.7e-13, $p_{adj\ (males)}$= 2.4e-16 **B)** Tissue specificity in females (F) and males (M) across scaffolds (see Supplemental Table 5), based on three somatic tissues. Scaffold 3, represented in orange, corresponds to the X chromosome, while other scaffolds are depicted in gray. Boxplots depict the median, the lower and upper quartiles, while the whiskers represent the minimum and maximum values, within 1.5x the interquartile range.

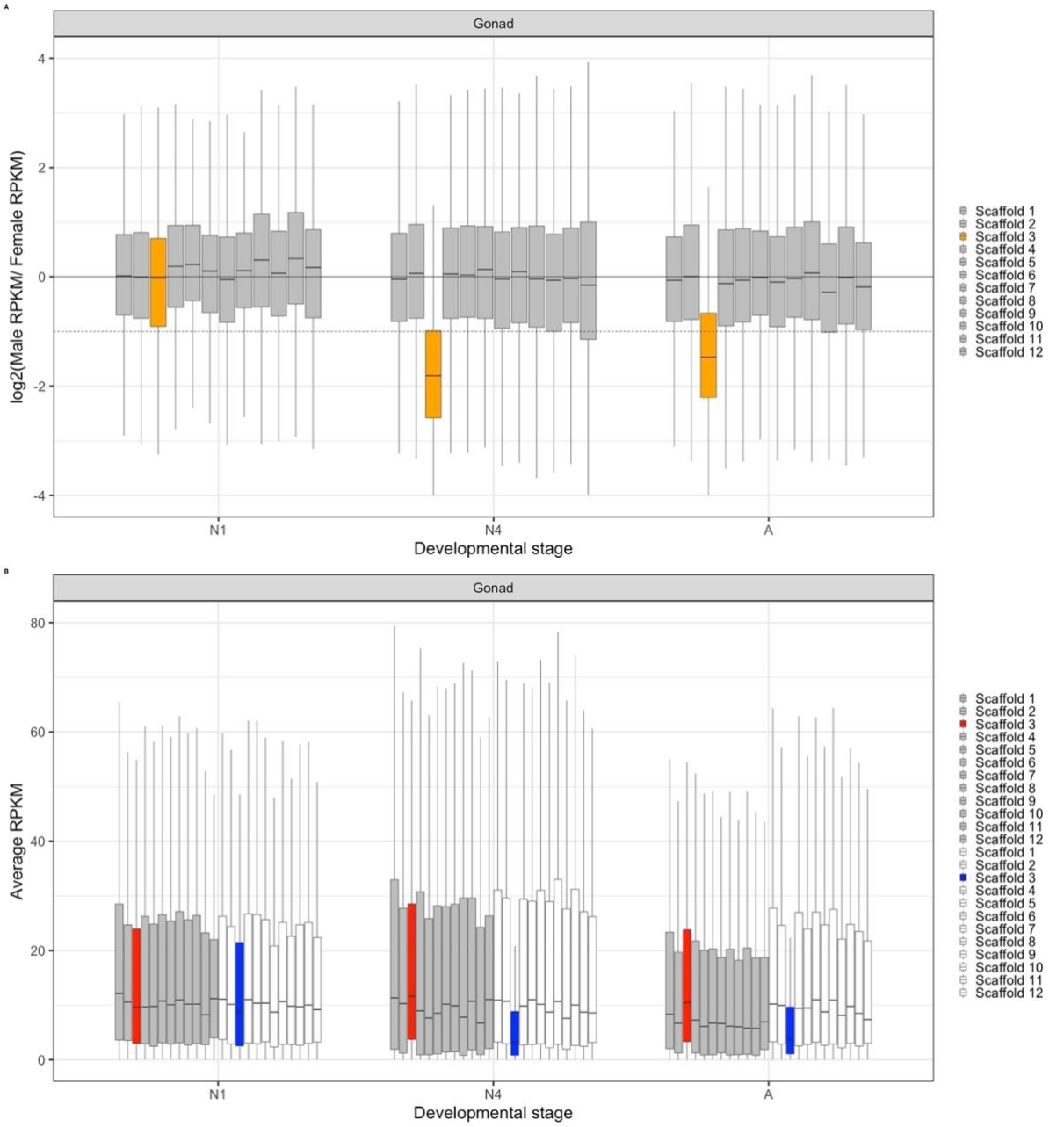

Supplemental Figure S5. A) The Log2 ratio of RPKM levels of expression between males and females across scaffolds at three developmental stages (N1, N4, and Adult) in the reproductive tract. Scaffold 3, represented in orange, corresponds to the X chromosome, while other scaffolds are depicted in gray. **B)** Average RPKM expression levels at three developmental stages (N1, N4, and adult) in the reproductive tract separated for different scaffolds (chromosomes) in females (grey) and in males (white) boxes, scaffold three corresponds to the X and is depicted in red (females) and blue (males). Boxplots depict the median, the lower and upper quartiles, while the whiskers represent the minimum and maximum values, within 1.5x the interquartile range.

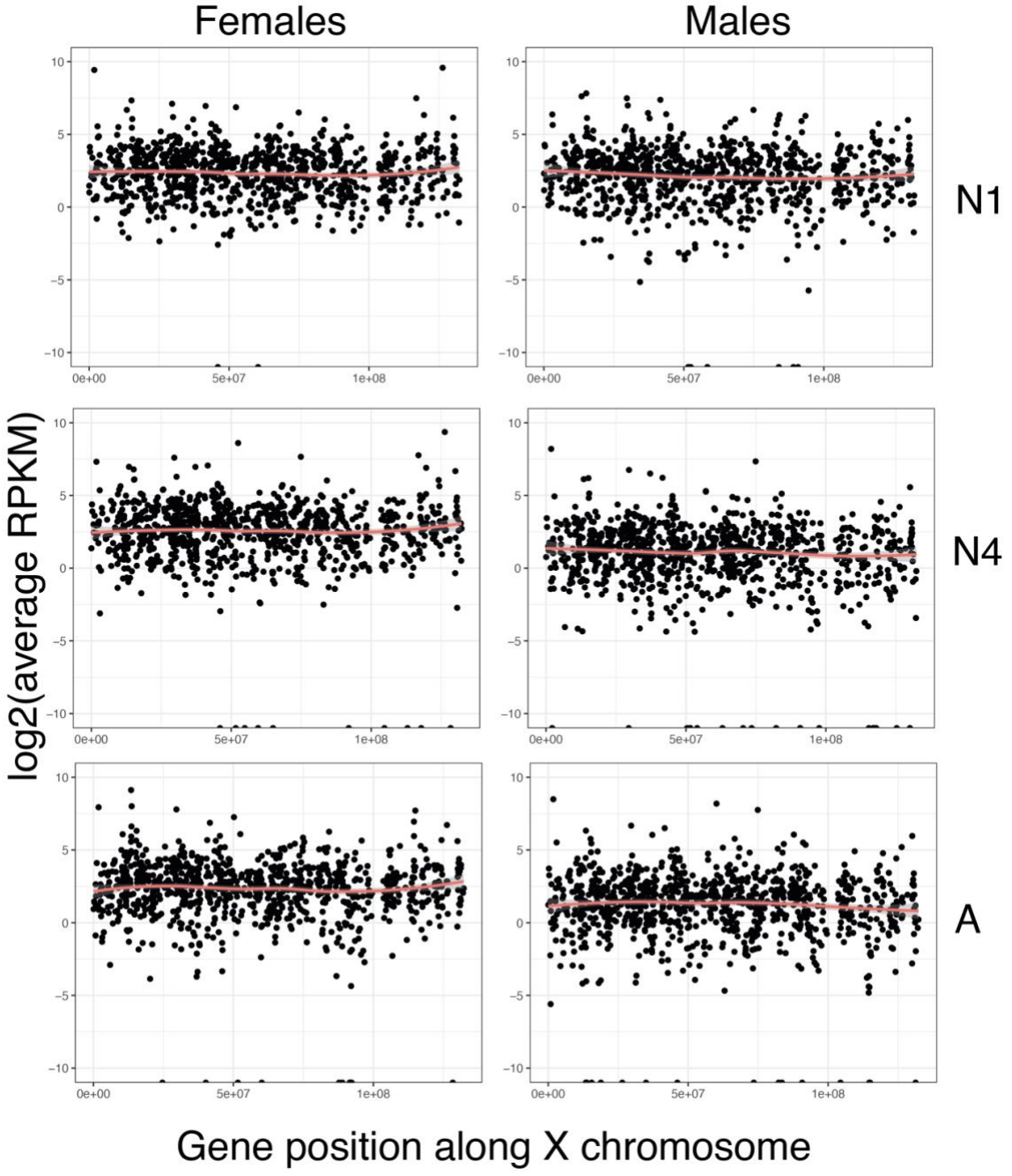

Supplemental Figure S6. Mean expression RPKM levels per gene along the X chromosome at 1st (N1), 4th (N4) and Adult (A) stages in reproductive tracts of females (left) and males (right) panels. The red line in each panel shows the loess smoothed curve.

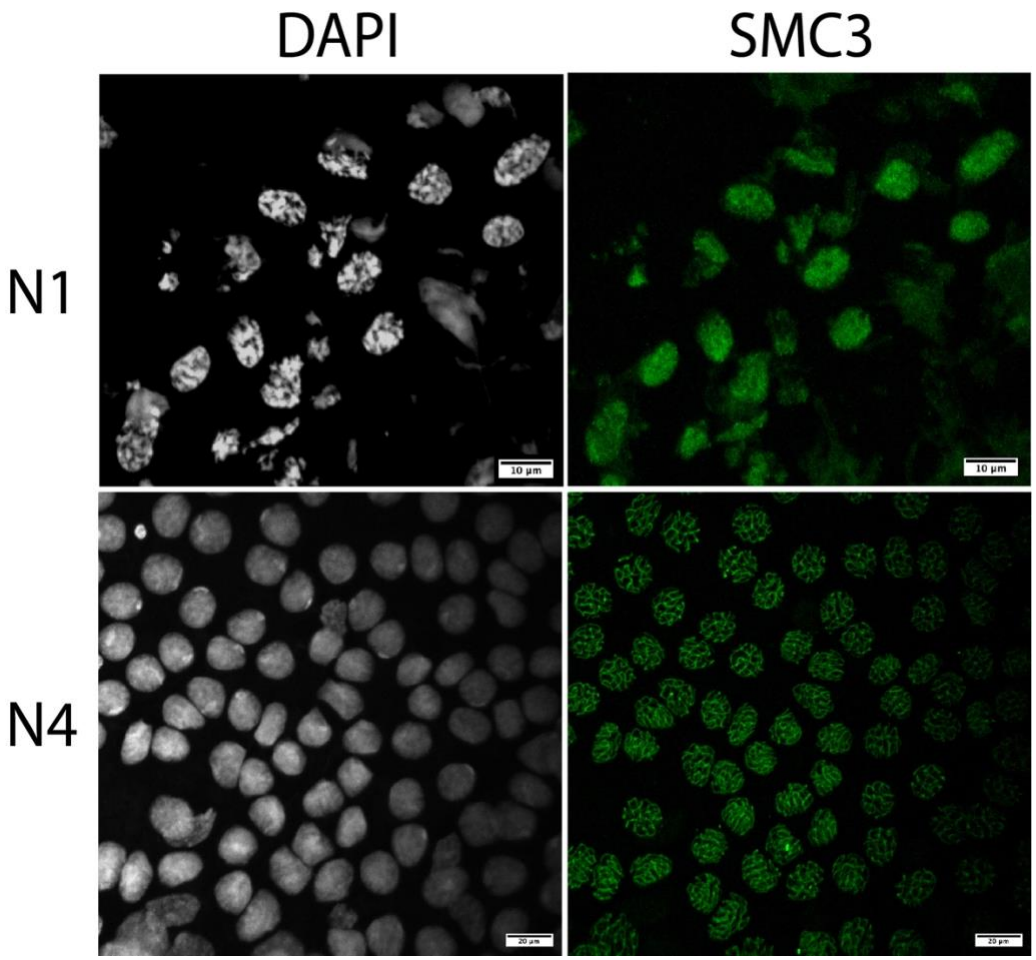

Supplemental Figure S7. DAPI, SMC3 staining applied to testes squashes of 1st (N1) and 4th (N4) nymphal stage males. No meiotic cells at N1, while there are numerous meiotic cells at (N4) with complete synapsis of chromosomes confirmed by the distinctive individualized thick chromatin threads marked by SMC3.

General discussion

The relationship between genotype and phenotype is complex and extends beyond alterations in gene coding sequences. Gene expression variation also contributes to the phenotypic diversification between and within species (Carroll, 2008; Harrison *et al*, 2012). However, how different phenotypes develop from the same shared genome remains an unanswered question. One such example is sexual dimorphism. The evolutionary interests differ between the two sexes, resulting in opposing direction of selection in males and females for different traits. Because of the shared genome, sexes might be constrained to achieve their optimal traits, resulting in sexual conflict. One way to overcome this is the sex specific regulation of gene expression.

Sexual conflict is expected to be strongest at the adult stage when the two sexes are the most differentiated. However, many sexually dimorphic traits begin developing before the adult stage. For example, in water striders (Heteroptera: Geridae), females struggle to resist multiple mating. Hence some species developed elaborated modifications in male antennae to grasp female and overcome her resistance (Khila, et al. 2012). This sexually dimorphic and sexually antagonistic trait shows early differentiation already in the 3rd instar. Despite sexual differentiation being a developmental process, little is known about the ontogeny of gene regulation underlying sexual dimorphism and how it relates to sexual conflict within species.

My thesis aims at understanding the effect of gene expression in the ontogeny of sexual dimorphism, by exploring the dynamics of sex-biased gene expression across development in *Timema* stick insects.

In chapter 1 of this thesis, we explored the dynamics of sex-biased gene expression during development in sexually reproducing *Timema californicum*. We used the whole body of individuals from three developmental stages: i) the first nymphal stage, with no evident sexual dimorphism, ii) the third nymphal stage, where some morphological differences between sexes can be observed, and iii) the adult stage, where sexual dimorphism is the most pronounced. We found a gradual increase in the amount of sex-bias, mirroring the morphological sexual dimorphism. Surprisingly, despite no morphological differences at the first nymphal stage, we observed some degree of sex-biased gene

expression. But many questions remain unanswered: how much different tissues contribute to sex-biased gene expression? Is the sex-biased gene expression still gradual when more developmental stages are analyzed? At which stage is sexual conflict the strongest?

We addressed those questions in chapter 2, where we analyzed sex-biased gene expression across development in multiple tissues in the sexual species *T. poppense* and in the parthenogenetic species *T. douglasi*. Sexual dimorphism in *Timema* is evident primarily through differences in body size, with females being larger compared to males. Additionally, differences in coloration appear in the antennae and legs, and there is a marked dimorphism in the shape and coloration of the cerci. The morphological and physiological variations between the sexes are generally attributed to sex-biased gene expression. Yet, it remains challenging to infer which genes, how many genes, and to which level of expression, they determine the sexually dimorphic traits. It is also unknown at which developmental stage the differences emerge, if it is a gradual, stepwise mechanism, or sudden differences in gene expression at a specific stage. In chapter 2, we show that levels of sex-biased gene expression correlate with levels of sexual dimorphism. There was minimal sex bias during development in somatic tissues, including the brain, gut, legs, and antennae, with a slight increase of sex-biased gene expression in antennae at the adult stage only. In contrast, the reproductive tract exhibited extensive sex-biased gene expression, starting from the first nymphal stage and persisting throughout development. High levels of sex-bias in the reproductive tract in contrast to somatic tissues, or whole bodies, occurs in many organisms. For instance, in plants, the majority of expressed genes were sex-biased in flowers (the reproductive part of plant), whilst only one gene was sex-biased in the leaf (the vegetative part) (Mank, 2017; Pointer *et al*, 2013; Sanderson *et al*, 2019; Whittle *et al*, 2021). However, we did not observe a gradual increase in sex-biased gene expression at the tissue level during development, suggesting that the results we obtained in chapter 1 were driven by the reproductive tissue. The reproductive tract, despite having little morphological differences between the sexes at the first nymphal stage, likely already differs in the developmental program underlying the production of separate gametes; i.e. sperm cells and eggs. In *Bacillus rossius,* at the first nymphal stage female ovaries already contain a few oocytes per ovariole,

indicating that this tissue is already differentiated (TADDEI *et al*, 1992). This may explain the high level of sex-biased gene expression that we observed in the reproductive tract at the first nymphal stage.

Besides sex-biased gene expression, other mechanisms such as alternative splicing can underlie sexual differentiation. In *Drosophila*, about 40 % of genes are alternatively spliced, with gonads having the most sex-specific splicing (Gibilisco, et al. 2016). Alternative splicing has a crucial role in sex-determination and sex-differentiation of insects (Salz 2011). For instance, the *Doublesex* (*dsx*) gene is alternatively spliced into male and female specific isoforms that have sex-specific effects on downstream sexual differentiation. The role of *Doublesex* in sex-determination is conserved in holometabolous insects and influences the development of the two sexes, while in hemimetabolous insects *dsx* seems to only affect males (Zhuo, et al. 2018; Wexler, et al. 2019). However, current evidence does not support sexual differentiation through sex-specific splicing of *dsx* in *Timema* (Gaudichau & Djordjevic, in preparation).

Sexual differentiation in insects can also be partially under hormonal control. The role of hormones in insect sexual differentiation has been neglected, as it challenges the conventional belief that sex determination in insects occurs in a cell-autonomous manner (Bear and Monteiro, 2013; Hopkins and Kopp, 2021). Nevertheless, some evidence suggests that hormones like ecdysone, 20-hydroxyecdysone, and juvenile hormones may influence sexual differentiation in insects. While the traditional understanding posits that hormones play a crucial role in sexual differentiation in mammals and birds, recent findings in insects, including beetle and butterfly species, indicate hormonal control over traits such as horn size and wing patterns (Bhardwaj *et al*, 2017; Emlen *et al*, 2005; Hopkins and Kopp, 2021). Hormones might target a few genes that cause large morphological changes. To test this hypothesis, future research should focus on hormone quantification and sex-biased gene expression over ontogeny across tissues. In *Timema*, cerci might be an interesting tissue to examine. This somatic tissue undergoes distinct morphological changes during development between males and females. Whether these changes co-occur with changes in hormone levels, or sex-biased gene expression, might

shed light on the role of hormones in sexual dimorphism. Another trait that could be investigated is the number of molts, which is also likely to be under hormonal control.

The postembryonic development of insects consists of series of developmental stages, where individuals grow, differentiate and achieve sexual maturity. The number of juvenile molts varies between species, but can also vary within species and between the sexes (Heming, 2003). Commonly, males have fewer instars than females, which has been shown across different insect orders and developmental types (Esperk *et al*, 2007). This tendency is associated with sexual size dimorphism, since the additional instars in females prolongs the growth period and final adult body size, which is important for female fecundity (Esperk *et al*, 2007; Honěk, 1993). In *Timema* as well, females are bigger and have an additional nymphal stage compared to males. This often raises questions about the homology between developmental stages in males and females. Our exploration of gene expression across nymphal stages in various tissues, of both males and females, in chapter 3 provides some valuable insight into this question. We found no specific separation by developmental stage within the tissues we compared. Instead, the 2nd to 6th nymphal stages form a group, separate from both the first nymphal stage and the adult stage. This result suggests that there is little differentiation between nymphal stages and sexes in sex-biased gene expression. Perhaps adding or removing nymphal stages would affect overall body size, but would have little effect on morphological or functional differentiation between sexes. However, whether the difference in the number of molts between sexes is driven by hormonal changes remains to be investigated. Artificially increasing or decreasing levels of relevant hormones during development might help us to understand their role in sexual dimorphism.

In chapter 2 we explored gene expression in parthenogenetic females, where sexual conflict is eliminated since they do not produce males. Comparisons between sexual and parthenogenetic females revealed masculinization in somatic tissues but a feminized gene expression in the reproductive tract during the 1st nymphal stage, suggesting potential unresolved sexual conflict in early gonadal development. The persistence of sexual conflict over gene expression in early gonads may be linked to the undifferentiated state of the reproductive tract at this stage. As development progresses, the

reproductive tract undergoes increased differentiation in morphology, function, and gene expression profiles, providing a better opportunity to resolve sexual conflict compared to earlier stages. This differentiation appears to be specific to the reproductive tract, as at the adult stage, this tissue displays distinct morphology and functions in each sex, almost resembling two distinct tissues. To further explore this phenomenon, additional experiments using another somatic tissue, such as the cerci, could provide valuable insights. Cerci initially lack sexual dimorphism in hatchlings, but later exhibit clear sexual dimorphism in adults, gradually differentiating between sexes during development (Figure 1, General Introduction). Given their role in mating for males, and in oviposition for females, these tissues are likely to be subject to sexually antagonistic selection. Following the premise of stronger conflict in undifferentiated tissues, similar feminization patterns in parthenogenetic females during the early nymphal stage would be expected.

Comparisons between sexual and parthenogenetic females revealed a surprising pattern, with the most extensive differences in gene expression occurring at the 1st nymphal stage in somatic and reproductive tissue. Subsequent nymphal stages showed minimal differential gene expression, with an increase at the adult stage. The observed pattern of gene expression resembles the "hourglass model" of evolutionary developmental biology. Under this model, early and late developmental stages represent periods of divergence where species evolve distinct characteristics, while the middle phase represents a period of constraint where there is a high degree of similarity. Results from transcriptomic analyses often mirror this morphological hourglass model (Liu *et al*, 2020). Although the model was proposed for species divergence during embryonic development, it might be applied to postembryonic development as well (Drost *et al*, 2017).

In chapter 3 we investigated dosage compensation mechanisms in *Timema* stick insects, where males possess a single X chromosome (X0) and females have two copies (XX). In somatic tissues (guts, brains, antennae, legs), males exhibit complete dosage compensation, with similar expression ratios of X-linked and autosomal genes compared to females. This is achieved by doubling the expression of genes on the single X in males. While present in somatic tissues, dosage compensation is often absent in the reproductive tract (Hu *et al*, 2022; Vicoso and Bachtrog, 2015). Other mechanisms such as

Meiotic Sex Chromosomes Inactivation (MSCI) can cause the imbalanced levels of X expression between sexes. For example, in mice and humans, early germ and gonadal somatic cells have complete dosage compensation, while it is lost in late germ cells (Sangrithi *et al*, 2017). Gene expression of the X chromosome was suggested to decrease gradually in germ cells from the leptotene/zygotene phase, followed by a complete silencing at the pachytene stage, due to MSCI (Sangrithi *et al*, 2017). Similarly, in *Anopheles gambiae* mosquitos (Culicidae: Diptera), the X in gonadal stem cells is compensated, while loss of dosage compensation begins in primary spermatogonia and gradually decreases until reaching its minimum in the mature spermatozoa (Page *et al*, 2023).

The level of X chromosome expression in the male reproductive tract during the 4th nymphal and adult stages, is below the levels expected due to absence of dosage compensation, resembling meiotic X-chromosome inactivation (MSCI). Immunolabeling and histone modification analysis further confirmed the occurrence of MSCI in *Timema*. We show that the dynamics of X-linked expression in the reproductive tract reflect the onset of meiosis, with complete dosage compensation observed in spermatogonia (1st nymphal stage) but not during meiotic divisions (4th nymphal and adult stages). In fact, this is likely true for all insects that have chiasmatic meiosis (McKee and Handel, 1993), which is not the case for *Drosophila* and some other Diptera. The absence of dosage compensation in the reproductive tract that has been recorded in different studies (Hu, et al. 2022; Parker, et al. 2022) could be driven by X chromosome inactivation. However, this is not the case in *Drosophila*, which shows absence of dosage compensation in germ cells, but not due to the MSCI.

In this thesis, I investigated the dynamics of sex-biased gene expression throughout development and its connection to sexual dimorphism and sexual conflict. I shed light on the distinct dynamics between early nymphal stage and adult stage, particularly regarding dosage compensation, sexual conflict, and gene expression patterns. Overall, these findings improve our understanding on sexual differentiation and sexual conflict during development.

Bibliography

Abbott JK, Lund-Hansen KK, Olito C. 2023. Why is measuring and predicting fitness under genomic conflict so hard? Current Opinion in Genetics & Development 81:102070.

Alexa A, Rahnenfuhrer J. 2023. topGO: Enrichment Analysis for Gene Ontology.

Alexa A, Rahnenführer J. 2009. Gene set enrichment analysis with topGO. Bioconductor Improv 27:1-26.

Anders S, Pyl PT, Huber W. 2014. HTSeq—a Python framework to work with high-throughput sequencing data. Bioinformatics 31:166-169.

Anderson J, Henikoff S, Ahmad K. 2023. Chromosome-specific maturation of the epigenome in the Drosophila male germline. In: eLife Sciences Publications, Ltd.

Argyridou E, Parsch J. 2018. Regulation of the X Chromosome in the Germline and Soma of Drosophila melanogaster Males. Genes 9:242.

Arnqvist G, Rowe L. 2002. Correlated evolution of male and female morphologies in water striders. Evolution 56:936-947.

Arnqvist G, Rowe L. 2005. Sexual conflict: Princeton university press.

Bachtrog D. 2013. Y-chromosome evolution: emerging insights into processes of Y-chromosome degeneration. Nature Reviews Genetics 14:113-124.

Bateman AJ. 1948. Intra-sexual selection in Drosophila. Heredity 2:349-368.

Benjamini Y, Hochberg Y. 1995. Controlling the false discovery rate: a practical and powerful approach to multiple testing. Journal of the Royal statistical society: series B (Methodological) 57:289-300.

Bioinformatics B. 2019. OmicsBox – Bioinformatics Made Easy.

Bolger AM, Lohse M, Usadel B. 2014. Trimmomatic: a flexible trimmer for Illumina sequence data. Bioinformatics 30:2114-2120.

Breer H. 1997. Molecular mechanisms of pheromone reception in insect antennae. In. Insect pheromone research: New directions: Springer. p. 115-130.

Brouard J-S, Bissonnette N. 2022. Variant Calling from RNA-seq Data Using the GATK Joint Genotyping Workflow. In: Ng C, Piscuoglio S, editors. Variant Calling: Methods and Protocols. New York, NY: Springer US. p. 205-233.

Catalán A, Briscoe AD, Höhna S. 2019. Drift and Directional Selection Are the Evolutionary Forces Driving Gene Expression Divergence in Eye and Brain Tissue of Heliconius Butterflies. Genetics 213:581-594.

Chen K, Rajewsky N. 2007. The evolution of gene regulation by transcription factors and microRNAs. Nature Reviews Genetics 8:93-103.

Chen Y, Lun AT, Smyth GK. 2016. From reads to genes to pathways: differential expression analysis of RNA-Seq experiments using Rsubread and the edgeR quasi-likelihood pipeline. F1000Research 5.

Chippindale AK, Gibson JR, Rice WR. 2001. Negative genetic correlation for adult fitness between sexes reveals ontogenetic conflict in Drosophila. Proceedings of the National Academy of Sciences 98:1671-1675.

Cline TW. 1993. The Drosophila sex determination signal: how do flies count to two? Trends in Genetics 9:385-390.

Colaco S, Modi D. 2018. Genetics of the human Y chromosome and its association with male infertility. Reproductive biology and endocrinology 16:1-24.

Connallon T, Knowles LL. 2005. Intergenomic conflict revealed by patterns of sex-biased gene expression. Trends in Genetics 21:495-499.

Cox RM, Calsbeek R. 2009. Sexually antagonistic selection, sexual dimorphism, and the resolution of intralocus sexual conflict. The American Naturalist 173:176-187.

Darwin C. 1871. The* descent of Man: 1: J. Murray.

Dean R, Mank JE. 2014. The role of sex chromosomes in sexual dimorphism: discordance between molecular and phenotypic data. Journal of Evolutionary Biology 27:1443-1453.

Deng X, Hiatt JB, Nguyen DK, Ercan S, Sturgill D, Hillier LW, Schlesinger F, Davis CA, Reinke VJ, Gingeras TR, et al. 2011. Evidence for compensatory upregulation of expressed X-linked genes in mammals, Caenorhabditis elegans and Drosophila melanogaster. Nature Genetics 43:1179-1185.

Djordjevic J, Dumas Z, Robinson-Rechavi M, Schwander T, Parker DJ. 2022. Dynamics of sex-biased gene expression during development in the stick insect Timema californicum. Heredity 129:113-122.

Dobin A, Davis CA, Schlesinger F, Drenkow J, Zaleski C, Jha S, Batut P, Chaisson M, Gingeras TR. 2013. STAR: ultrafast universal RNA-seq aligner. Bioinformatics 29:15-21.

Ellegren H, Parsch J. 2007. The evolution of sex-biased genes and sex-biased gene expression. Nature Reviews Genetics 8:689-698.

Ernst C, Eling N, Martinez-Jimenez CP, Marioni JC, Odom DT. 2019. Staged developmental mapping and X chromosome transcriptional dynamics during mouse spermatogenesis. Nature Communications 10:1251.

Evans JD, Shearman DC, Oldroyd BP. 2004. Molecular basis of sex determination in haplodiploids. Trends in Ecology & Evolution 19:1-3.

Foresta C, Ferlin A, Moro E. 2000. Deletion and expression analysis of AZFa genes on the human Y chromosome revealed a major role for DBY in male infertility. Human molecular genetics 9:1161-1169.

Gibilisco L, Zhou Q, Mahajan S, Bachtrog D. 2016. Alternative splicing within and between Drosophila species, sexes, tissues, and developmental stages. PLOS Genetics 12:e1006464.

Gibson JR, Chippindale AK, Rice WR. 2002. The X chromosome is a hot spot for sexually antagonistic fitness variation. Proceedings of the Royal Society of London. Series B: Biological Sciences 269:499-505.

Goodfellow PN, Lovell-Badge R. 1993. SRY and sex determination in mammals. Annual review of genetics 27:71-92.

Götz S, García-Gómez JM, Terol J, Williams TD, Nagaraj SH, Nueda MJ, Robles M, Talón M, Dopazo J, Conesa A. 2008. High-throughput functional annotation and data mining with the Blast2GO suite. Nucleic Acids Research 36:3420-3435.

Grath S, Parsch J. 2016. Sex-biased gene expression. Annual review of genetics 50:29-44.

Gu L, Walters JR. 2017. Evolution of Sex Chromosome Dosage Compensation in Animals: A Beautiful Theory, Undermined by Facts and Bedeviled by Details. Genome Biology and Evolution 9:2461-2476.

Gu L, Walters JR, Knipple DC. 2017. Conserved Patterns of Sex Chromosome Dosage Compensation in the Lepidoptera (WZ/ZZ): Insights from a Moth Neo-Z Chromosome. Genome Biology and Evolution 9:802-816.

Gupta V, Parisi M, Sturgill D, Nuttall R, Doctolero M, Dudko OK, Malley JD, Eastman PS, Oliver B. 2006. Global analysis of X-chromosome dosage compensation. Journal of Biology 5:3.

Hamada FN, Park PJ, Gordadze PR, Kuroda MI. 2005. Global regulation of X chromosomal genes by the MSL complex in Drosophila melanogaster. Genes & development 19:2289-2294.

Hansson BS, Stensmyr MC. 2011. Evolution of insect olfaction. Neuron 72:698-711.

Harrison PW, Wright AE, Mank JE. 2012. The evolution of gene expression and the transcriptome–phenotype relationship. Seminars in Cell & Developmental Biology 23:222-229.

Hollis B, Houle D, Yan Z, Kawecki TJ, Keller L. 2014. Evolution under monogamy feminizes gene expression in Drosophila melanogaster. Nature Communications 5:3482.

Hopkins BR, Perry JC. 2022. The evolution of sex peptide: sexual conflict, cooperation, and coevolution. Biological Reviews 97:1426-1448.

Hu Q-L, Ye Y-X, Zhuo J-C, Huang H-J, Li J-M, Zhang C-X. 2022. Chromosome-level Assembly, Dosage Compensation and Sex-biased Gene Expression in the Small Brown Planthopper, Laodelphax striatellus. Genome Biology and Evolution 14.

Hudry B, de Goeij E, Mineo A, Gaspar P, Hadjieconomou D, Studd C, Mokochinski JB, Kramer HB, Plaçais P-Y, Preat T. 2019. Sex differences in intestinal carbohydrate metabolism promote food intake and sperm maturation. Cell 178:901-918. e916.

Hurst LD, Ghanbarian AT, Forrest ARR, consortium F, Huminiecki L. 2015. The Constrained Maximal Expression Level Owing to Haploidy Shapes Gene Content on the Mammalian X Chromosome. PLoS biology 13:e1002315.

Huylmans AK, Macon A, Hontoria F, Vicoso B. 2021. Transitions to asexuality and evolution of gene expression in Artemia brine shrimp. Proceedings of the Royal Society B 288:20211720.

Huylmans AK, Parsch J. 2015. Variation in the X:Autosome Distribution of Male-Biased Genes among Drosophila melanogaster Tissues and Its Relationship with Dosage Compensation. Genome Biology and Evolution 7:1960-1971.

Ingleby FC, Flis I, Morrow EH. 2015. Sex-biased gene expression and sexual conflict throughout development. Cold Spring Harbor perspectives in biology 7:a017632.

Janzen FJ, Paukstis GL. 1991. Environmental sex determination in reptiles: ecology, evolution, and experimental design. The Quarterly review of biology 66:149-179.

Jaron KS, Parker DJ, Anselmetti Y, Van PT, Bast J, Dumas Z, Figuet E, François CM, Hayward K, Rossier V, et al. 2020. Convergent consequences of parthenogenesis on stick insect genomes. bioRxiv:2020.2011.2020.391540.

Kelly WG, Aramayo R. 2007. Meiotic silencing and the epigenetics of sex. Chromosome research 15:633-651.

Kelly WG, Schaner CE, Dernburg AF, Lee M-H, Kim SK, Villeneuve AM, Reinke V. 2002. X-chromosome silencing in the germline of C. elegans. Development 129:479-492.

Khalil AM, Boyar FZ, Driscoll DJ. 2004. Dynamic histone modifications mark sex chromosome inactivation and reactivation during mammalian spermatogenesis. Proceedings of the National Academy of Sciences 101:16583-16587.

Khila A, Abouheif E, Rowe L. 2012. Function, developmental genetics, and fitness consequences of a sexually antagonistic trait. Science 336:585-589.

Kiefer BI. 1966. Ultrastructural Abnormalities in Developing Sperm of X/0 DROSOPHILA MELANOGASTER. Genetics 54:1441-1452.

Kodric-Brown A, Brown JH. 1987. Anisogamy, sexual selection, and the evolution and maintenance of sex. Evolutionary Ecology 1:95-105.

Kottler VA, Schartl M. 2018. The Colorful Sex Chromosomes of Teleost Fish. Genes 9:233.

Kramer M, Kranz A-L, Su A, Winterkorn LH, Albritton SE, Ercan S. 2015. Developmental dynamics of X-chromosome dosage compensation by the DCC and H4K20me1 in C. elegans. PLOS Genetics 11:e1005698.

Lande R. 1980. Sexual dimorphism, sexual selection, and adaptation in polygenic characters. Evolution 34:292-305.

Langfelder P, Horvath S. 2008. WGCNA: an R package for weighted correlation network analysis. BMC Bioinformatics 9:559.

Larose C, Lavanchy G, Freitas S, Parker DJ, Schwander T. 2023. Facultative parthenogenesis: a transient state in transitions between sex and obligate asexuality in stick insects? Peer Community Journal 3.

Larschan E, Bishop EP, Kharchenko PV, Core LJ, Lis JT, Park PJ, Kuroda MI. 2011. X chromosome dosage compensation via enhanced transcriptional elongation in Drosophila. Nature 471:115-118.

Lawrence M, Huber W, Pagès H, Aboyoun P, Carlson M, Gentleman R, Morgan MT, Carey VJ. 2013. Software for Computing and Annotating Genomic Ranges. PLOS Computational Biology 9:e1003118.

Loyau A, Jalme MS, Sorci G. 2005. Intra-and intersexual selection for multiple traits in the peacock (Pavo cristatus). Ethology 111:810-820.

Lucchesi JC. 1998. Dosage compensation in flies and worms: the ups and downs of X-chromosome regulation. Current Opinion in Genetics & Development 8:179-184.

Lyon MF. 1961. Gene Action in the X-chromosome of the Mouse (Mus musculus L.). Nature 190:372-373.

Mahadevaraju S, Fear JM, Akeju M, Galletta BJ, Pinheiro MM, Avelino CC, Cabral-de-Mello DC, Conlon K, Dell'Orso S, Demere Z. 2021. Dynamic sex chromosome expression in Drosophila male germ cells. Nature Communications 12:892.

Mank JE. 2013. Sex chromosome dosage compensation: definitely not for everyone. Trends in Genetics 29:677-683.

Mank JE. 2017. The transcriptional architecture of phenotypic dimorphism. Nature Ecology & Evolution 1:0006.

Mank JE, Nam K, Brunström B, Ellegren H. 2010. Ontogenetic complexity of sexual dimorphism and sex-specific selection. Molecular Biology and Evolution 27:1570-1578.

McCarthy DJ, Chen Y, Smyth GK. 2012. Differential expression analysis of multifactor RNA-Seq experiments with respect to biological variation. Nucleic Acids Research 40:4288-4297.

McKee BD, Habera L, Vrana JA. 1992. Evidence that intergenic spacer repeats of Drosophila melanogaster rRNA genes function as X-Y pairing sites in male meiosis, and a general model for achiasmatic pairing. Genetics 132:529-544.

McKee BD, Handel MA. 1993. Sex chromosomes, recombination, and chromatin conformation. Chromosoma 102:71-80.

McKenna A, Hanna M, Banks E, Sivachenko A, Cibulskis K, Kernytsky A, Garimella K, Altshuler D, Gabriel S, Daly M, et al. 2010. The Genome Analysis Toolkit: A MapReduce framework for analyzing next-generation DNA sequencing data. Genome research:1297-1303.

Meiklejohn CD, Tao Y. 2010. Genetic conflict and sex chromosome evolution. Trends in Ecology & Evolution 25:215-223.

Meisel RP, Malone JH, Clark AG. 2012. Disentangling the relationship between sex-biased gene expression and X-linkage. Genome research 22:1255-1265.

Meller VH. 2000. Dosage compensation: making 1X equal 2X. Trends in cell biology 10:54-59.

Meyer B, McDonel P, Csankovszki G, Ralston E editors. Cold Spring Harbor symposia on quantitative biology. 2004.

Meyer BJ, Casson LP. 1986. Caenorhabditis elegans compensates for the difference in X chromosome dosage between the sexes by regulating transcript levels. Cell 47:871-881.

Namekawa SH, Lee JT. 2009. XY and ZW: is meiotic sex chromosome inactivation the rule in evolution? PLOS Genetics 5:e1000493.

Nguyen DK, Disteche CM. 2006. Dosage compensation of the active X chromosome in mammals. Nature Genetics 38:47-53.

Ohno S. 1967. Sex chromosomes and sex-linked genes. Verlag: Springer.

Oliver B, Parisi M. 2004. Battle of the Xs. BioEssays 26:543-548.

Parisi M, Nuttall R, Naiman D, Bouffard G, Malley J, Andrews J, Eastman S, Oliver B. 2003. Paucity of Genes on the Drosophila X Chromosome Showing Male-Biased Expression. Science 299:697-700.

Parker DJ, Bast J, Jalvingh K, Dumas Z, Robinson-Rechavi M, Schwander T. 2019. Sex-biased gene expression is repeatedly masculinized in asexual females. Nature Communications 10:4638.

Parker DJ, Jaron KS, Dumas Z, Robinson-Rechavi M, Schwander T. 2022. X chromosomes show relaxed selection and complete somatic dosage compensation across Timema stick insect species. Journal of Evolutionary Biology 35:1734-1750.

Parker GA. 1979. Sexual selection and sexual conflict. Sexual selection and reproductive competition in insects 123:166.

Parker GA, Baker RR, Smith VGF. 1972. The origin and evolution of gamete dimorphism and the male-female phenomenon. Journal of Theoretical Biology 36:529-553.

Parsch J, Ellegren H. 2013. The evolutionary causes and consequences of sex-biased gene expression. Nature Reviews Genetics 14:83-87.

Perry JC, Harrison PW, Mank JE. 2014. The Ontogeny and Evolution of Sex-Biased Gene Expression in Drosophila melanogaster. Molecular Biology and Evolution 31:1206-1219.

Perry JC, Rowe L. 2015. The evolution of sexually antagonistic phenotypes. Cold Spring Harbor perspectives in biology 7:a017558.

Pessia E, Engelstädter J, Marais GAB. 2014. The evolution of X chromosome inactivation in mammals: the demise of Ohno's hypothesis? Cellular and Molecular Life Sciences 71:1383-1394.

Pointer MA, Harrison PW, Wright AE, Mank JE. 2013. Masculinization of Gene Expression Is Associated with Exaggeration of Male Sexual Dimorphism. PLOS Genetics 9:e1003697.

Rago A, Werren JH, Colbourne JK. 2020. Sex biased expression and co-expression networks in development, using the hymenopteran Nasonia vitripennis. PLOS Genetics 16:e1008518.

Rayner JG, Hitchcock TJ, Bailey NW. 2021. Variable dosage compensation is associated with female consequences of an X-linked, male-beneficial mutation. Proceedings of the Royal Society B 288:20210355.

Raz AA, Vida GS, Stern SR, Mahadevaraju S, Fingerhut JM, Viveiros JM, Pal S, Grey JR, Grace MR, Berry CW. 2023. Emergent dynamics of adult stem cell lineages from single nucleus and single cell RNA-Seq of Drosophila testes. Elife 12:e82201.

Rice W, Chippindale A. 2001. Intersexual ontogenetic conflict. Journal of Evolutionary Biology 14:685-693.

Rice WR. 1984. Sex chromosomes and the evolution of sexual dimorphism. Evolution:735-742.

Rico-Guevara A, Hurme KJ. 2019. Intrasexually selected weapons. Biological Reviews 94:60-101.

Robinson MD, McCarthy DJ, Smyth GK. 2009. edgeR: a Bioconductor package for differential expression analysis of digital gene expression data. Bioinformatics 26:139-140.

Rodríguez-Montes L, Ovchinnikova S, Yuan X, Studer T, Sarropoulos I, Anders S, Kaessmann H, Cardoso-Moreira M. 2023. Sex-biased gene expression across mammalian organ development and evolution. Science 382:eadf1046.

Roy D, Seehausen O, Nosil P. 2013. Sexual dimorphism dominates divergent host plant use in stick insect trophic morphology. BMC Evolutionary Biology 13:135.

Ruta V, Datta SR, Vasconcelos ML, Freeland J, Looger LL, Axel R. 2010. A dimorphic pheromone circuit in Drosophila from sensory input to descending output. Nature 468:686-690.

Salz HK. 2011. Sex determination in insects: a binary decision based on alternative splicing. Current Opinion in Genetics & Development 21:395-400.

Schoenmakers S, Wassenaar E, Hoogerbrugge JW, Laven JSE, Grootegoed JA, Baarends WM. 2009. Female Meiotic Sex Chromosome Inactivation in Chicken. PLOS Genetics 5:e1000466.

Schwander T, Crespi BJ. 2009. MULTIPLE DIRECT TRANSITIONS FROM SEXUAL REPRODUCTION TO APOMICTIC PARTHENOGENESIS IN TIMEMA STICK INSECTS. Evolution 63:84-103.

Schwander T, Crespi BJ, Gries R, Gries G. 2013. Neutral and selection-driven decay of sexual traits in asexual stick insects. Proceedings of the Royal Society B: Biological Sciences 280:20130823.

Shorey HH. 1973. Behavioral responses to insect pheromones. Annual review of entomology 18:349-380.

Signor SA, Nuzhdin SV. 2018. The evolution of gene expression in cis and trans. Trends in Genetics 34:532-544.

Stingele S, Stoehr G, Peplowska K, Cox J, Mann M, Storchova Z. 2012. Global analysis of genome, transcriptome and proteome reveals the response to aneuploidy in human cells. Molecular Systems Biology 8:608.

Straub T, Becker PB. 2007. Dosage compensation: the beginning and end of generalization. Nature Reviews Genetics 8:47-57.

Straub T, Gilfillan GD, Maier VK, Becker PB. 2005. The Drosophila MSL complex activates the transcription of target genes. Genes & development 19:2284-2288.

Stuart OP, Cleave R, Magrath MJL, Mikheyev AS. 2023. Genome of the Lord Howe Island Stick Insect Reveals a Highly Conserved Phasmid X Chromosome. Genome Biology and Evolution 15.

Team RC. 2023. R: A Language and Environment for Statistical Computing. Version 4.3.1. Vienna. Austria: R Foundation for Statistical Computing.

Toubiana W, Armisén D, Dechaud C, Arbore R, Khila A. 2021. Impact of male trait exaggeration on sex-biased gene expression and genome architecture in a water strider. BMC biology 19:1-17.

Toubiana W, Armisén D, Viala S, Decaras A, Khila A. 2021. The growth factor BMP11 is required for the development and evolution of a male exaggerated weapon and its associated fighting behavior in a water strider. PLoS biology 19:e3001157.

Toups MA, Vicoso B. 2023. The X chromosome of insects predates the origin of Class Insecta. bioRxiv:2023.2004.2019.537501.

Trivers RL. 1972. Parental investment and sexual selection. In. Sexual selection and the descent of man: Routledge. p. 136-179.

Turner JM. 2015. Meiotic silencing in mammals. Annual review of genetics 49:395-412.

Turner JMA. 2007. Meiotic sex chromosome inactivation. Development 134:1823-1831.

Veltsos P, Fang Y, Cossins AR, Snook RR, Ritchie MG. 2017. Mating system manipulation and the evolution of sex-biased gene expression in Drosophila. Nature Communications 8:2072.

Vickery VR, Sandoval CP. 2001. Descriptions of three new species of Timema (Phasmatoptera: Timematodea: Timematidae) and notes on three other species. Journal of Orthoptera Research 10:53-61.

Vicoso B, Bachtrog D. 2015. Numerous Transitions of Sex Chromosomes in Diptera. PLoS biology 13:e1002078.

Vicoso B, Charlesworth B. 2009a. The Deficit of Male-Biased Genes on the D. melanogaster X Chromosome Is Expression-Dependent: A Consequence of Dosage Compensation? Journal of Molecular Evolution 68:576-583.

Vicoso B, Charlesworth B. 2009b. Effective population size and the faster-X effect: an extended model. Evolution 63:2413-2426.

Vicoso B, Charlesworth B. 2006. Evolution on the X chromosome: unusual patterns and processes. Nature Reviews Genetics 7:645-653.

Viera A, Parra MT, Arévalo S, García de la Vega C, Santos JL, Page J. 2021. X Chromosome Inactivation during Grasshopper Spermatogenesis. Genes (Basel) 12.

Waters PD, Wallis MC, Graves JAM. 2007. Mammalian sex—Origin and evolution of the Y chromosome and SRY. Seminars in Cell & Developmental Biology 18:389-400.

Wexler J, Delaney EK, Belles X, Schal C, Wada-Katsumata A, Amicucci MJ, Kopp A. 2019. Hemimetabolous insects elucidate the origin of sexual development via alternative splicing. Elife 8:e47490.

Whitehead A, Crawford DL. 2006. Variation within and among species in gene expression: raw material for evolution. Molecular ecology 15:1197-1211.

Whittle CA, Kulkarni A, Extavour CG. 2021. Evolutionary dynamics of sex-biased genes expressed in cricket brains and gonads. Journal of Evolutionary Biology 34:1188-1211.

Wickham H. 2016. ggplot2: Elegant Graphics for Data Analysis: Springer-Verlag New York.

Wigby S, Chapman T. 2005. Sex peptide causes mating costs in female Drosophila melanogaster. Current Biology 15:316-321.

Williams TM, Carroll SB. 2009. Genetic and molecular insights into the development and evolution of sexual dimorphism. Nature Reviews Genetics 10:797-804.

Witt E, Shao Z, Hu C, Krause HM, Zhao L. 2021. Single-cell RNA-sequencing reveals pre-meiotic X-chromosome dosage compensation in Drosophila testis. PLOS Genetics 17:e1009728.

Wu C-I, Xu EY. 2003. Sexual antagonism and X inactivation–the SAXI hypothesis. Trends in Genetics 19:243-247.

Xia Q, Cheng D, Duan J, Wang G, Cheng T, Zha X, Liu C, Zhao P, Dai F, Zhang Z. 2007. Microarray-based gene expression profiles in multiple tissues of the domesticated silkworm, Bombyx mori. Genome biology 8:1-13.

Yamamoto D, Koganezawa M. 2013. Genes and circuits of courtship behaviour in Drosophila males. Nature Reviews Neuroscience 14:681-692.

Yanai I, Benjamin H, Shmoish M, Chalifa-Caspi V, Shklar M, Ophir R, Bar-Even A, Horn-Saban S, Safran M, Domany E, et al. 2004. Genome-wide midrange transcription profiles reveal expression level relationships in human tissue specification. Bioinformatics 21:650-659.

Zhuo J-C, Hu Q-L, Zhang H-H, Zhang M-Q, Jo SB, Zhang C-X. 2018. Identification and functional analysis of the doublesex gene in the sexual development of a hemimetabolous insect, the brown planthopper. Insect biochemistry and molecular biology 102:31-42.